University of Turin
Doctoral School of Sciences and Innovative Technologies

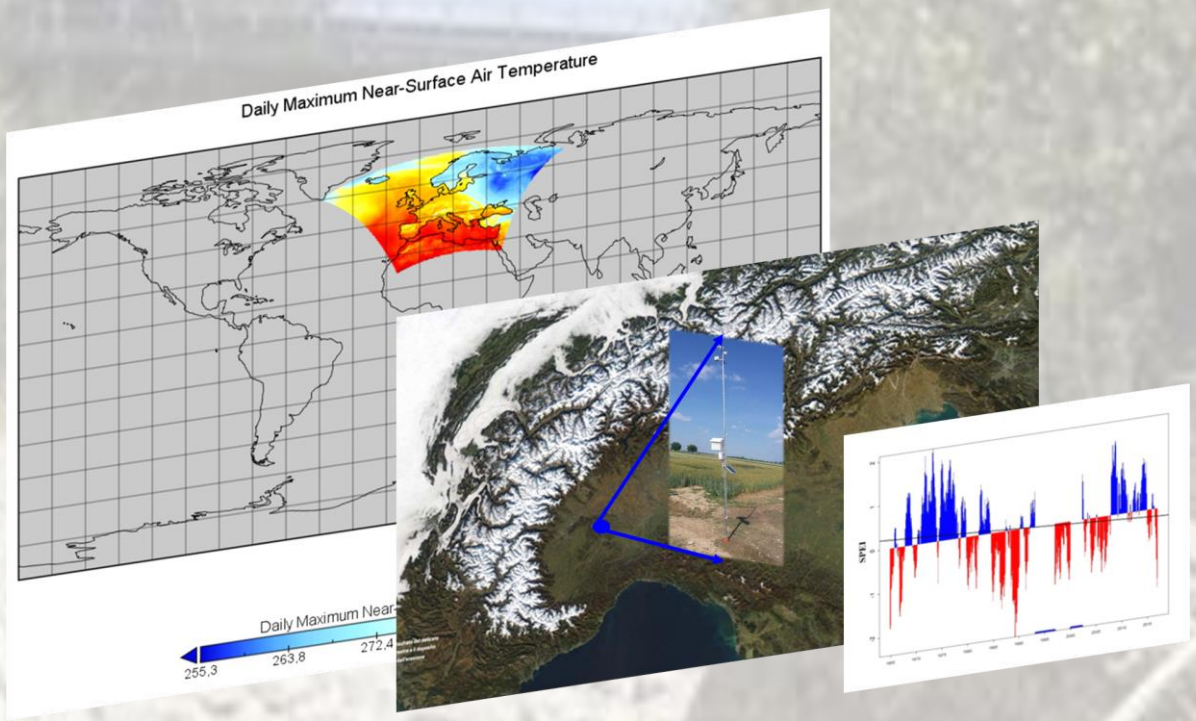

Analysis and projections of drought in northern Italy

Alice BARONETTI

EARTH SCIENCES

DIPARTIMENTO DI SCIENZE DELLA TERRA
UNIVERSITÀ DEGLI STUDI DI TORINO

University of Torino

Doctoral School of Sciences and Innovative Technologies

Doctorate in Earth Sciences

(XXXIII Cycle)

Analysis and projections of drought in northern Italy

Candidate: Alice Baronetti

Tutors: Prof.ssa Simona Fratianni

Prof. Pierluigi Pieruccini

Co-Tutor: Dott.ssa Fiorella Acquaotta

ABSTRACT

Drought is not an instantaneous phenomenon; its effects often take weeks or months to appear. Drought has the greatest consequences, compared to all other natural hazards, in terms of the number of people affected, both directly, i.e. by water scarcity, and indirectly, e.g. due to famine and consequent food shortages. In central Mediterranean basin (Southern Italy) several efforts were devoted in the study of drought episodes, due to the very significant rainfall reduction recorded in the southern Italian regions during the last 50 years. On the other hand, northern Italy is historically rich in water resources, and one of the most fertile and productive agricultural area. But recently drought events increased influencing the hydrological behaviour of the Po river. The specific focus of this study is to characterise for the first time in the international literature drought in northern Italy in the context of climate change. Past (1965-2017), near future (2020-2049) and far future (2070-2099) weekly drought events for the northern Italy, based on weather stations and Euro-CORDEX and Med-COREX ensembles were expressed and mapped.

The Standardised Precipitation Index (SPI) and the Standardised Precipitation Evapotranspiration Index (SPEI) are used to characterise the main drought events at different time scales, and duration in weeks, magnitude according to index values, and the percentage of area affected under specific thresholds for past and expected episodes were established. The spatial and temporal propagation of future drought events were then investigated and discussed possible mechanisms and triggering factors.

The results, because of the combined use of historical ground series and future projections, figure out an intensification of drought events in northern Italy since 2000s, influencing the prolongation of the Po river lean period. This positive trend continues in the future and the Alpine chain is expected to be the sector mostly involved. This study clearly showed the value of combining multiple drought indices, demonstrating that two different triggering factors influenced the characteristics of past and future drought events. The findings provide support in the development of knowledge and techniques that can help policymakers and decision makers to plan for and adapt to changing climatic conditions.

***Key words**: Climate Change, Global Climate Models, Drought, Regional Climate Models, Weather Stations, Standardised Precipitation Evapotranspiration Index, Standardised Precipitation Index, Propagation Gradient, Precipitation, Temperature.*

ACKNOWLEDGEMENTS

A special thanks goes to my tutor and beloved friend Prof. Simona Fratianni, for the many hours devoted to my work, and for her support, motivation and kindness. She always believed in me during this challenging time of my life, and she well be always with me.

I also thank my tutor Prof. Pierluigi Pieruccini, that decided to follow and support me and my work in this difficult period.

Dr. Fiorella Acquaotta for her precious help in all the stages of my PhD journey, in particular for her advices on statistical analysis and collection of meteorological data.

I would also like to thanks Dr. Antonello Provenzale Director of the Istituto di Geoscienze e Georisorse del Consiglio Nazionale delle Ricerche (CNR, Italia), for his interest and enthusiasm in my work.

I deeply grateful to Prof Vincent Dubreuil of the Université Rennes 2 (France), Département de Géographie for his suggestion on the research topic during the French adventure and the interest in this work, the willingness to revise this dissertation and the helpful suggestions to improve the thesis.

Special thanks for the precious suggestions and tips during my Spanish Erasmus also goes to Prof. José Carlos González Hidalgo of the Universidad de Zaragoza, (Spain), Departamento de Geografía y Ordenación del Territorio, and Dr. Sergio Vicente Serrano of the Istituto Pirenaico de Ecologia (Saragoza, Spain) and his staff.

Other special thanks goes also to Prof. Guillaume Fortin of the Université de Moncton (Canada), Département d'Histoire et de Géographie, for his mentorship during my first transcontinental experience in Canada.

I extend an additional thank you to those who helped me in the collection of future projection models:

Dr. Renan Le Roux of the of the UR Forêts et Sociétés of CIRAD (Montpellier, France) and Dr. Nicola Colombo of the Università di Torino (Italia), Dipartimento di Scienze della Terra.

Dr. Francesco Faccini of the Dipartimento di Scienze della Terra, dell'Ambiente e della Vita – DISTAV, Università di Genova (Italy) who revised this manuscript and gave helpful ideas to improve the thesis.

I would also like to thank my family for their loving support throughout these years and finally Alessandro (Peppo), for the special person he is, his constant encouragement has been my strength and my inspiration.

CONTENTS

INDEX OF TABLES

INDEX OF FIGURES

LIST OF ABBREVIATION

AED Atmospheric Evaporative Demand

AR4 Fourth Assessment Report of the Intergovernmental Panel on Climate Change

AR5 Fifth Assessment Report of the Intergovernmental Panel on Climate Change

ARPA Regional Environmental Protection Agencies

ASCE American Society of Civil Engineers

a.s.l. above the sea level

CH_4 Methane

CO_2 Carbon Dioxide

CORDEX COordinated Regional climate Downscaling EXperiment

CMIP3 Coupled Model Intercomparison Project Phase 3

CMIP5 Coupled Model Intercomparison Project Phase 5

COP21 Conference of the Parties

CRAN Comprehensive R Archive Network

CRED Centre for Research on the Epidemiology of Disasters

DRMKC Disaster Risk Management Knowledge Center

EDO European Drought Observatory

ET Evapotranspiration

ET_0 Potential or reference Evapotranspiration

ET_a Actual Evapotranpiration

Euro-CORDEX Coordinated Downscaling Experiment - European Domain

FAO Food and Agriculture Organization of the United Nations

GCM Global Climate Models

GHG GreenHouse Gases

GMT Global Mean Temperture

HG Hargreaves method

IPCC Intergovernmental Panel on Climate Change

ICID International Commission for Irrigation

ISPRA Italian National Institute for Environmental Protection and Research

KED Kriging with External Drift

LST Land Surface Temperature

OK Ordinary Kriging

MAE Mean Absolute Error

Med-CORDEX Coordinated Downscaling Experiment – Mediterranean Domain

MK Mann-Kendall test

MO Mediterranean Oscillation

NAO North Atlantic Oscillation

NAP National Action plan

NAS National Adaptation Strategy

NCDA National Climate Data Archive

N_2O Nitrous Oxides

PCI Precipitation Condition Index

PM Penman–Monteith method

QC Quality control

RCMs Regional Climate Models

RCP Representative Concentration Pathways

RK Regression Kriging

SCIA National System for the Collection, Processing, and Dissemination of Climatic Data of Environmental Interest

SEAP Sustainable Energy Action Plan

SPEI Standardised Precipitation Evapotranspiration Index

SPI Standardised Precipitation Index

SSD Snow Survey Database

SNHT Standard Normal Homogeneity Test

SK Simple Kriging

STRK Spatio-temporal regression kriging

TCI Temperature Condition Index

UK Universal Kriging

ULMOi Upper-Level Mediterranean Oscillation index

UNCCD United Nations Convention to Combat Desertification

UTM-32N Universal Transverse Mercator Zone 32N

WeMO Western Mediterranean Oscillations

WGS84 World Geodetic System 1984

WHO World Health Organization

WMO World Meteorological Organization

CHAPTER 1: INTRODUCTION

1.1. State of arts

Drought is not an instantaneous phenomenon; its effects often take weeks or months to appear. Drought is a normal, recurring feature of climate that occurs virtually in all climatic regimes. It is a temporary aberration, in contrast to aridity, which is a permanent feature of climate and is restricted to low rainfall areas. Whenever it becomes a disaster depends on its impact on local people, economies, agriculture, and the environment (Magno, 2014). Therefore, it is important to monitor and analyse the potential impact of drought in order to identify areas that are more vulnerable (Tadesse, 2004).

Drought is one of the most important consequences of climatic change for natural and socioeconomic systems. Wilhite and Glantz (1985) classified drought in into four general types: 1) meteorological (precipitation deficit), 2) agricultural (meteorological drought with consequences for agriculture), 3) hydrological (meteorological drought with reduced surface/sub-surface water supply), and 4) socioeconomic (drought combined with excess demand on the available supply of water, with consequences for society)

With respect to other extreme climatic events, drought effects appear after a long period with a shortage of precipitation, making it very difficult to determine their onset, extent and end (Dubreuil, 1997). Thus, it is hard to objectively quantify the characteristics of drought episodes in terms of their intensity and magnitude. Therefore, several efforts have been devoted to developing techniques for drought analysis and monitoring. Among these, the definition of quantitative indices is the most widespread approach. Many drought indices have been developed by using meteorological data, but is very difficult to establish a unique and universal drought index.

Among the available meteorological drought indices, the widely used are the Standardized Precipitation Index (SPI, McKee et al., 1993) and the Standardized Precipitation-Evapotranspiration Index (SPEI, Vicente-Serrano et al., 2010). The Standardized Precipitation Index (SPI) is the predominant meteorological drought index used in Europe and is recommended by the "Lincoln declaration on drought indices", which encourages Meteorological and Hydrological Services around the world to use the SPI (Hayes et al., 2011). By the other hand, the SPEI, uses a similar methodology, but is based

on the climatic water balance, which may better quantify drought. It has been widely used in the Iberian Peninsula, but is increasing applied also in other part of Europe, specially in the Mediterranean Basin.

The popularity of these two indices is due to their multiscalar flexibility. The multiscalar characteristic is viewed as a major benefit, in fact it allows to perform the drought investigation at short (for example 3, and 6 months) or long (for example 12, 24 and 36 months) time scales, allowing the user to approximate meteorological, agricultural, hydrological, and socioeconomic drought by adjusting the time scale of the indices (Vicente-Serrano et al., 2012). However, this prerogative of the index is rarely tested, in fact only few studies identify the most properly drought index and accumulation period for the different drought type and climatic region.

However, problems in drought quantification and data uncertainty has made difficult to determine changes in drought severity and to correlate these with climate drivers. This has promoted, in recent years, the creation of different available online services, that provide droughts forecasting, reports and bulletins for Europe and Mediterranean Basina. For example the European Drought Observatory (EDO, http://edo.jrc.ec.europa.eu), the Drought Management Centre (http://www.dmcsee.org/) and the SPEI Global Drought Monitor (http://sac.csic.es/spei/).

The Mediterranean Basin it has been identified by Diffenbaugh and Giorgi (2012) as a potential climate change “hot spot”. In the 20th century it experienced a noticeable increase in temperature coupled with a generalized decrease (in many cases not significant) in precipitation and soil moisture. Consequently, several studies have suggested that the area suffered the highest increase of drought magnitude, and different researches have analysed their impact on agriculture practices and hydrological conditions (Sellami et al., 2016). It is interesting to notice that usually drought in dry season capture the mass media attention, even if long spells of shortage of precipitation during the wet season could seriously damage agricultural economics (Raymond et al., 2016; Lamy and Dubreuil, 201).

Looking at future projections, due to the increasing public interest of climate change, the past decades have seen a rapid development in the methods for future climate scenario generation. Part of this evolution has involved downscaling techniques, which aim at translating 100-250 km resolution information obtained from Global Climate Models (GCMs) into Regional Climate Models (RCMs) with typical spatial resolution in the range 10-50 km. At European scale, the CORDEX (Coordinated Regional Climate

Downscaling Experiment, Giorgi et al., 2009) has provided high spatial resolution models for different European regions, in particular the two subprojects Euro-CORDEX (Jacob et al., 2014) and Med-CORDEX (Ruti et al., 2015) for the north-western Mediterranean region have produced present and future simulations at 12 km for the Representative Concentration Pathways (RCP 2.6, RCP 4.5 and RCP 8.5).

A detailed analysis of future projections in the Mediterranean basin is provided by Spinoni et al (2020), who analysed a large number of simulations based on a combination of GCMs and RCMs. Their analysis highlighted a significant climatic change over the Mediterranean basin. The marked negative precipitation trend linked with the significant increase of temperature could lead to more severe drought episodes. Spinoni et al (2020) and Diodato et al., 2020 showed that these changes are associated with a dominant anticyclonic circulation linked with a northward displacement of the Atlantic circulation. For Italy, the Italian National Institute for Environmental Protection and Research (ISPRA) has collected four RCMs models with spatial resolution of 50 km, belonging to the Med-CORDEX subproject, to obtain future climate projections (Desiato et al., 2015). The authors found a temperature increase of 2.5°C for RCP 4.5 and of 4.4°C for RCP 8.5 in the period 2061-2090, compared to the reference period 1971-2010. For precipitation, a decrease of about 1.5% with respect to the reference period is expected.

With regards of northern Italy few efforts were devoted in the study of past and future drought events. In fact, due to the typical Mediterranean climate and a very significant rainfall reduction recorded in the southern Italian regions during the last 50 years, the majority of studies on drought were performed in Calabria (Sirangelo et al., 2017, Buttafuoco et al., 2015), Basilicata (Piccarreta et al., 2004) and Campania (Alfio et al., 2020). At the same time, significant precipitation decrease will be expected and future drought events have been mostly investigated for the southern part of Italy (Critto et al., 2016).

On the other hand, the northern Italy even if falls completely within the Mediterranean area, it is a borderline Mediterranean climate region historically rich in water resources, and one the most fertile and productive agricultural area with different agriculture production of high quality such as wines, but also cereals, industrial crops, fruits and vegetables, that account for the 82% of the total agricultural production, and 40% of the total cultivated area, in the Po river basin (Musolino et al., 2017). But recently drought events

have increased even in this part of Italy. In fact, since the 2000s an increase of the prolongation of the Po river lean period was recorded, and in particular the dry and warm conditions observed across northern Italy in the years 2003, 2012, 2015 and 2017 have influenced the hydrological behaviour of the Po river (Marchina et al., 2017). In fact, in the last forty years, an antycyclonic synoptic system moved on western Mediterranean with high 500 geopotential over northern Europe, preventing from prolonged snow and precipitation events (Diodato at al., 2020).

1.2. Climate modelling

The atmospheric weather and the ocean circulation are governed by the fundamental laws of physics that describe the conservation of mass, energy and momentum (Figure 1). These basically well-known laws form the backbone of climate models. This solid physical basis gives a strong reason to believe that the models are a useful tool for exploring the behaviour of the climate system and its response to changes in external forcing such as increases in greenhouse gas concentrations (Raäisaänen, 2007).

In this regard climate models are the primary tools available for investigating the response of the climate system to various forcings, for making climate predictions on seasonal to decadal time scales and for making projections of future climate over the coming century and beyond.

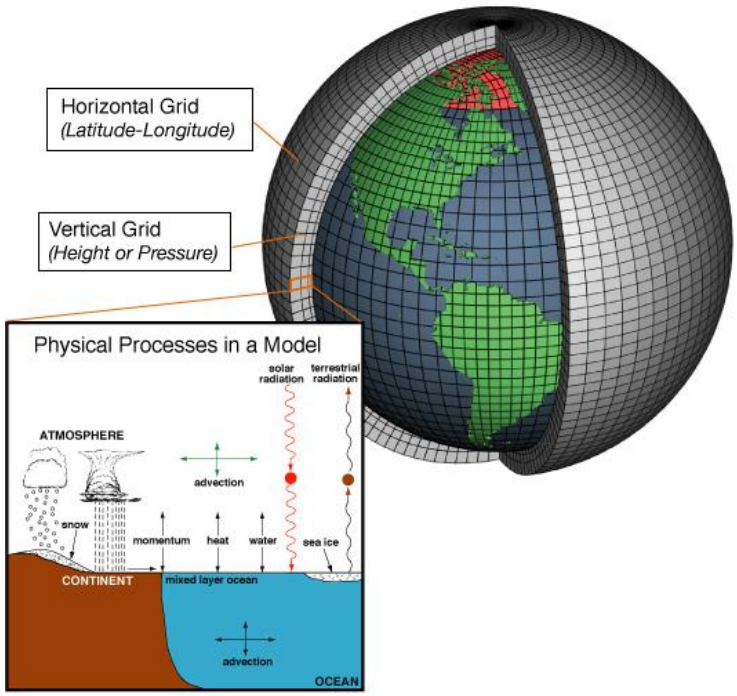

Figure 1: This image shows the concept used in climate models. Each of the thousands of 3-dimensional grid cells can be represented by mathematical equations that describe the way energy moves through the materials (https://celebrating200years.noaa.gov/breakthroughs/climate_model/modeling_schematic.html).

The main inputs into models are the external factors that change the amount of the sun's energy that is absorbed by the Earth, or how much is trapped by the atmosphere. These external factors are called "forcings". They include changes in the sun's output, as greenhouse gases (carbon dioxide (CO_2), methane (CH_4), nitrous oxides (N_2O)) and tiny particles called aerosols that reflect incoming sunlight and influence cloud formation. Typically, all these individual forcings are run through a model either as a best estimate of past conditions or as part of future "emission scenarios".

These are potential pathways for the concentration of greenhouse gases in the atmosphere, based on how technology, energy and land use change over the centuries ahead. In fact, in 2013, the Intergovernmental Panel on Climate Change (IPCC) defined a new set of scenarios that focused on the level of greenhouse gases in the atmosphere in 2100. These scenarios are known as Representative Concentration Pathways or RCPs. Each RCP indicates the

amount of climate forcing, that would result from greenhouse gases in the atmosphere in 2100. There are four pathways: RCP8.5, RCP6, RCP4.5 and RCP2.6. RCP 8.5 is generally considered as the worst scenario; it represents the condition where emissions continue to rise throughout the 21st century. The RCP 4.5 is described by the IPCC as an intermediate scenario, while the RCP 2.6 is a "very stringent" pathway. In fact, is assumed that carbon dioxide emissions start declining by 2020 and go to zero by 2100 (Flato et al., 2013).

Models also use as input estimates of past forcings to examine how the climate has changed over the past years. Past forcings are estimated using evidence of changes in the Earth's orbit, historical greenhouse gas concentrations, past volcanic eruptions, changes in sunspot counts, and other records of the distant past.

Subsequently, climate models generate a complete picture of the Earth's climate, including thousands of different variables across hourly, daily and monthly timeframes. These outputs include temperatures and humidity of different layers of the atmosphere from the surface to the upper stratosphere. Models also produce estimates of snowfall, rainfall, snow cover and the extent of glaciers, ice sheets and sea ice. They generate wind speed, strength and direction, as well as climate features, such as the jet stream and ocean currents.

Climate models also produce an estimate of climate sensitivity. They calculate how sensitive the Earth is to the increase in greenhouse gas concentrations, taking into account various climate feedbacks, such as water vapour and changes in reflectivity, or albedo, of the Earth surface associated with ice loss (Stocker, 2011).

The models widely used in climate research range from Global Climate Models (GCMs) and Regional Climate Modes (RCMs). The choice of model depends directly on the scientific question being addressed Applications include simulating palaeo or historical climate, predicting near-term climate variability and change on seasonal to decadal time scales, making projections of future climate change over the coming century or more and downscaling such projections to provide more detail at the regional and local scale.

1.2.1. Global Climate Models (GCMs)

Global Climate Models or General Circulation Models are the standard climate models. Their primary function is to understand the dynamics of the physical components of the climate system (atmosphere, ocean, land and sea ice), and for making projections based on future greenhouse gas (GHG) and

aerosol forcing. These models are extensively used, and in particular are run for seasonal to decadal climate prediction applications (Flato et al., 2013)

Global Climate Models typically have a grid spacing of 200–300 km in the horizontal direction. In the vertical direction there are typically about 30 levels between the surface and the model top at 30–50 km height, the spacing of the levels increasing from a few hundred metres in the boundary layer to several kilometres in the stratosphere (Raäisaänen, 2007)

The Intergovernmental Panel on Climate Change (IPCC) gathers and reviews global climate models as part of the international climate change Assessment Reports. The ensemble of the models are called the Climate Model Intercomparison Project (CMIP) CMIP is a framework for climate model experiments, allowing scientists to analyse, validate and improve GCMs in a systematic way:

- CMIP3 is the model ensemble for the IPCC's Fourth Assessment Report (AR4) and was released in 2010.
- CMIP5 is the model ensemble for the IPCC's Fifth Assessment Report (AR5) and was released in 2013(Figure 2).

Actually, CMIP6 is now underway, which will involve more than 30 modelling centres around the world.

The two greatest differences between CMIP3 and CMIP5 dataset is that CMIP5 contains more models than CMIP3 and the CMIP5 models are more advanced. The IPCC's Fifth Assessment Report (AR5) is based primarily on results from the CMIP5 modelling using RCPs, but it also uses results from the CMIP3 modelling. The IPCC notes that, for both large-scale climate patterns and the magnitudes of climate change, there is overall consistency between the projections based on CMIP3 and CMIP5.

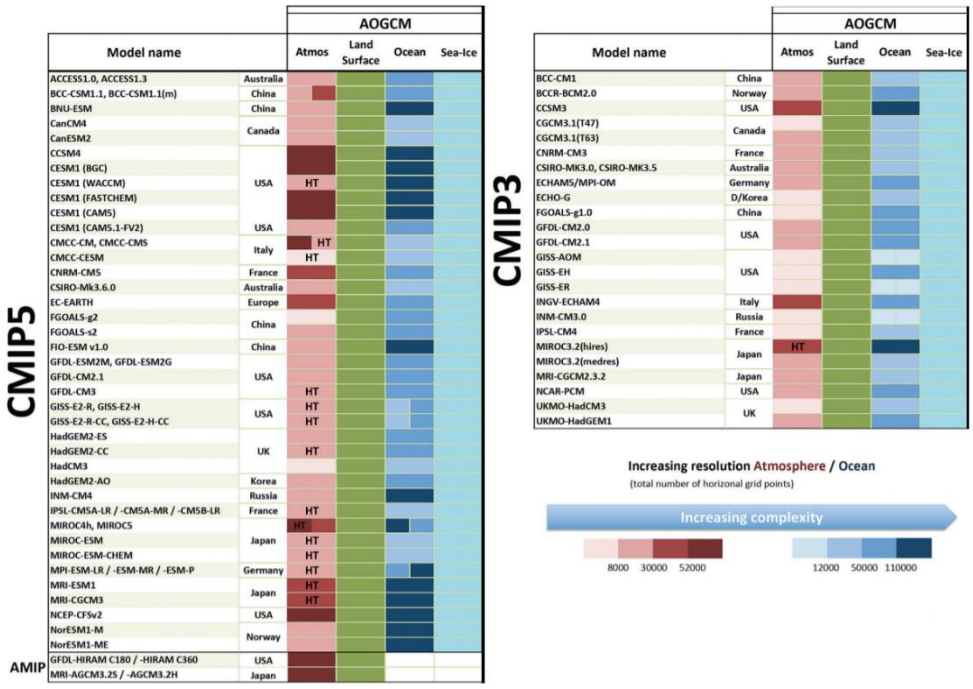

Figure 2: Main features of the General Circulation Models (GCMs) participating in Coupled Model Intercomparison Project Phase 5 (CMIP5), and a comparison with Coupled Model Intercomparison Project Phase 3 (CMIP3, modified by Flauti et al., 2013).

1.2.2. Regional Climate Models (RCMs)

One of the main limitations of global climate models is that their spatial resolution is typically around 100km in the mid-latitudes. This means that in regional analysis GCMs miss the geographical features that characterise a particular location.

Regional climate models (RCMs) are a complementary research method, allowing more detailed process studies and simulation of regional and even local conditions. In fact, Reginal Climate Models (RCMs) are limited-area models with representations of climate processes comparable to the Global Climate Models (GCMs). RCMs are often used to dynamically downscale global model simulations for some particular geographical region to provide more detailed information. By contrast, statistical downscaling method constitute a range of techniques to provide similar regional or local detail. The technique of dynamical downscaling allows for a higher spatial resolution over the domain of interest, and for a more realistic representation of important

surface heterogeneities (such as topography, coast lines, and land surface characteristics, Kotlarski et al., 2014).

Research projects such as MERCURE (e.g., Hagemann et al., 2004), PRUDENCE (Christensen et al., 2007), NARCCAP (Mearns et al., 2009), and ENSEMBLES (van der Linden and Mitchell, 2009) are the milestones in both regional model development. If the previous cited projects are widely used by the climate impact community and are considered as state-of-the-art. The next generation of regional climate projections falls in the frame of the CORDEX project (Coordinated Regional Climate Downscaling Experiment, Giorgi et al., 2009). CORDEX aims to provide provided high spatial resolution models for different regions in the World. Euro-CORDEX (Jacob et al., 2014) and Med-CORDEX (Ruti et al., 2015) are the European branches of CORDEX, which provide regional climate projections for the north-western Mediterranean at grid resolutions of about 12 and 50 km.

1.3. Research aims and Objectives

Nowadays, few efforts were devoted in the study of past and future droughts in northern Italy. Because it is a borderline Mediterranean climate region, this area is historically rich in water resources, and availability of water resources for irrigated and rainfed farming, and for other uses, is used to be high. In this regard, the level of economic development and economic vivaciousness in northern Italy is very high: 34% of the value added of Italy is created in the Po Plain, due to a remarkable concentration of a wide range of agricultural, industrial and services activities (Musolino et al., 2017). However, recently drought events have risen. Since 2000, a further increase in the prolongation of the Po river lean period has been recorded, and the dry and warm conditions observed across northern Italy in the years 2003, 2011, 2015, and 2017 influenced the lean period of the Po river.

The present work addresses, for the first time, the high-resolution analysis of drought episodes in northern Italy, by using two indices, SPEI and SPI. Two study period were investigated:

- Past (1965-2017) drought events. The main drought events, their characteristics, the spatial propagation, and information on the possible triggering factors are identified.
- Near (2020-2049) and far future (2070-2099). The expected frequency of events and their magnitude, the percentage of area affected under specific

thresholds and the temporal trends are quantified. The spatial propagation of future drought events and the possible mechanisms and triggering factors are also investigated.

1.4. Dissertation structure

This dissertation is divided into eight chapters. This **first chapter** contains the research state of arts and objectives. Moreover, the chapter explains the principles of climate modelling, describing two models widely used in climate research, Global Climate Models (GCMs) and Regional Climate Models (RCMs).

The other chapters are as follows (**Errore. L'origine riferimento non è stata trovata.**):

Chapter 2 – DROUGHT, this chapter is focused on drought, its definition, types, causes, effects and methods of investigation. A further description is given of the impacts of drought and future climate scenarios.

Chapter 3 – CLIMATIC CHARACTERISTICS OF NORTHERN ITALY; in this chapter will be presented the study area (with geographical information and climatic classification) and the main climatic zones that characterise the northern Italy.

Chapter 4 – DATASETS; this chapter provides information about the data used and their sources. Procedure and methods of quality control, homogenization and reconstruction of the historical series and the technique of validation of the climatological models were presented.

Chapter 5 – METHODS and ANALYSIS; this chapter provides the analysis of the historical series and of the climatological models comprises the methodology used to study drought, in order to extract the main drought episodes and detect temporal and spatial trends.

Chapter 6 – RESULTS; this chapter shows the results obtained from the different calculations performed. Graphs, tables and summaries most representative images are shown.

Chapter 7 – DISCUSSION; this chapter provides a discussion of research finding

In the last **chapter 8**, there are the conclusions and some ideas for further works.

CHAPTER 2: DROUGHT

Drought is one of the most important natural hazards, that occurs virtually in all climatic regimes. It is a temporary precipitation aberration, in contrast to aridity, which is a permanent feature of climate and is restricted to low rainfall areas (Mishra and Sigh, 2010).

Due to the complexity of the phenomenon, yet a universal definition of the term has proven to be elusive. The World Meteorological Organization (1992) glossary defines drought as an insidious natural hazard characterized by lower than expected or lower than normal precipitation, that is insufficient to meet the demands of human activities and the environment.

Reducing the definition of drought solely on precipitation deficit, is to neglect the importance of evaporation and transpiration as moisture carries. Further, the definition provided by the WMO is lack in the reference to the timing of the precipitation deficit. In fact, it is a crucial factor in the determination of many drought impacts. Sheffield and Wood (2012) gave an accurate and brief definition of drought as "a deficit of water relative to normal conditions". This definition echoes the one made by Palmer (1965), that defined drought as "an interval of time, generally of the order of months or years in duration, during which the actual moisture supply at a given place rather consistently falls short of the climatically expected or climatically appropriate moisture supply".

This definition captures the two essential drought features, the first one is the length of the dry period and the second one is the region to be considered (Lloyd-Hughes, 2014). Drought is difficult to quantify, its effects often appear after a considerable period and may delay for years after the ending of the event, determining the onset and end of drought problematic to detect. (Wilhite, 2000). Moreover, the drought severity, magnitude, and frequency can vary from region to region, and it is not an easy task to determine their spatial and temporal distribution, that is influenced by different factors, including low precipitation, high temperature, strong wind, solar radiation and relative humidity (Vicente-Serrano et al., 2010).

2.1. Drought types

Because of these different points of views of droughts, there is not a single definition that assess and describe drought severity. Wilhite and Glantz (1985) categorized the definitions of drought in: meteorological, hydrological,

agricultural, and socioeconomic. The first three approaches treat drought as a physical phenomenon, while the last one treat drought in terms of the effects of water shortfall on socioeconomic systems.

2.1.1. Meteorological drought

Meteorological drought (Figure 3) is defined usually on the basis of the degree of dryness and the duration of the dry period. It is characterised by a shortage of precipitation (Keyantash and Dracup, 2002), aggravated by hot temperatures (Vicente-Serrano et al., 2015). It develops quickly and it appears in the first three months. Moreover, meteorological drought is the primary cause of a drought, while the other types describe secondary effects on specific ecological and economic compartments (e.g. soil moisture, river flows, reservoirs, and economic sectors, Spinoni et al., 2020).

Definitions of meteorological drought must be considered as region specific, since the atmospheric conditions that result in deficiencies of precipitation are highly variable from region to region. In fact, drought definition based only on the number of days with precipitation below a certain threshold are unrealistic in those regions where precipitation distribution is seasonal, and extended periods without rainfall are common (e.g. Mediterranean basin). Actually, the greatest part of meteorological drought definitions is based on precipitation amounts below the monthly, seasonal, water year, or annual average of a specific region (Wilhite, 2000).

2.1.2. Agricultural drought

Agricultural drought (Figure 3) links the characteristics of the meteorological drought to agricultural impacts, focusing not only on precipitation shortages but also in differences between actual and potential evapotranspiration, soil water deficits, and reduced groundwater.

Plant water demand depends on the biological characteristic of the plant, on its state of growth, on soils features, but also on the main weather conditions. Moreover, a good definition of agricultural drought should take into account the variable susceptibility of the plant during the different phenological stages. In fact, during the early stage of growth a low subsoil moisture will impact less on the final crop yield if the topsoil is well moisturised and if it is sufficient to satisfy the early growth requirements, or if rainfall meets plant water needs (Wilhite, 2000).

Usually agriculture is the first economic sector interested by drought, in fact, during high temperature and windy period, soil moisture supplies are often quickly depleted. Furthermore, drought impact is crop specific in fact, the most weather-sensitive phenological stages can vary between crops. For example, a period characterised by high temperature and low precipitation conditions may coincide with a critical weather-sensitive growth stage for one crop, while missing a critical stage for another crop. In this regard agricultural drought mitigation strategies act to reduce the risk of drought altering the crop genotype, planting date, and cultivation practices (Winkler et al., 2017).

2.1.3. Hydrological drought

Hydrological drought (Figure 3) is the result of the effect of periods of precipitation lack on surface or subsurface water supply. Hydrological drought is usually out of phase or lag the occurrence of meteorological and agricultural droughts. It develops slowly instead of meteorological and agricultural drought and the effects occur after 6 months and can continue over the years, since recharge of reservoirs and groundwater is a long process. In fact, for the hydrological drought, precipitation shortage takes more time to result in the component of the hydrological system such as soil moisture, streamflow, and groundwater and reservoir levels (Wilhite, 2000).

The frequency and severity of hydrological drought is often defined on river basin scale, comparing the actual flow with the long-term runoff threshold to consider the progression of the drought. In fact, if a monitored flow for a selected period falls below a specific threshold, hydrological drought is considered to be in act. However, the defined threshold is somewhat arbitrary, and the criteria can vary between streams and river basins.

Hydrological drought that interests the upstream portion of a river basin could interest the downstream part, resulting in lower reservoirs and groundwater levels, even if meteorological drought does not exist at this level of the basin. The impacts of hydrological drought in reservoir and in groundwater levels may seriously impact the economic system, since water is used for hydroelectric power production, recreation, transportation, agriculture, and other sectors.

2.1.4. Socioeconomic drought

Among the four types of drought, the socioeconomic drought (Figure 3) has a direct impact on human production and daily life. The socioeconomic definition of drought is linked with the supply and demand of some economic good with elements of meteorological, hydrological, and agricultural drought. In fact, economic good such as water, forage, food grains, fish, and hydroelectric power, depends on weather. The socioeconomic drought could be defined when the demand of economic goods exceeds the supply, as a result of weather condition related to a precipitation shortage (Guo et al., 2019).

This definition of socioeconomic drought, support the strong connection between drought and human activities. In fact, most of the time, the demand for economic goods is increasing as a result of increasing population. In the future the incidence of drought could increase because of a change in the frequency of the physical event, a change in societal vulnerability to water shortages, or both.

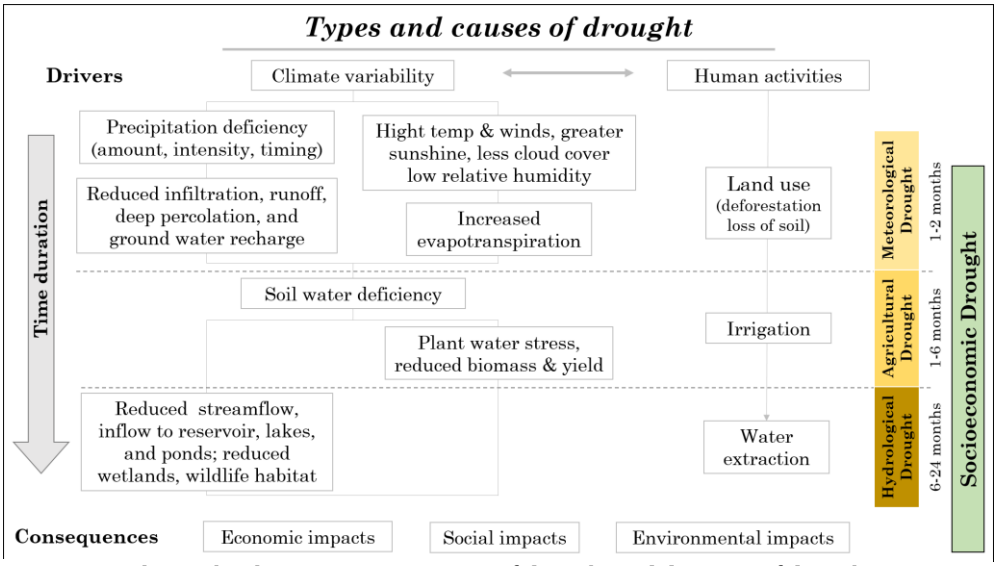

Figure 3: Relationship between various types of drought and duration of drought events (Wilhite, 2000).

2.2. Drought as natural hazard

A natural hazard is a naturally occurring event that have a negative impact on people or the environment. Drought is a natural hazard that is aggravated by the growing water demand. The reason why the occurrence of drought episodes is complex, is because it depends not only on the atmosphere but also on the hydrologic cycle that apport moisture to the atmosphere. In fact, once dry hydrologic conditions are established, the positive feedback mechanism of drought is triggered, and low evapotranspiration levels at the upper soil layers promote a reduction of the atmospheric relative humidity. Lesser relative humidity in the atmosphere reduces the probability that precipitation events happen. This makes harder to reach saturation conditions for a regular low-pressure system over the region. Only the arrival of enough moisture from outside the dry region will be able to produce sufficient rainfall to end drought conditions (Mishra and Singh, 2010).

Droughts rank first among the natural hazards in terms of the number of people affected, but it differs from the others in three essential characteristics: intensity, length or duration and spatial prorogation. Intensity is the degree of precipitation shortage or the severity of impacts correlated with the event of shortage. This feature is identified by the application of climatic indices. Usually the widespread method used to detect the intensity of a drought event is to compare actual precipitation with normal or average precipitation for time periods ranging from one to twelve months. The great limitation of this method is to fix a precipitation threshold that define a shortage. The second drought feature is the length or duration, the onset and the end of a drought are difficult to determine. Drought increases slowly, it needs from one to three months to become established and it can continue for months or years after termination. The magnitude of a drought impact is the result of the timing of the onset of the precipitation shortfall, the intensity and the duration of the event. The third characteristic is the spatial prorogation, differently from the other natural hazards, drought is not structured and spreads over large geographical areas (Wilhite, 2000). Human activities play also an important role in drought propagation, irrigation, dam and reservoir operations, and water diversion may significantly alter the propagation process (Wang et al., 2016).

2.3. Impact of climate change on droughts

The Intergovernmental Panel on Climate Change (IPCC) Fifth Assessment Report recognised that climate change is one of the major threats for the Earth

planet in the twenty-first century. Temperature have risen globally over the last 157 years, with significant regional variations. For the global average, warming was occurred in two phases, a first one from the 1910s to the 1940s with +0.35° of warming and a second one more pronounced from the 1970s to the present with +0.55°C of increase (Hartmann et al., 2013). In general, this temperature increase has intensified the global hydrological cycle, and is well known that earth's temperature surface has been increasing since the last glacial maximum 21000 years ago, thus has increased evapotranspiration, precipitation and runoff (Mishra and Singh, 2010). As concern precipitation the IPCC AR5 reported that precipitation trends in the twentieth century are not equally distributed over the Earth, and precipitation has increased over the equatorial and subpolar regions, while negative trends in the subtropical and mid-latitude regions are observed (Ren et al., 2013). The consequences of climate change are not only the increase or decrease of mean values, but the overall increase of extreme events. Among the extreme events drought is the most slowly developing one, that has the longest duration and the lowest predictability.

2.3.1. Global drought

Droughts, as described in previous sub-chapters, is part of the natural climate cycle that commonly affects large areas and can last for several months or even years. It is a complex phenomenon with wide-ranging environmental and socioeconomic impacts and is considered globally to be one of the costliest natural hazards (EEA, 2010).

In the last few years, in the newspapers, on the internet, or in the media, it is not uncommon to find claims that the latest event, such as the California drought of 2014 (Science News, 2014), Moscow's heatwave in summer 2016 (Russia Beyond, 2016), and the South Asia flood of 2017 (The Guardian, 2017), broke century or millennial records. Specially since 1950s drought events increased their frequency and they are mostly influenced by El Niño.

Spinoni et al. (2020) identified globally 52 mega-droughts since 1951. Among them are remarkable, The great drought of 1952 in the Central United States and the drought of 1963 in the North-Eastern United States. The devastating Sahel (Sub-Saharan Africa) drought in the 1970s, was widely reported in literature and it was one of the main reasons that promoted the creation of the United Nations Convention to Combat Desertification (UNCCD). The heavy drought event in 1972 that interested the Eastern Russia. Moreover, Ethiopia and Sudan were hit by recurrent droughts in 1982–1984, in 1987, and in 1990.

The World Health Organization (WHO) collaborating Centre for Research on the Epidemiology of Disasters (CRED) reported that the drought event between 1983 and 1985 resulted in more than half million deaths in Ethiopia and Sudan. In late 1990s a severe drought hit Borneo with devastating forest fires and it was also the worst drought event in Papua. The new millennium started with the so-called Millennium Drought in Australia (1995-2012). The 2001-2002 drought event interested Canada and United States. The 2002 drought interested also India with 300 million people affected. Important is the summer 2003 drought that hit the Mediterranean area and Central Europe (Ouzeau et al., 2016). Globally the drought event of 2015-2016 interested the highest percentage of area in the post-1950 record. Every month of 2016 had at least 12% of global land experiencing severe drought conditions, matched only by 1984 and 1985 (Osborn et al., 2017). This event was more marked over the Mediterranean Basin and Africa, and it became more extensive across large parts of Brazil (except for the south) and other tropical countries in the northern half of South America (Jimenez-Munoz et al. 2016).

2.3.2. Mediterranean Basin drought

In a contest of drought increase around the world, the Mediterranean region emerges as a prominent regional climate change hotspot. In particular, the Mediterranean basin is affected by strong drought episodes due to the high interannual variability of precipitation which combined with high evapotranspiration losses can lead to deficit in soil moisture. Consequently, drought can cause a wide range of impacts affecting the environment, society and economy, where impacts on agriculture and public water supply are most frequently reported. It is interesting notice that drought episodes during the wet season have significative impacts on agriculture economy which implies a massive use of water availability. At the same time, the reduction of water availability has effect on soil moisture and reservoirs during the dry season, with a hight attention of the mass media. (Drumond et al., 2017).

Mediterranean prolonged droughts with severe impacts, became more frequent since 1970s. In particular, the last decades were characterised by mega heatwaves such as the major drought in summer 2003. This event mainly affected the Central Europe regions and the Mediterranean region. The main triggering factor for the 2003 drought was the increase of extreme warm temperature events. The mean temperature anomaly recorded in 2003 was of 0.46 °C in relation with the reference period 1961-1990 (Luterbacher et al., 2004). Another major event is the drought of 2008 over the Iberian Peninsula.

It was the most intense hydrological drought recorded in the Jucar and Turia basins (Easter Spain) in the recorded history of hydrological flows (since 1940, Andreu et al., 2009). The year 2015 was characterised by another important drought event that mainly interested the south-western Europe (France, Greece, Northern Italy and Spain). Summer 2015 was one of the warmest summers in the Mediterranean Basin since 1910 (after 2003), with a temperature anomaly of 0.90°C in August. Subsequently, during the 2016-2017 period most of south and western Europe suffered for a major drought episode. García-Herrera et al. (2019) figured out that this drought episode was generated by a significant decrease of moisture transport from the Atlantic Ocean. During this event in Spain and Italy crops were severely affected by the resulting reduction in agricultural production, especially for cereals, olives, tomatoes, wine grapes, and almonds. In Italy, Coldiretti estimates losses of two billion euros, and 11 regions on 20 asked for an emergency declaration to fight against the drought.

2.3.3. Future scenario

Looking at future projections, in the fifth report (AR5), the IPCC (2014) used a new set of scenarios, called Representative Concentration Pathways (RCPs), for the new climate model simulations developed under the Coupled Model Intercomparison Project Phase 5 (CMIP5, Taylor et al., 2012) of the World Climate Research Programme. Future climate projection models suggest that drought will be more frequent in the future due to global climate change, which is expected to cause increases in temperature (and heat wave events) and changes in precipitation. In fact, even though global rainfall is projected to increase, the activities contributing to global warming will influence the extent to which drought is triggered. This is due to the variation in precipitation characteristics (amount, frequency, intensity, duration, type) and extremes events (Trenberth et al., 2003). Global future projections also predict for the twenty-first century a reduction of renewable surface water and groundwater resources in most dry subtropical regions, intensifying competition for water among sectors.

For the near future (next 15-20 years), Perini et al. (2011) predicted a strong decrease in winter and spring precipitation in northern and southern Italy, and a reduction of summer rainfall in Southern Italy and the islands. While, by the 2100s, a general temperature increase of about 3 °C is expected in all seasons across the whole of Italy, peaks of 4 °C are projected for the Po Valley in winter and over the whole north-west region in summer (Bucchignani et al.,

2016), according to the RCP4.5 scenario, with increasingly frequent and long-lasting heat waves, which will extend to more than thirty days over the entire summer season (González-Hidalgo et al., 2018). On the contrary, the RCP8.5 scenario predicts a strongly significant reduction in precipitation in spring and summer in the Alpine area with a negative anomaly from 0.1 to 0.4mm day-1 (Bucchignani et al. 2016). The future projections of climate change over the 21st century also predict a reduction of renewable surface water and groundwater resources in most dry subtropical regions, intensifying competition for water among sectors. According to the RCP8.5 scenario, the frequency of droughts will likely increase by the end of the 21st century in presently dry regions, while in contrast, water resources are projected to increase at high latitudes.

Climate change is already affecting the food and agriculture sectors, and these effects are projected to grow, along with global average temperatures, especially when the shortage of precipitation during the growing season imposes on crop production or ecosystem function in general (due to soil moisture drought). Responses to decreased food production and quality and adaptation options for agriculture include technological responses, and developing new crop varieties adapted to changes in CO2, temperature, and drought; enhancing the capacity for climate risk management; and offsetting economic impacts of land use change. Improving financial support and investing in the production of small-scale farms can also provide benefits.

2.4. Drought impacts

Droughts are a recurrent feature of climate and their impact on the environment and human activities depends on the interaction between this natural event and water demand for several purposes, from agriculture to civil and industrial needs. Drought can affect both ecosystems and society in multiple ways, for instance it is the main driver for land degradation and desertification. It could involve socio- economic impacts such as crop failure, food shortages, famine, malnutrition, deaths and mass migration (Masih et al., 2014).

It is important to analyse droughts at the regional or continental scale since droughts may persist for long periods and affect large areas, unlike many other natural extreme events. Heat waves, forest fires and vegetation stress are potential processes that increase droughts with impacts on a large scale.

Agriculture and food production are the primary sectors affected by drought due to high water demands by farming. The impact of drought on water resources and agriculture is a complex process, it responds to the particular characteristics of a region and its effects can vary from region to region (Renza et al., 2010). Agricultural activity itself, including water flow regulation and irrigation practices, may also lead to reduced water availability and, thus, conditions of agricultural drought. Conservation agriculture increases the capacity of agriculture to adapt to the impacts of drought. Integrated crop, soil and water management measures can be employed to reduce soil degradation and increase the resilience of agricultural production systems. Crop diversification and adoption of drought-tolerant crops, adoption of improved irrigation techniques (i.e. drip irrigation), moisture conservation methods and maintaining vegetation can reduce the negative effects of water shortage. A healthy agricultural system and so a stable food production guarantee food security, while an unstable food production because of drought and others extreme weather events, can have dramatic impacts on society, safety, and stability between countries.

Drought impacts also have severe environmental and socio-economic impacts and depend upon human and ecosystem demands for water, available water-resource management capabilities and practices, and the meteorological and hydrological characteristics of the drought (Loucks and Gladwell, 1999). They are controlled to a large degree by the duration of droughts, rather than their severity, because recovery from the cumulative damage of consecutive drought years is more difficult (Cook et al., 2007).

Many societies do not have the economic resources to overcome single drought or multiple-year droughts, particularly in water- stressed regions where resources are inadequate to meet local needs even during normal years. Especially in the context of climate change, the recurrent nature of droughts requires pro-actively planned policy instruments both to be well-prepared to respond to droughts when they occur, and to undertake ex-ante actions to mitigate their impacts by strengthening the societal resilience to drought (Gerber and Mirzabaev, 2017).

Moreover, urban areas depending on surface water are more vulnerable to drought because the impacts of reduced precipitation are more immediate. Desalination water systems may reduce vulnerability to drought (Wilhite, 2000). The undefined onset of drought events increases the difficulties of planning for, and adapting to, this phenomenon. Droughts are usually recognized only when the water shortage conditions are already established.

Moreover, the undefined end of drought creates more difficulties with taking defensive actions (Pereira et al. 2002).

CHAPTER 3: CLIMATIC CHARACTERISATION OF NORTHERN ITALY

This chapter describes the study area and the main climatic zones that characterise the northern Italy. The climate description of the study area is then provided by mean of the Köppen classification.

3.1. Study region

The study was conducted in the area of the northern Italy (Figure 4). It consists of eight administrative Regions: Aosta Valley, Piedmont, Liguria, Lombardy, Emilia-Romagna, Veneto, Friuli-Venezia Giulia and Trentino-Alto Adige/Südtirol. Northern Italy includes the Po Plain, surrounded by two mountain chains, the Alps at the northern and north-western boundaries and the northern Apennines at the southern boundary. The northern Adriatic Sea constitutes the eastern boundary. It is characterized by the presence of some big urban agglomerations, like Milan and Turin, several medium size urban centres, and vast rural areas, either in plain or in hilly and mountain areas.

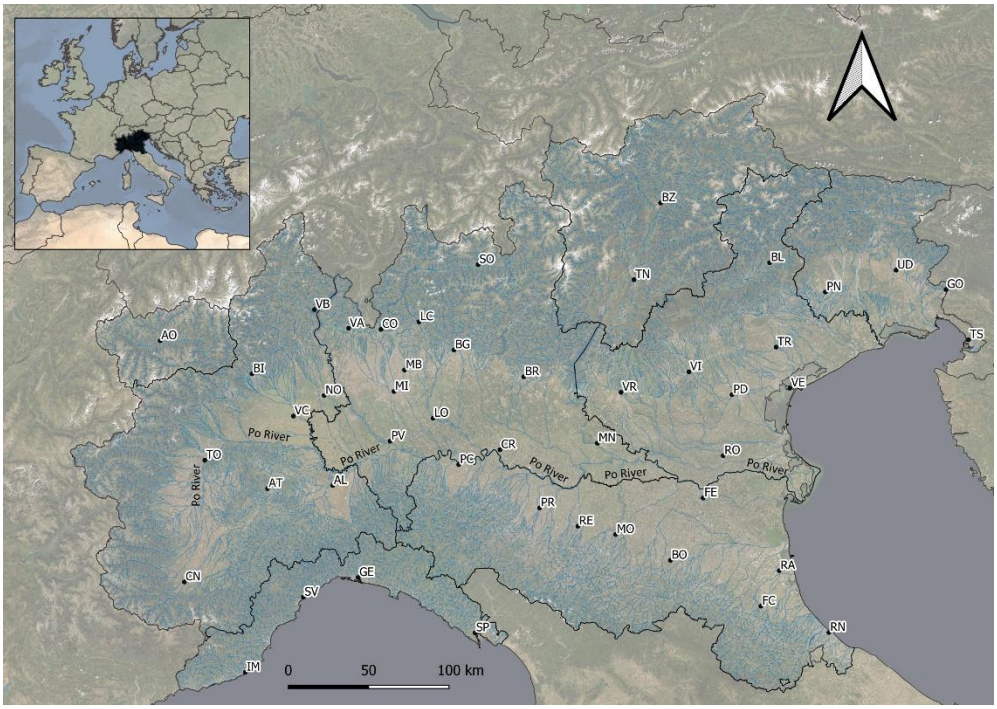

Figure 4: Study area. In figure are highlighted the main northern Italy cities. Aosta (AO) for Aosta Valley region; Alessandria (AL), Asti (AT), Biella (BI), Cuneo (CN), Novara (NO), Torino (TO), Verbania (VB) and Vercelli (VC) for Piedmont region; Genova (GE), Imola (IM), La Spezia (SP) and Savona (SV) for Ligura region; Bergamo (BG), Brescia (BR), Como (CO), Cremona (CR), Lecco (LC), Lodi (LO), Mantova (MN), Milano (MI), Monza Brianza (MB), Pavia (PV), Sondrio (SO) and Varese (VA) for Lombardy region; Belluno (BL), Padova (PD), Rovigo (RO), Treviso (TR), Venezia (VE), Verona (VR) and Vicenza (VI) for Veneto region; Bolzano (BZ) and Trento (TN) for Trentino-Alto Adige/Südtirol region; Gorizia (GO), Pordenone (PN), Trieste (TS) and Udine (UD) for Friuli-Venezia Giulia; Bologna (BO), Ferrara (FE), Forlì Cesena (FC), Modena (MO), Parma (PR), Piacenza (PC), Ravenna (RA), Reggio Emilia (RE) and Rimini (RI) for Emilia Romagna region.

The Po Plain is the most extensive plain in Italy and it covers approximately 46000 km and an average population density of 450 inhabitants/km2.It is crossed by the 652 km long Po river, the largest Italian river. The Po valley is not a valley scoured by the Po rives, but it is a foredeep structure of both the Alps and Apennine filled by mostly marine Pliocene and Quaternary sediments and drained by the Po river. Furthermore, the location of the Po river in the Po Plain is mainly structurally controlled, but also driven by the opposed thrust of the Alpine and Apennine river sediment. The Po river flows

eastward to the Adriatic Sea, where it feeds the Po Delta. The valley is crossed also by a number of affluents running down from the Alps in the north and from the Apennines in the south. The Quaternary uplift of the Apennine front in the western portion of the Plain, has resulted in the two hills of Langhe and Monferrato, located in the Piedmont region (Castaldini et al, 2019). The northern border of the Po Plain, at Alpine foothills, is characterise by several glacial amphitheatres, where they fringe several large lakes. This testify the advance of glacial tongues along the main Alpine valleys, during the Pleistocene period.

The orogenesis of the Alps and northern Apennines influenced the evolution of northern Italy, resulting in a complex topographical structure. With an area of 5200 km², the Italian Alps represents the 27.3% of the European Alps. The mean elevation of the mountain peaks is 2500 m, and the highest peaks is Mont Blanc (4810 m) and the second one is Monte Rosa (4634 m). The Alps mountain system forms an arc extended from the Ligurian coast to the Austria and Slovenia. The width of the mountain chain is decreasing westward, and where the chain bends, around the Piedmont region, a width of approximately 150 km is observed (Bartolini, 2010). The mountain chain is divided in Western Alps and Eastern Alps. The first one tends to be more compressed than the second, due to the collision between the African and the European plate. As consequence, the highest peaks are observed in the western portion, while the Eastern Alps have the greatest diameter, with a width of 300 km (Bartolini 2010). Glaciers are located mainly in the western sector, which from the Little Ice Age to 2000 suffered of a reduction of 50%. This regression has been accelerating in recent years due to the effects of climate warming.
The Apennine due to their young, they rather make a mountain system rather a mountain range, consisting of parallel smaller chains extending approximately 1200 km along the length of Italy. Apennines forms an arc enclosing the Ligurian and Tyrrhenian sea to the west and the Adriatic Sea to the east, thus dividing Italy into a Tyrrhenian and an Adriatic sector. In northern Italy, the Apennine is in contact with the Western Alps at north and with the Central Apennine at south. From a geographical point of view, the northern Apennine consist of two sub-chains: the Ligurian and Tuscan-Emilian. The highest peaks are reached in Monte Cimone with 2165 m asl and Monte Cusna with 2121 m als (Bartolini et al., 2010).

Two main factors induce the thermal-pluviometric characteristics of the area: the orography, the greater internal factor, and the atmospheric circulation with

dry continental air flowing in from Po Valley in the east and relatively moist Mediterranean and Atlantic air coming in with north-western flows. The orographic configuration promotes the formation of foehn airflows. The foehn is a katabatic wind occurring when a deep layer of air is forced to cross mountainous ridges. In fact, the air mass forced to move upslope, due to positive atmospheric pressure difference between the upwind and the downwind sides of the mountain, expands and cools. The cool and dehydrated air mass crosses the crest and starts its downsloping motion, generating an increment of the temperature surface of even 20 °C in short time. In the case of the Alpine foehn, a pressure difference of 4-8 hPa is sufficient to generate a weak foehn episode, while a difference of 14 hPa produce intense and long-lasting foehn events with winds speeds up to 30m/s coming from North, North-West and West especially during February, March and April (Fratianni et al., 2009).

3.2. Altitudinal Zonation

The northern Italy is characterised by three geomorphological areas: mountain, hill and plain. Therefore, northern Italy includes several climatic zones, for example the largest climate zone is the one that includes the Po Plain, in this area the climate is mainly continental. Altitudinal zonation in this region describes the natural layering of ecosystems that occurs at distinct altitudes due to varying environmental conditions. Temperature, humidity, soil composition, and solar radiation are important factors in determining altitudinal zones, which consequently support different vegetation and animal species (Pedrotti, 2018).

Altitudinal zonation was first hypothesized by geographer Alexander von Humboldt who noticed that temperature drops with increasing elevation (Salter et al. 2005). It is possible to split the altitudinal gradient into six main climatic zones used by ecologists under varying names, each with different vegetation. The lowest zone is the planar zone, followed by the colline zone, the montane zone, the sub-Alpine, the Alpine zone and the highest, the glacial zone (figure 5).

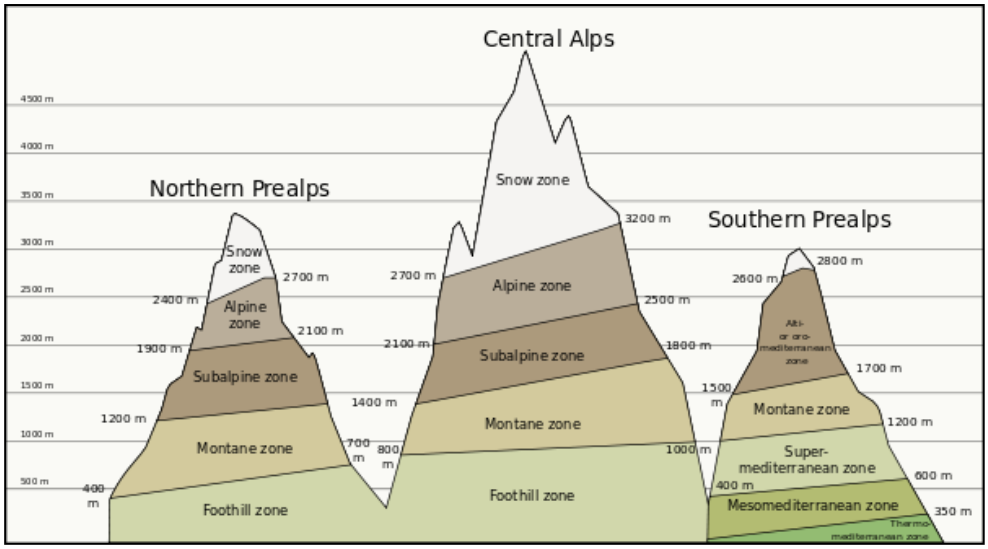

Figure 5 Altitudinal zonation of northern Italy.

The following constitutes the classifications found in the literature related to the altitudinal zones in northern Italy

3.2.1. Planar zone

The Planar zone is the lowest zone it extends from a certain initial share up to 300-700 m asl. This share beginning is imposed by the orography and the morphology of the places.

The climate of the Venetian-Po Plain is temperate continental, with hot summers and often wet and cold winters, similar, in values, to the Colline zone, but much more uniform and less ventilated. Nor suffers sudden changes and has an average rainfall constant. The minimum winter temperatures drop slightly below the 0 °C, but are persistent, as maximum summer ones, that do not exceed 40 °C but with relative humidity often quite high. In the transitional seasons the thermal variations have long times, for the density, and the relative atmospheric thermal inertia.

3.2.2. Colline zone

The Colline zone is roughly extended between 400-600 m asl and 800–1200 m asl (Daubenmire 1943). It corresponds to the first reliefs that do not have a clear mountain or alpine morphology. On these hills, almost never snow, at least up to 1000 m, or otherwise, in the highest parts, covered with little snow intermittently and never stable.

The maximum winter temperatures are mainly slightly below the 0 °C, with variations from +5 °C to -5 °C. The snow rarely appears and remains an episodic phenomenon and short. On the contrary, in the band above the presence of snow coincides with the meteorological winter season and the maximum summer temperature, never above 30 ºC, it can go down to 10 - 18 °C. The daily summer temperature swings so between 28 °C and 15 °C at 800 m asl, and between the 32 °C and the 22 °C, at 600 m asl.

3.2.3. Sub-Alpine and Montane zone

The Montane level (Nagy and Grabherr 2009; Daubenmire 1943) Extends from the mid-altitude forests to the tree line (roughly between 800–1200 m asl and 2000–2400 m asl). The exact level of the tree line varies with local climate, but typically the tree line is found where mean monthly soil temperatures never exceed 10 °C and the mean annual soil temperatures are around 6.7 °C. In the tropics, this region is typified by montane rain forest while at higher latitudes coniferous forests often dominate.

This level is divided in two zones: Sub-Alpine zone and Montane zone.

- **Sub-Alpine zone** (1600-2400). The most characteristic feature of this region is the prevalence of coniferous trees that form vast forests that cover a large part of the surface. These play a most important part in the natural economy of the country. They retain the soil by their roots, protect the valleys from destructive avalanches and mitigate the destructive effects of heavy rains.
- **Montane zone** (800-1700). It corresponds to the first reliefs which present a clearly mountainous and alpine morphology. Its slopes are covered in rich arboreal vegetation, originally continuous and dense forests. The winter season is the meteorological one (December to March) with maximum temperatures that were only slightly above the 0 °C, but which can rise up to + 10 °C, or down to -10 °C. During

transition months, the sudden changes in temperature are blunted by the air thermal inertia. The difference between night and day is usually contained (except places particularly exposed to the sun or cold drafts) within 10-15 °C and that between sunniest parts and parts in shadow does not exceed 5-7 °C. The summer maximum value, consistently higher than 0 °C, can go down to 5-8 °C for the coverage of the sky or for fresh winds, while the summer daily temperature fluctuates between 27 °C and 10 °C at 1000 m asl, and among the 20 °C and 5 °C at 1800 m. The slopes of the mountain zone, moreover, can be affected by hot downdraft or updraft winds from the plains below

3.2.4. Alpine zone

The Alpine climate (or Alpine level; Nagy and Grabherr 2009) is typical of the Alps, between the tree line, up to the permanent snow line, roughly between 1800-2200 m asl and 2500-3000 m asl.

The winter season is shorter and runs from October to April, with maximum temperatures slightly below 0 °C, but can drop down to -25 °C. Even the summer period (May to September) presents significant variations in temperature, especially in the transitional months (March, April and October). The temperature difference between night and day reaches 15 - 20 °C, and the difference between parts exposed to the sun and in the shade 5 - 10 °C. The summer maximum value, always higher than 0 °C, can drop of 5-10 °C with covered sky, while the daily summer temperature ranges between +20 and 0 °C to 2000 m asl, and between +15 and -5 °C 2500 m asl.

3.2.5. Glacial zone

The Glacial zone, known also as Nival level (Stahr and Langenscheidt 2015; Hanks 2011) or Snow zone. Located above the snow line, is covered in snow throughout most of the year.
Usually in the higher parts of Alps more snow falls in each year than melts. A large portion of snow accumulates in hollows and depressions of the surface and is gradually converted into glacier ice which descends by slowly flowing into the deeper valleys where it helps swell perennial streams.

The climatic snow line is the point above which snow and ice cover the ground throughout the year. The actual snow line may seasonally be significantly lower. The interplay of altitude and latitude affects the precise placement of the snow line at a particular location, just below 3,000 meters in the Alps. In addition, the relative location to the nearest coastline can influence the altitude of the snow line. Areas near a coast might have a lower snow line than areas of the same altitude and latitude situated in a landmass interior.
The climate of the glacial region is characterized by intense solar radiation by day, which raises the surface when dry to a temperature approaching 27°C, alternates with severe frost by night. Also, the upper region of the Alps sustains a varied and brilliant vegetation.

3.3. Köppen Climate Classification

The system is based on the concept that native vegetation is the best expression of climate. Thus, climate zone boundaries have been selected with vegetation distribution in mind. It combines average annual and monthly temperatures and precipitation, and the seasonality of precipitation (Pinna 1978). The Köppen climate classification scheme divides climates into five main groups (A, B, C, D, E), each having several types and subtypes. Each particular climate type is represented by a two- to four-letter symbol. The second letter indicates the precipitation pattern, while the third letter indicates the degree of summer heat.

The northern Italy falls completely within the Mediterranean area (Figure 4), in reality, besides the typical Mediterranean climate, it is characterized by other meso-thermal climates, or areas with situations of micro-thermal or altitude climates (Fratianni and Acquaotta, 2017). The climatic classification in northern Italy is outlined below.

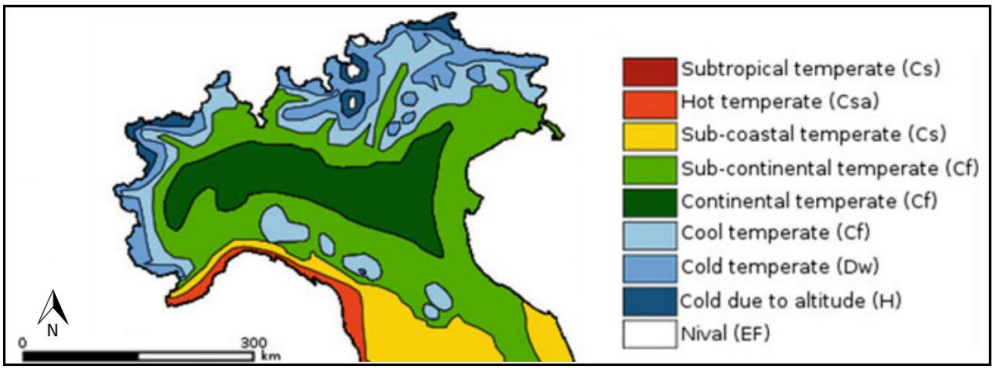

Figure 6 Map of climatic classification by Köppen and Geige (Modified by Fratianni and Acquaotta 2017).

Group C

These climates have an average monthly temperature above 10°C in their warmest months (April to September in northern hemisphere), and temperature of coldest month less than 18°C but greater than –3°C.

- **Hot temperate (Csa)** - This climate is usually characterized by summer droughts (Csa). Mean annual temperature ranges from 14.5°C to 16.9°C and the mean temperature of the coldest month is from 6°C to 9.9°C. In this area four months with a mean temperature >20°C are observed. In the northern Italy this climate is typical of the coastal area of the Ligurian Region (Figure 6).
- **Sub-coastal temperate (Cs)** – This climate is typical of the lower slopes of the Apennines, and it characterise the inland of the Ligurian region. Mean annual temperature ranges from 10°C to 14.4°C; mean temperature of the coldest month is from 4°C to 5.9°C. The sectors characterised by this climate, record three months with mean temperature >20°C (Figure 6).
    - **Continental temperate (Cf)** – This climate interest all the Po Plain and part of the Venetian Plain. The mean annual temperature ranges from 9.5°C to 25°C and the mean temperature of the coldest month is from −1.5°C to 3°C. Three months with a mean temperature >20°C are typical of this climate. Two sub-types can be identified:**Hot summer temperate climate Cfa -** A relatively "continental" and "four-

season" version of the humid subtropical Cfa climate can be found in the Po and Adige's valleys. It's marked by hot and wet summers, while winters are moderately cold. The precipitation is higher and there is no dry season. Average temperatures are around 1°C to 3°C in the winter and more than 22°C in the summer (Figure 6)

    - **Temperate Oceanic climate Cfb -** It can be found in the alpine foothills. Summers are between 17°C and 21°C. The presence of several lakes in this area has a mitigating influence, allowing the cultivation of Mediterranean crops (wine, olives, citrus fruits, Figure 6).
- **Cool temperate climate (Cf)** – This climate is typical of the Pre-Alpine area, which sometimes presents sub-continental characteristics. The mean annual temperature is between 6°C and 9.9°C. The mean temperature of the coldest month ranges from 0°C to −3°C and the mean temperature of the hottest month is from 15°C to 19.9°C (Figure 6).

Group D

These climates have an average temperature above or equal to 10°C in their warmest months, and a coldest month average below −3°C (or 0°C in some versions, as noted previously). These usually occur in the interiors of continents and on their upper east coasts, normally north of 40°N.

In the northern Italy a **cold temperate climate (Dw)** can be identified, and it affects the area of the Alps. The mean annual temperature ranges from 3°C to 5.9°C. The mean temperature of the coldest month is above−3°C, while the mean temperature of the hottest month is from 10°C to 14.9°C (Figure 6).

Group E and H

In the Köppen climate classification, the alpine climate is part of "Group E", and "Group H". These climates are characterized by an average temperature of the warmest month less than 10°C (Fratianni and Acquaotta, 2017).

- **Cold due to altitude (H) –** This climate affects the highest sectors of the Alps (Figure 6).
- **Nival EF -** which affects the Alpine zone above 3500 m, with the presence of perennial snow. All the months with average below 0°C (Figure6).

3.4. Precipitation distribution

The spatial distribution of precipitation in northern Italy is strongly influenced by latitude, longitude and aspect. In fact, the mountainous zones in northern Italy receive a greater quantity of water than the plains and the coasts, especially when they are exposed to moist currents from the sea (Figure 7).

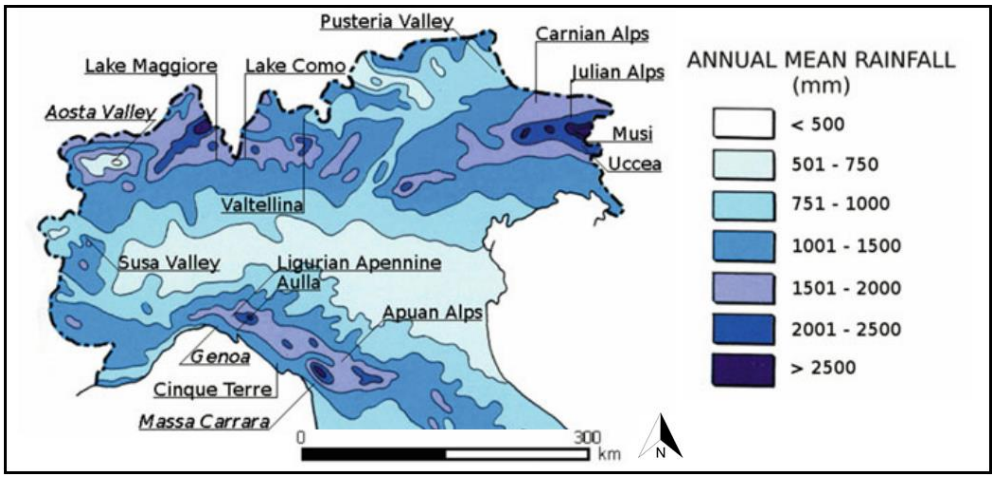

Figure 7: Annual mean precipitation from 1961 to 1990 in northern Italy (Modified by Acquaotta and Fratianni 2017).

The rainiest areas in the North of Italy are three (Figure 7). The first one is located in the eastern part with and annual precipitation between 1500 mm and 2500 mm, peaks of annual precipitation are observed in proximity of the Carnian and Julian Alps with an annual average between 2500 and 3000 mm. This area is mostly influenced by Scirocco and Libeccio winds, which are two moist and rainy flows coming from respectively south-east and south-west (Acquaotta and Fratianni, 2017). The second rainiest area is the norther part of the Occidental Alps with annual precipitation between 1700 mm and 1950 mm, with peaks greater than 2000m in proximity of the Maggiore Lake. In

this area the highest rates of snow fall are recorded (Terzago et al., 2013). The third rainiest sector is the eastern Ligurian Apennines, in proximity of the Tuscan-Emilian Apennines, with an annual average precipitation of 2300 mm (Acquaotta et al., 2018; Sacchini et al., 2012). The high amounts of precipitation observed in this area are due to mesoscale convective systems generated on the sea, because of the convergence of a cold and dry flow coming from the north and a warm and wet south-eastern flow (Acquaotta et al; 2019). The interaction of these currents with the orography forced them to persist in that area for a long period (Fiori et al., 2017; Parodi et al., 2017).

Less abundant rainfall amounts are reached in the Po Plain (Figure 7) with an east-west decrease, as it does from the high altitudes to the low plain. In this area an annual average precipitation between 500-1000 mm is recorded. In the Valtellina and Pusteria Valley, at the eastern edge of the domain, and Susa and Aosta Valley, at the western edge of the domain, annual precipitation amounts below 500 mm are common. In fact, these areas are surrounded by high mountain peaks that affect the local circulation (Fazzini et al., 2004; Uboldi and Lussana 2018).

The pluviometric regime presents a remarkable variability in northern Italy, and Pinna and Vittorini 1985 distinguished three main types (Figure 8):

- **Continental regime.** It is characterized by an accentuated precipitation maximum in summer and an accentuated minimum in winter. It is typical of the Alpine area in Lombardy and Trentino Alto Adige.
- **Pre-Alpine regime.** This regime is the most common in northern Italy. It is characterised by a main precipitation maximum in spring and a second maximum in autumn, and two minimum periods in summer and winter. In some zones, at the foothill, the main precipitation maximum is in autumn (**Sub-Alpine regime**).
- **Sub-Littoral regime.** This regime presents a main maximum rainfall period at the end of autumn and a minimum period in summer; a main minimum occurs at the end of winter. This regime is more common in the southern part of the North Italy, in proximity of the Ligurian region.

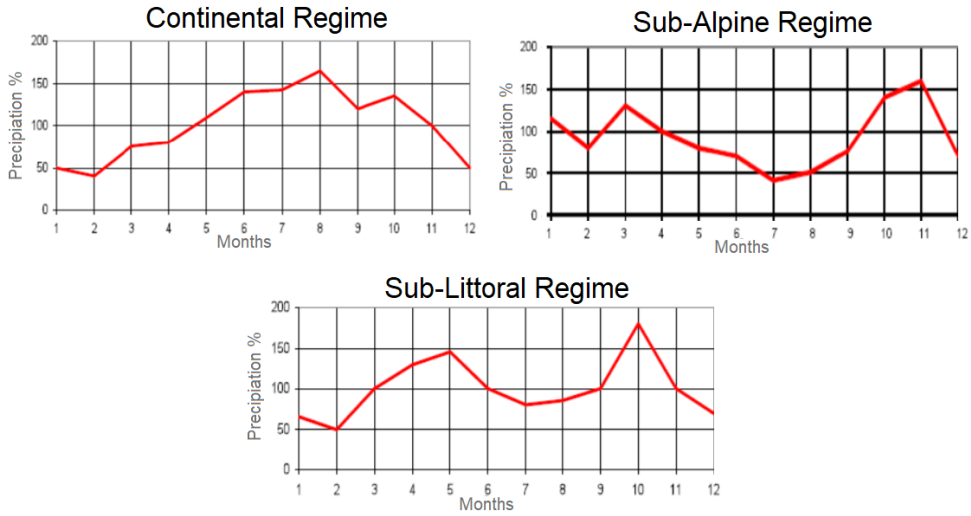

Figure 8: Three main pluviometric regimes in northern Italy (modified by Pinna and Vittorini, 1985)

CHAPTER 4: DATASET

In this chapter are described the data and techniques applied in this study to produce a high-quality database.

4.1. Datasets

The meteorological data used in this research belongs form two different datasets in northern Italy. The first one consists of historical precipitation and temperature series from weather ground stations. The second one is made up of temperature and precipitation ensembles from GCMs/RCMs models couples simulated over Europe.

4.1.1. Historical series

The North of Italy database is made up by 88 daily maximum and minimum temperature and precipitation historical series from January 1, 1965 to December 31, 2017, collected from the National System for the Collection, Processing, and Dissemination of Climatic Data of Environmental Interest (SCIA, Figure 9 and Table 1). SCIA is a national system of climatological data collection, elaboration and release, developed since 2006 by the Italian National Institute for Environmental Protection and Research (ISPRA) with the collaboration of the Regional Environmental Protection Agencies (ARPA) and other public and private authorities located over the whole National territory. The need for such system derives from the fact that meteorological data are sparse among several national and regional organizations and that climate indicators need to be calculated using quality checked data and homogenous statistical procedures. The main goal of this system is to harmonise and standardise the several methodologies available and to provide, climatic data, indices useful to study variation and tendencies of the main climatic variables in Italy. Because the collected data belongs to different meteorological networks the available data are integrated with metadata to highlight inhomogeneities in the series, such as changes in instrumentation and station relocation. (Desiato et al, 2007).

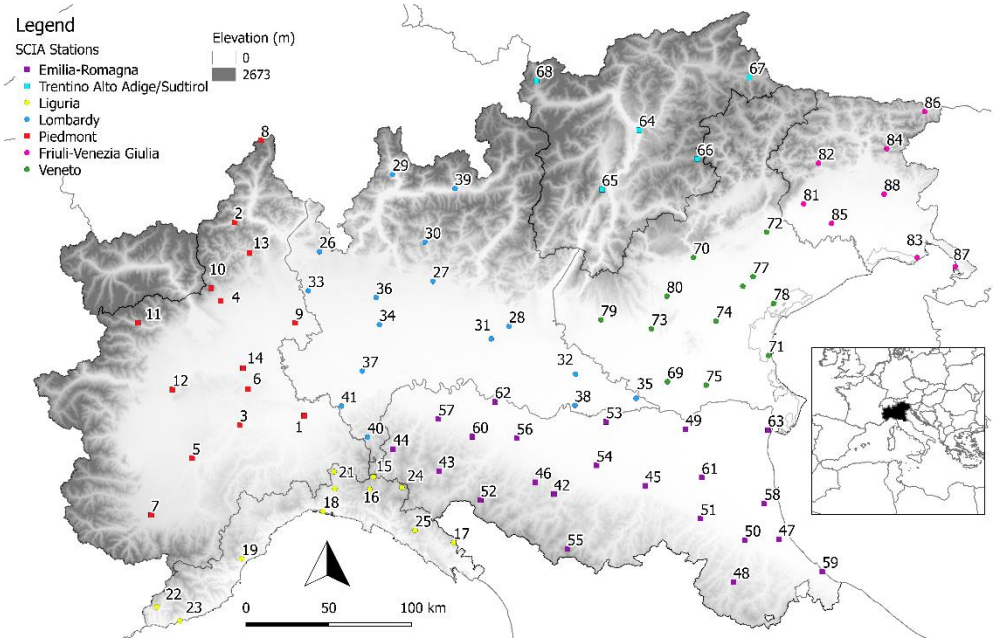

Figure 9: Map of Italy and location of the meteorological stations in the northern Italy.

Table 1: List of the 88 selected stations in Northern Italy, organised per regions. For each station, the corresponding number, the name, the elevation and the coordinate expressed in WGS84 Zone 32N were reported.

	N.	Name	Elev. (m als)	UTMX	UTMY
PIEDMONT	1	Alessandria	90	476644	4976003
	2	Anzino	669	434627	5092919
	3	Asti	175	437790	4970464
	4	Biella	405	426362	5045454
	5	Bra	285	409014	4950399
	6	Casale	136	442781	4992128
	7	Cuneo	550	384289	4915998
	8	Lago Toggia	2165	450696	5142404
	9	Novara	162	471305	5032039
	10	Oropa	1186	420585	5053083
	11	Rosone	701	376293	5032323
	12	Torino	239	397030	4991748
	13	Varallo	470	443587	5074258
	14	Vercelli	131	439689	5004655
	15	Alpe Gorreto	915	518690	4938955
LIGURIA	16	Brugneto	775	516281	4931466
	17	Calice	70	566975	4899307
	18	Genova	30	488058	4918201
	19	Loano	5	438945	4889495
	20	Mignanego	270	495214	4931830
	21	Passo dei Giovi	475	494686	4942185
	22	Rocchetta	215	387688	4860449
	23	Sanremo	61	401589	4852035
	24	S Stefano D'Aveto	1322	535750	4932607
	25	Tavarone	603	543751	4906755
LOMBARDY	26	Azzate	332	486020	5075175
	27	Bergamo	249	554527	5057288
	28	Brescia	149	600384	5030076
	29	Chiavenna	333	530062	5121899
	30	Cornalita	393	549664	5080914
	31	Manerbio	64	589736	5022470
	32	Mantova	19	640711	5001172
	33	Milano	122	479183	5051530
	34	Milano Linate	119	522136	5031092
	35	Moglia	20	677304	4986524
	36	Monza	162	520284	5047417
	37	Pavia	77	511785	5002957
	38	Poggio	20	640340	4982270
	39	Sondrio	307	567931	5113312
	40	Varzi	485	515022	4962973
	41	Voghera	96	499212	4981840

	N.	Name	Elev. (m als)	UTMX	UTMY
EMILIA-ROMAGNA	42	Baiso	542	627652	4928560
	43	Bardi	597	558125	4942531
	44	Bobbio	270	530403	4955794
	45	Bologna	78	682743	4933648
	46	Canossa	519	616398	4935772
	47	Cervia	6	763613	4901272
	48	Civitella	460	736167	4875368
	49	Ferrara	33	707187	4967686
	50	Forli	42	742974	4900851
	51	Imola	53	716242	4913811
	52	Marra	618	583309	4924991
	53	Mirandola	18	659231	4972277
	54	Modena	73	653432	4945970
	55	Monte Cimone	2165	635838	4895492
	56	Parma	53	605213	4962483
	57	Piacenza	72	557855	4973992
	58	Ravenna	16	754768	4922949
	59	Rimini	8	789836	4881901
	60	Salsomaggiore	17	578371	4963323
	61	Santonio	8	716990	4938663
	62	Volano	3	592034	4984385
	63	Zibello	31	757012	4967304
TRENTINO-ALTO ADIGE/ SUDTIROL	64	Bolzano	262	679121	5148581
	65	Paganella	1850	656761	5112717
	66	Passo Rolle	2006	714323	5131145
	67	Dobbiaco	2906	745782	5180521
	68	S. Valentino	1499	617089	5178524
VENETO	69	Badia Polesine	12	696274	4996540
	70	Bassano del Grappa	129	712072	5071729
	71	Chioggia	11	757351	5012459
	72	Conegliano	85	756193	5086912
	73	Lonigo	31	686632	5028570
	74	Padova	12	725596	5033283
	75	Rovigo	9	719645	4994494
	76	Treviso	46	741762	5054281
	77	Treviso A	23	748014	5060090
	78	Venezia	1	760394	5043902
	79	Verona	69	656060	5033990
	80	Vicenza	39	695889	5048227
FRIULI-VENEZIA GIULIA	81	Aviano	150	778584	5104017
	82	Chevolis	475	787510	5128590
	83	Fossalon	0	847140	5071508
	84	Musi	612	828771	5137358
	85	S Vito	21	795435	5092221
	86	Tarvisio	794	851643	5159815
	87	Trieste	6	870107	5066144
	88	Udine	91	827201	5109970

4.1.2. Future projection models

The future drought investigation is performed analysing GCMs-RCMs couples belonging to the Euro-CORDEX and Med-CORDEX sub-projects at 12km^2 resolution. Because RCMs simulations, in particular for those sectors that are characterised by a complex topography, exhibit uncertainties that arise

from the nature of model design. It is recommended to analyse an ensemble of simulations (Teutschbein and Seibert, 2012).

In the following study RCMs of the two sub-projects Euro-CORDEX (https://www.euro-cordex.net/) and Med-CORDEX (https://www.medcordex.eu/) were collected and processed. 12 daily maximum and minimum temperature and 12 daily precipitation ensembles from the RCMs: RACMO22E, HIRHAM5, CCLM4 and ALADIN52, combined with the GMCs: EC-EARTH, MPI-ESM, HadGEM2 and CM5 at a spatial resolution of 0.11 degree (12 km, Table 2). To compare future drought events according to the possible mitigation strategies two representative concentration pathways were investigated: RCP 4.5 (stabilization strategies of greenhouse gasses) and RCP 8.5 (very high greenhouse gas emissions). The selected ensembles were then cropped on the Northern Italy area with the following vertices, expressed in WGS84 coordinates: 47.667 North, 43.242 South, 14.566 East and 6.032West.

Table 2: GCM-RCM model couples selected from the Euro-CORDEX and Med-CORDEX sub-projects. The models that provided the less reliable results for northern Italy during the validation phase are shaded in grey.

N°	***RCP4.5***	***N°***	***RCP8.5***
1	EC-EARTH-RACMO22	**7**	EC-EARTH-RACMO22
2	EC-EARTH-HIRHAM5	**8**	EC-EARTH-HIRHAM5
3	MPI-ESM-CCLM4	**9**	MPI-ESM-CCLM4
4	HadGEM2-CCLM4	**10**	HadGEM2-CCLM4
5	HadGEM2-RACMO22	**11**	HadGEM2-RACMO22
6	CM5-ALADIN52	**12**	CM5-ALADIN52

4.2. Quality control of the historical series

Quality control (QC) of surface data refers to the application of methods that determine whether data meet overall quality goals and defined quality criteria for individual values. In order to determine if whether data are good it is necessary to set of quality goals and specific criteria against which data are evaluated (WMO, 2018). In the following it is discussed the quality and homogeneity checks performed to find erroneous data or discontinuities due to non-climatic factors and the gap-filling technique used to estimate the missing data in the ground series.

To analyse the main drought episode, 53 years of a common period of study from January 1, 1965 to December 31, 2017 were identified and quality

control performed. A preliminary analysis was conducted on the whole dataset, and in this regard, only climatic series with less than 20% of gaps, calculated over the whole period, and no more than six consecutive days without records were analysed.

4.2.1. Errors and outliers check

The first step of quality control consists in the detection of digitizing errors, in fact maximum temperature lower or equal than minimum temperature and negative precipitation were detected and flagged. Next, temperature and precipitation outliers were identified and flagged. Precipitation outliers, as a weekly accumulation transcribed into the value of 1 day, were analysed, and the most recurrent errors detected. Temperature outliers were observed by means of the standard deviation thresholds, and all of the daily temperature data greater or lesser than the ± fourth standard deviation were considered as potential outliers. Subsequently, a visual quality control was performed, and the daily precipitation and temperature data were plotted, permitting outliers and the variance of data to be identified, according to Aguilar et al. (2005). Finally, the detected outliers were compared with values recorded in the surrounding stations for final outlier identification.

4.2.2. Data aggregation

Daly data were then aggregated over weekly scale. In this regard a week with at most 1 day of missing value was deemed not available for precipitation, whereas for temperature weeks with at least 80% of daily data were analysed. To facilitate the inter-annual comparison of the climatic series, and avoid the problem of leap years, each month was divided into 4 weeks: first week from the first to the eighth day; second week from the 9th to the 15th day; third week from the 16th to the 22nd day; and fourth week from the 23rd until the end of the month.

4.2.3. Series reconstruction

The 88 precipitation and temperature weekly series are continuous except for few cases when isolated weekly values are missing. In this case the fragmented weekly series (candidate) were reconstructed by means of a gap-filling process based on weighted averages of measurements made at nearby stations

(reference). The selection of nearby stations was based on three parameters, that is, the overlapping period, the difference in elevation and the distance. Reference series need to have more than 5 year of overlapping period with the candidate. According with Acquaotta et al. (2015) on the precipitation gradient, the difference in elevation between reference and candidate series must be less than 200 m. The distance between the two series must be less than 40 km (Acquaotta et al., 2019b). Once the nearby reference series were selected, the first step of correlation was checked evaluating that the Pearson's correlation test, between the candidate and the selected reference series was grater that 0.8. Subsequently the correlation analysis between the candidate series with the remaining reference series was computed by mean of the statistical analysis developed in the Co.Rain script (Guenzi et al., 2017) for precipitation, and Co.Temp script (Guenzi et al., 2019) for temperature.

Co.Temp and Co.Rain are free open source software published on the Github platform (https://github.com/UniToDSTGruppoClima). Both the software aims to detect, by mean of a set of well-known statistical tools, dissimilarities between the reference and candidate series, with the classification of events in several classes. Co.Temp classify events in extremely cold, cold, mean, warm and extremely warm. While Co.Rain classify precipitation events in weak, mean, heavy and extreme. This procedure has allowed to show the percentage of precipitation and temperature events that can be considered equal between the pairs of reference and candidate series. At the same time, the classes with the greater difference between the two investigated series were highlighted. All the stations matching this methodological scheme were considered reference series for the process of gap filling.

In order to avoid biases in the filling due to differences in the distribution parameters (mean and variance) between the candidate and the objective data series, Vicente-Serrano et al., (2017) has develop a bias correction procedure on the reference data before computing the weighted average. Therefore, the normal distribution mapping was applied for bias correction and the gamma distribution was used for both precipitation and temperature series. The data of the reference series were re-scaled to match the statistical distribution of the series to be filled, based on the overlapping period between them. Once the weighted average was computed, a posterior bias correction was again performed using the same procedure in order to correct for bias in the variance of the filling data caused by the averaging of many reference series.

Table 3: Percentage of missing values in the weekly temperature and precipitations series before and after the reconstruction. %NAPrec, %NATx and %NATn are the percentage of missing values in the raw precipitation, maximum and minimum series. %NAPrecR, %NATxR and %NATnR are the percentage of missing values in the precipitation, maximum and minimum series after the reconstruction

	Station	%NA Prec	%NA Tx	%NA Tn	%NA PrecR	%NA TxR	%NA TnR
PIEDMONT	Alessandria	8.87	4.75	4.75	0.00	0.00	0.00
	Anzino	4.01	0.08	0.08	0.08	0.00	0.00
	Asti	4.59	3.70	3.70	0.00	0.00	0.00
	Biella	5.50	9.34	9.34	0.00	0.00	0.00
	Bra	2.93	5.89	5.89	0.00	0.00	0.00
	Casale	0.12	8.90	8.94	0.00	0.00	0.00
	Cuneo	8.72	8.51	8.51	0.00	0.00	0.00
	Lago Toggia	8.31	0.50	0.46	0.31	0.00	0.00
	Novara	5.80	0.12	0.12	0.12	0.00	0.00
	Oropa	0.27	3.70	3.70	0.00	0.00	0.00
	Rosone	3.99	3.32	3.32	0.19	0.00	0.00
	Torino	1.16	0.04	0.04	0.00	0.00	0.00
	Varallo	1.47	1.62	1.58	0.00	0.00	0.00
	Vercelli	0.12	0.19	0.19	0.00	0.00	0.00
LOMBARDY	Azzate	4.32	3.64	3.96	0.04	0.00	0.00
	Bergamo	4.69	3.73	3.77	0.23	0.00	0.00
	Brescia	6.48	0.23	0.23	0.08	0.00	0.00
	Chiavenna	5.93	2.02	1.78	0.08	0.00	0.00
	Cornalita	10.42	3.39	2.95	0.08	0.00	0.00
	Manerbio	8.26	9.77	9.77	0.00	0.00	0.00
	Mantova	9.41	7.79	7.79	0.08	0.00	0.00
	Milano	4.89	4.90	4.90	0.89	0.00	0.00
	Milano Linate	9.54	3.24	3.24	0.04	0.00	0.00
	Moglia	7.72	6.28	6.20	0.00	0.00	0.00
	Monza	2.98	0.27	0.66	0.31	0.00	0.00
	Pavia	2.70	19.68	18.67	0.00	0.00	0.00
	Poggio	9.90	8.26	8.99	0.08	0.00	0.00
	Sondrio	10.03	3.12	3.86	0.08	0.00	0.00
	Varzi	9.38	9.65	9.65	0.12	0.00	0.00
	Voghera	4.17	5.86	5.86	0.08	0.00	0.00
TRENTINO-ALTO ADIGE/ SUDTIROL	Bolzano	7.82	2.67	2.67	0.62	0.00	0.00
	Dobbiaco	3.59	0.00	0.00	0.69	0.00	0.00
	Paganella	1.30	1.93	1.93	1.30	1.93	1.93
	S Valentino	8.33	4.86	4.86	8.33	4.86	4.86
	Passo Rolle	7.68	0.42	0.42	0.12	0.00	0.00
FRIULI-VENEZIA GIULIA	Aviano	8.53	0.08	0.08	0.50	0.00	0.00
	Chevolis	4.28	2.43	3.33	0.04	0.00	0.00
	Fossalon	0.58	0.00	0.00	0.00	0.00	0.00
	Musi	8.76	4.98	4.98	0.00	0.00	0.00
	S Vito	9.26	5.35	5.63	0.08	0.00	0.00
	Tarvisio	9.65	1.85	1.85	0.08	0.00	0.00
	Trieste	9.08	1.54	2.12	9.26	0.00	0.00
	Udine	9.52	7.99	7.99	0.31	0.00	0.00

	Station	%NA Prec	%NA Tx	%NA Tn	%NA PrecR	%NA TxR	%NA TnR
LIGURIA	Alpe Gorreto	0.00	0.00	0.00	0.00	0.00	0.00
	Brugneto	4.59	4.17	4.09	0.12	0.00	0.00
	Calice	8.48	9.95	9.95	0.08	0.00	0.00
	Genova Sestri	9.81	3.24	3.24	0.00	0.00	0.00
	Loano	6.91	1.49	1.49	0.00	0.00	0.00
	Mignanego	7.05	7.52	7.52	0.00	0.00	0.00
	Passo dei Giovi	10.97	5.78	5.78	10.97	0.00	0.00
	Rocchetta	9.30	9.77	9.77	0.08	0.00	0.00
	Sanremo	6.98	6.71	6.71	0.08	0.00	0.00
	S Stefano D'Aveto	0.08	0.00	0.00	0.00	0.00	0.00
	Tavarone	9.56	9.22	9.22	0.08	0.00	0.00
EMILIA-ROMAGNA	Baiso	0.00	0.00	0.00	0.00	0.00	0.00
	Bardi	0.08	0.00	0.00	0.00	0.00	0.00
	Bobbio	0.08	0.00	0.00	0.00	0.00	0.00
	Bologna	0.15	1.77	1.77	0.00	0.00	0.00
	Canossa	0.08	0.00	0.00	0.00	0.00	0.00
	Cervia	1.50	1.54	1.54	0.00	0.00	0.00
	Civitella	0.89	0.00	0.00	0.04	0.00	0.00
	Ferrara	0.08	1.54	1.54	0.00	0.00	0.00
	Forli	0.58	0.00	0.00	0.00	0.00	0.00
	Imola	0.00	0.00	0.00	0.00	0.00	0.00
	Marra	0.00	0.00	0.00	0.00	0.00	0.00
	Mirandola	0.35	0.00	0.00	0.00	0.00	0.00
	Modena	0.00	0.00	0.00	0.00	0.00	0.00
	Monte Cimone	1.50	0.00	0.00	0.00	0.00	0.00
	Parma	0.54	0.00	0.00	0.00	0.00	0.00
	Piacenza	0.46	1.54	1.54	0.00	0.00	0.00
	Ravenna	0.15	0.00	0.00	0.00	0.00	0.00
	Rimini	0.12	1.77	1.77	0.00	0.00	0.00
	Salsomaggiore	0.00	0.00	0.00	0.00	0.00	0.00
	Santonio	0.66	0.62	0.62	0.04	0.00	0.00
	Volano	0.00	0.73	0.73	0.00	0.00	0.00
	Zibello	1.20	0.00	0.00	0.00	0.00	0.00
VENETO	Badia Polesine	6.06	6.21	6.21	0.35	0.00	0.00
	Bassano del Grappa	2.35	1.93	1.93	1.47	0.00	0.00
	Chioggia	5.81	7.56	5.71	0.42	0.00	0.00
	Conegliano	5.23	2.28	2.28	0.31	0.00	0.00
	Lonigo	5.58	2.04	2.04	0.69	0.00	0.00
	Padova	5.58	1.85	1.85	0.85	0.00	0.00
	Rovigo	5.66	2.58	2.58	0.31	0.00	0.00
	Treviso	2.43	0.19	0.19	0.04	0.00	0.00
	Treviso A	3.24	1.16	1.16	0.04	0.00	0.00
	Venezia	9.54	3.24	3.24	9.54	0.00	0.00
	Verona	2.47	0.00	0.00	0.04	0.00	0.00
	Vicenza	4.63	0.19	1.93	0.08	0.00	0.00

The procedure of gap filling has highlighted that, before the reconstruction the weekly precipitation and temperature series had no more than 10% of gaps. Table 3 shows that precipitation series are more discontinuous, and in the regions of Lombardy and Friuli-Venezia Giulia the highest percentage of

missing values was observed. While for the Emilia-Romagna region the lowest percentage of gaps was detected with no more than 1.54% for both precipitation and temperature series. In general, for the whole database the gaps are concentrated in the first 5-6 years of records (1965-1970). In fact, since the '60 the Italian Hydrographic Mareographic Service (SIMN), that was the main meteorological network in Italy, experienced a progressive reduction in the number of active instrumentation and stations, this probably due to a reduction at the Hydrographic Office of employers, instrumentation and economic resources. This decrease has continued until the passage of the meteorological networks to the Regional Agencies (ARPA).

Table 3 has figured out that after the gap filling procedure the greatest part of the temperature series did not presented gaps. While for the precipitation series, the percentage of missing values was considerably decreased, and no more than 1.30% of gaps is observed for the new reconstructed series. Table 3 figured out also that for the station of Paganella (1850 m als) and S. Valentino (1499 m asl) in Trentino Alto Adige/Südtirol region, weekly temperature and precipitation series were not reconstructed, in fact, no neighbouring stations were detected (distance with the other stations > 40 km, Table 4).

For Passo dei Giovi (475 m als) in Liguria region, Trieste (20 m asl) and Venezia (1 m asl) in Veneto region, weekly precipitation series were not reconstructed (Table 3). In detail table 4 has figured out:

- For Passo dei Giovi eight neighbouring stations were observed but only Bobbio (270 m asl) and Mignanego (270 m als) stations have an elevation difference with Passo dei Giovi below 200 m. At the same time, weekly precipitation series were not reconstructed because, the Pearson's correlation coefficients calculated between the candidate and the two references series were below 0.8. On the contrary the Pearson's correlation test applied on the temperature series has showed values above 0.8, and maximum and minimum temperature series were gap filled.
- For Trieste only one neighbour station was detected (Fossolan 0 m als) with an elevation difference below 200m. The weekly precipitation series was not reconstructed because, the Pearson's correlation coefficient between the candidate and the reference series was 0.66 (<0.8). While maximum and minimum temperature series were gap filled.
- For Venezia four neighbouring stations with an elevation difference below 200 m were identified. For the precipitation series, a Pearson's

correlation coefficient between candidate and reference series below 0.8 was observed, and the reconstruction was not performed. On the contrary for maximum and minimum temperature the Pearson's coefficients were between 0.96 and 0.99 and the series were reconstructed.

Table 4: Selection of the reference series for the station of Paganella (1850 m als) and S. Valentino (1499 m asl) in Trentino Alto Adige/Sudtirol region, Passo dei Giovi (475 m als) in Liguria region, Trieste (1 m asl) and Venezia (6 m asl) in Veneto region. Where Elev. is the elevation (m als), Pearson Prec is the Perasons' coefficient for precipitation, Pearson Tx is the Perasons' coefficent for maximum temperature and Pearson Tn is the Perasons' coefficent for minimum temperature. In grey are the suspicious values.

CANDIDATE SERIES		REFERENCE SERIES				
Station	**Elev (m asl)**	**Station**	**Elev (m asl)**	**Pearson Prec**	**Pearson Tx**	**Pearson Tn**
Paganella	1850	**NA**	NA	NA	NA	NA
S. Valentino	1499	**NA**	NA	NA	NA	NA
Passo dei Giovi	475	**Alessandria**	90	-0.046	0.96	0.96
		Voghera	96	-0.072	0.97	0.97
		Varzi	485	-0.202	0.97	0.96
		Bobbio	270	-0.079	0.97	0.96
		Alpe Gorreto	915	-0.044	0.95	0.96
		Brugneto	775	-0.107	0.98	0.97
		Mignaego	270	-0.050	0.96	0.96
		Genova	30	-0.102	0.98	0.97
Trieste	1	**Fossolan**	0	0.66	0.98	0.97
Venezia	6	**Chioggia**	11	0.61	0.99	0.96
		Padova	12	0.59	0.99	0.99
		Treviso	46	0.69	0.99	0.99
		Treviso A	23	0.69	0.99	0.99

4.2.4. Homogenisation

To perform an accurate analysis of the main drought event in the norther Italy, the reconstructed weekly precipitation and temperature historical series should be as homogeneous as possible. A time series can be only defined temporally homogeneous if temporal variations are exclusively influenced by weather and climate (Domonkos and Coll, 2017). In practice, the most of the historical meteorological stations have undergone to a number of factors that have corrupted the homogeneity. These factors include station relocations, changes of instrumentation, instrument position, site changes around the instrument, changes of the timing of reading instruments (Acquaotta et al., 2016). Some changes can cause strong discontinuity while others, such as station relocation can cause a systematic bias in the measurements. All these inhomogeneities can lead to an erroneous interpretation of the results in the climate analysis.

Therefore, it is important to identify and remove any inhomogeneity, or at least to determinate the extent of error that can cause them. Certain data quality problems can be eliminated a by general quality control or with the analysis of the metadata. However, the statistical homogenisation procedure of data provides a more accurate quality control of the climatic series and allows the temporal and spatial comparisons between data for scientific purposes.

The homogeneity analysis was performed to the 88 weekly precipitation and temperature historical series, and the Standard Normal Homogeneity Test (SNHT) was used to detect any changepoint in the time-series (Alexandersson, 1986). The SNHT-CRAN Package was used for the investigation of both indices (Browning and Schneider, 2017). SNHT is a homogeneity test frequently used in climate studies. The Standard Normal Homogeneity Test assumes changepoint as a shift in the mean value of a time-series. In fact, for each observation, the test computes two means: one for the N days prior to observation and one for the N days following. If there are not N observations both before and after the current observation, no test is performed. If the test detects any observation that exceeds some threshold, a change point occurred and all the observations after and before were adjusted. The inhomogeneities identified were corrected using the mean ratio or difference between the series before and after the inhomogeneity.

The final climate database of the northern Italy included 88 series for precipitation, 88 for temperature, with less than 10% of gaps for each weekly series.

4.3. Models validation

Scenarios of regional climate change are in general based on downscaled atmosphere ocean coupled general circulation models (GCMs). The downscaling is either based on regional climate models (RCMs), statistical methods, or a combination of both. As explained in the paragraph **1.2.2. Regional Climate Models (RCMs)**, the dynamical downscaling of GCM output can today be considered as a well-established standard technique for the generation of regional climate change scenarios. Kotlarski et al. (2014) shows that RCMs are able to reproduce the most important climatic features at regional scales, particularly if driven by perfect boundary conditions. For a given emission scenario, the skill of regional climate change projections is limited by uncertainties. Some of these deficiencies are specific to individual models. Others seem to be a common and more systematic feature across

different RCMs, such as a dry and warm summer bias in south-eastern Europe (Hagemann et al., 2004) and an overestimation of interannual summer temperature variability in central Europe (Fischer et al., 2012), are partly related to parametric uncertainty and choices in model configuration and can be affected by internal variability as well as by uncertainties of the observational reference data themselves (Bellprat et al., 2012).

In order to improve the model's reliability is important design validation experiment. In fact, an integral part of regional model development is the evaluation and quantification of model performance by comparison against observation-based reference data. Furthermore, the validation should in particular consider aspects that have limited attention, such as extreme events observation (Maraun et al., 2015).

In the following study a model validation analysis to detect what GCM/RCM couple perform best in northern Italy was performed. For this purpose, for each simulation, 10 daily precipitation and temperature series (reference series) were extracted and compared with the corresponding quality-controlled and homogenised data series recorded at the ground (candidate series), obtained from the database created for northern Italy. In order to understand the impact of the elevation on the reliability of the analysed ensembles, the 10 climatic series were extracted both in the plain/hill and in the mountain sectors. The statistical comparison between reference and candidate series was then developed for the 30-years control period 1971-2000 by means of Co.Temp (Guenzi et al., 2019) for the temperature and Co.Rain (Guenzi et al., 2017) software for precipitation. The results of model validation performed for the ground stations located in the plain/ hill sector is reported in Table 5. The average number of precipitation events present both in the model and the data (obviously at different times) decreases moving from weak to extreme episodes. Especially marked differences between ground data and model outputs are observed for the extreme event class. The couples EC-EARTH-RACMO22E and MPI-ESM -CCLM4 provide the worse comparisons, with the highest Root Mean Square Error (RMSE) in the extreme event class (59.56 mm in the first and 56.11 mm in the second), while the other GMC/RMC couples give RMSE that are no larger than 25.59 mm. Table 5 also shows that for the mean, heavy and extreme precipitation classes the GCM/RCM couples have a tendency to overestimate the precipitation amounts.

Table 5: Results of the model precipitation validation for the selected GCM/RCM couples in the plain/hill area. For each precipitation class, the number of common events between models and ground stations, the average precipitation amount of common events and the corresponding RMSE are RMSE are reported. The less reliable models are shaded in grey.

	Class	N. common events	Common events models (mm)	Common events ground stations (mm)	RMSE
EC-EARTH-RACMO22	**weak**	82	273.6	250.91	2.82
	mean	18	260.4	221.49	6.56
	heavy	5	153.6	146.45	6.29
	R95	2	438.8	27.51	59.56
EC-EARTH-HIRHAM5	**weak**	76	240.6	239.78	2.4
	mean	11	156.8	139.15	6.41
	heavy	3	103.2	105.19	14.5
	R95	4	527	430.62	25.59
MPI-ESM-CCLM4	**weak**	77	264	259.46	2.41
	mean	29	340.6	321.97	5.29
	heavy	6	202.2	165.49	10.06
	R95	5	409.2	25.83	56.11
HadGEM2-CCLM4	**weak**	88	309.8	292.98	2.39
	mean	20	250	241.36	5.87
	heavy	6	182	145.27	10.58
	R95	3	529	500.75	12.66
HadGEM2-RACMO22	**weak**	92	267.4	290.44	2.46
	mean	25	342	314.82	5.52
	heavy	8	259.8	219.24	10.46
	R95	3	527.6	450.99	15.51
CM5-ALADIN52	**weak**	130	405	430.15	2.52
	mean	51	617.6	658.94	4.75
	heavy	3	91.8	82.28	9.02
	R95	2	501.8	494.77	12.72

Table 6 reports the precipitation model validation performed in the mountain sector. Like the results performed for the plain/hill area, the greatest differences between ground station and data estimated by the GCM/RCM couples are observed in the extreme events class. In particular the EC-EARTH-RACMO22E and MPI-ESM -CCLM4 couples provide the worst comparison, with a RMSE of 67.39 mm in the first and 67.01 mm in the second. While for the other couples no more than 36.55 mm of RMSE is recorded. Table 6 also pointed out that in comparison with the plain/hill in the mountain the GCM/RCM used to underestimate precipitation except for the extreme class.

Table 6: Results of the model precipitation validation for the selected GCM/RCM couples in the mountain area. For each precipitation class, the number of common events between models and ground stations, the average precipitation amount of common events and the corresponding RMSE are RMSE are reported. The less reliable models are shaded in grey

	Class	N. common events	Common events models (mm)	Common events ground stations (mm)	RMSE
EC-EARTH-RACMO22	**weak**	75	167.2	183.99	1.57
	mean	40	291.3	315.05	2.57
	heavy	18	343.6	383.89	6.96
	R95	6	206.3	405.2	67.39
EC-EARTH-HIRHAM5	**weak**	107	269.4	278.76	1.7
	mean	36	272.6	257.6	2.33
	heavy	17	280.2	279.24	5.62
	R95	3	102.6	116.15	35.33
MPI-ESM-CCLM4	**weak**	89	248.8	228.43	1.91
	mean	26	203.5	206	2.69
	heavy	12	206.9	221.93	6.14
	R95	10	387.3	30.05	67.01
HadGEM2-CCLM4	**weak**	109	305.8	297.76	1.72
	mean	39	331	341.03	3.03
	heavy	16	279.8	297.02	5.87
	R95	12	441.6	26.25	36.4
HadGEM2-RACMO22	**weak**	91	235.3	252.98	1.62
	mean	28	225.8	212.31	2.65
	heavy	13	214.5	234.42	4.8
	R95	12	386	28.66	30.17
CM5-ALADIN52	**weak**	138	357.7	412.45	1.77
	mean	46	359.5	390.42	2.87
	heavy	15	289.6	274.55	6.75
	R95	6	259.9	45.69	36.55

Table 7 reports the temperature validation in the plain/hill area for the ensemble, while in table 8 are showed the results for the mountain sector. In all cases, there is a bias of the model outputs to higher temperature values. This phenomenon is noticeable for the mountainous area, in fact table 8 shows a clear overestimation of temperature estimated by the model couples. In

particular in the extreme cold and extreme warm classes, where the RMSE ranges between 2.16°C and 5.27°C. As concern the plain/hill area the RMSE is lower and ranges between 2.0 °C and 2.48°C.

At variance with precipitation, the temperature analysis did not identify GCM/RCM couples that are more biased than others. In table 5 and table 6, were marked in grey the GCM/RCM couples that are more biased in northern Italy.

One the models were validated, daily data were converted in weekly, following the same procedure described in the paragraph **4.2.2. Data aggregation** for the historical series.

Table 7: Results of the model temperature validation for the selected GCM/RCM couples in the plain/hill area. For each temperature class, the number of common events between models and ground stations, the average temperature of common events and the corresponding RMSE are reported.

	Class	N. common events	Common events ground stations (°C)	Common events models (°C)	RMSE
EC-EARTH-RACMO22	**Extr_Cold**	26	-3.82	-2.25	2.43
	Cold	271	0.94	0.92	1.44
	Warm	244	28.14	28.70	1.63
	Extr_Warm	165	32.59	32.74	2.35
EC-EARTH-HIRHAM5	**Extr_Cold**	47	-2.46	-2.46	2.02
	Cold	306	1.44	1.15	1.44
	Warm	230	27.62	27.93	1.48
	Extr_Warm	109	31.14	31.70	2.26
MPI-ESM-CCLM4	**Extr_Cold**	19	-1.77	-1.52	2.00
	Cold	220	1.31	1.06	1.41
	Warm	199	27.83	28.36	1.70
	Extr_Warm	93	32.17	32.51	2.22
HadGEM2-CCLM4	**Extr_Cold**	13	-2.80	-0.85	2.52
	Cold	237	1.86	1.53	1.40
	Warm	188	27.56	27.98	1.67
	Extr_Warm	98	31.88	32.05	2.48
HadGEM2-RACMO22	**Extr_Cold**	9	-0.73	-1.01	0.91
	Cold	236	3.80	2.40	2.13
	Warm	238	27.61	28.07	1.61
	Extr_Warm	135	31.70	32.50	2.44
CM5-ALADIN52	**Extr_Cold**	3	-8.44	-7.00	2.15
	Cold	100	-4.50	-3.83	1.58
	Warm	118	24.80	24.66	1.08
	Extr_Warm	19	30.10	31.38	2.33

Table 8: Results of the model temperature validation for the selected GCM/RCM couples in the mountain area. For each temperature class, the number of common events between models and ground stations, the average temperature of common events and the corresponding RMSE are reported.

	Class	N. common events	Common events ground stations (°C)	Common events models (°C)	RMSE
EC-EARTH-RACMO22	Extr_Cold	17	-8.29	-7.20	2.84
	Cold	186	-3.46	-3.45	1.73
	Warm	169	21.32	22.40	2.14
	Extr_Warm	110	26.23	29.00	3.62
EC-EARTH-HIRHAM5	**Extr_Cold**	25	-8.53	-8.10	2.98
	Cold	194	-3.35	-2.90	1.94
	Warm	203	22.04	23.00	2.26
	Extr_Warm	119	26.90	28.00	3.39
MPI-ESM-CCLM4	**Extr_Cold**	12	-8.45	-6.90	2.44
	Cold	189	-3.08	-3.00	1.63
	Warm	106	18.59	20.45	2.89
	Extr_Warm	19	24.35	26.00	3.06
HadGEM2-CCLM4	**Extr_Cold**	15	-7.63	-7.60	2.18
	Cold	158	-3.12	-2.90	2.07
	Warm	181	21.01	22.40	2.36
	Extr_Warm	84	25.85	27.55	3.32
HadGEM2-RACMO22	**Extr_Cold**	26	-9.94	-9.25	3.14
	Cold	214	-3.49	-3.00	1.85
	Warm	179	22.14	22.80	1.97
	Extr_Warm	104	26.55	28.00	2.75
CM5-ALADIN52	**Extr_Cold**	13	-10.28	-9.00	2.45
	Cold	129	-5.68	-4.40	2.22
	Warm	115	19.16	21.10	2.45
	Extr_Warm	23	24.05	27.80	5.27

CHAPTER 5: METHODS OF ANALYSIS

This chapter describes all the methods of analysis applied to the historical time series and the future projection models in order to detect and characterise the main past (1965-2017), near future (2020-2049) and far future (2070-2099) drought events in northern Italy.

5.1. Interpolation of precipitation and temperature historical series

Precipitation and temperature data are measured at a limited number of locations. Moreover, the observations made by a single station are only representative of a restricted area in the neighbourhood. But in order to study droughts in northern Italy a spatially distributed field is required, in fact gridded products of the main climatological variables with high quality and spatial resolution are needed for the application of drought indices.

The goal was to find an appropriate method for the spatial interpolation of the weekly temperate and precipitation series. Kriging has become a very popular interpolation method for temperature, precipitation and other meteorological variables due to its ability to take into account spatial correlation, to estimate target variables at unobserved locations, and to quantify the uncertainty associated with the estimator. Courault and Monestiez (1999) used ordinary kriging (OK) to interpolate maximum and minimum temperatures for southeast France. Subsequently regression kriging (RK) was introduced, and it was proven that it gives better results than OK (Hunter and Meentemeyer 2005). Carrera-Hernández and Gaskin (2007) interpolated then precipitation and temperature for Mexico by mean of the kriging with an external drift (KED). Later Brinckmann et al. (2016) and Milovanović et al. (2017) used the simple kriging (SK) to interpolate monthly temperature and precipitation for Europe. Spatio-temporal regression kriging (STRK) recently become popular due to the development of R gstat (Pebesma 2004) and spacetime (Pebesma 2012) packages.

Here it is presented an approach that integrate the interpolation of the main climatological data with several auxiliary variables. Weekly precipitation and temperature data were interpolated into a spatial grid at 20 km resolution, with the following vertices, expressed in WGS84 UTM-32N cartographic coordinates: North 5220300 m 4847300 m South, East and West 882908 m 312908 m.

A semivariogram (γ) is one of the basic geostatistical tools that is used to determine spatial dependence. Calculation of an experimental semivariogram is necessary input for different geostatistical interpolation techniques, like Kriging. In this regard, for each week of the period 1965-2017 the experimental variogram of the precipitation and temperature data was calculated. The semivariogram is calculated as half the average squared difference between the paired data values.

$$\gamma(h) = \frac{1}{2N(h)} \sum_{n=1}^{N(h)} [z_n - z_{n+h}]^2 \qquad (5.1)$$

Where, $N(h)$ is the number of data pairs at separate distance "h" (inside searching neighbourhood area); z_n is the value at location n (in this case precipitation or temperature data); z_{n+h} - value at location n+h.

In this study, the maximum separation distance considered (h) is taken at 250 km and a maximum of 25 neighbouring observatories ($N(h)$) were considered to obtain weights for the interpolations ($N(h)/h^2$).

To assure that the kriging equations have a unique and stable solution. A given semivariogram is then approximated by the theoretical model. In the interpretation of climatological variables, commonly used theoretical models are Spherical, Exponential and a Gaussian model. Several models were tested and the Spherical was chosen (Isaaks and Srivastava, 1989):

$$\gamma(h) = C_0 + C\left[\left(\frac{3h}{2a}\right) - \left(\frac{h^3}{2a^3}\right)\right] \qquad h \le a$$

$$\gamma(h) = C_0 + C \qquad h > a \qquad (5.2)$$

Where $\gamma(h)$ is the variogram value at distance "h"; C_0 is the nugget constant; $C_0 + C$ is the Sill and "a" is the range. The parameters of the variogram models were fitted and figure 10 shows the example of spherical semivariograms used to interpolate maximum temperature layer.

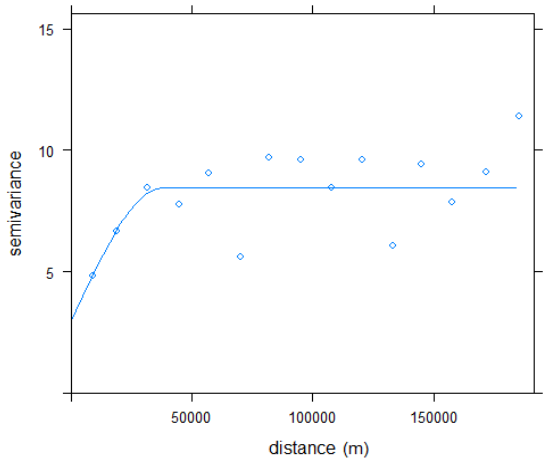

Figure 10: Example of spherical semivariogram used to develop the weekly maximum temperature gridded layer

The universal kriging (UK) was applied to the weekly historical precipitation, maximum and minimum temperature series recorded in the northern Italy (Wang et al., 2014). Taking into account the causes of climate determining temperature and precipitation distribution in northern Italy a set of potential environmental predictors including: latitude, longitude, distance to shoreline and elevation were used directly to solve the kriging weights, as auxiliary predictors. All variables were prepared as raster layers of 20 km resolution, projected to the Italian local coordinate system WGS84-32N.

The Universal kriging is a spatial prediction technique commonly used in geostatistics that combines a regression of the dependent variable (precipitation and temperature in this case) on auxiliary/predictive variables (latitude, longitude, distance to shoreline and elevation) with kriging of the regression residuals. UK is mathematically equivalent to the interpolation method variously called regression kriging and kriging with external drift.

The aim of the UK method is to predict Z(x) at an unsampled area as well. The universal kriging model splits the random function into a linear combination of deterministic functions, the smoothly varying and nonstationary trend, that is also called a drift $\mu(x) \in \mathbb{R}$, and a random component $Y(x) := Z(x) - \mu(x)$ representing the residual random function (Wackernagel, 2003). In contrast to the Ordinary Kriging, that assume a stationary of the constant mean of the underlying real-valued random function Z(x). The mean value varies, it is

often not constant across the entire study area and the variable is nonstationary. A nonstationary regionalized variable can be considered as having two components; drift (average or expected value of the regionalized variable) and a residual (difference between the actual measurements and the drift). The method of UK assumes that the mean m(x) has a functional dependence on the spatial location and can be approximated by a model with the equation (Kumar, 2007):

$$\mu(x) = \sum_{l=1}^{k} a_l f_l\,(x) \qquad (5.3)$$

a_l is the lth coefficient to be estimated from the data; f_l is the lth basic function of spatial coordinates that describes the drift; "k" is the number of functions used in modelling the drift.

UK is also known as kriging with a trend or kriging in the presence of a drift. Spatial trend or a drift represents any detectable tendency for the values to change as a function of the coordinate variables. The mean can be a function of the coordinates in linear, quadratic or higher form. The UK considering linear trend was used for the spatial interpolation of the variable. The mathematical model with two auxiliary variables (i.e. latitude and longitude) is (Kastelec and Košmelj, 2002):

$$Z(s) = \beta_0 + \beta_1 x_1 + \beta_2 x_2 + \delta(s) \qquad (5.4)$$

$Z(s)$ predicted variable at location s; x_1 (s) is the latitude at location s; β_0, β_1, β_2 are the coefficients of the linear trend; δ(s) is the intrinsic stationary random process with existing semivariogram ɣ(h).

The kriging estimate is as follows (Kumar, 2007):

$$Z'(s_0) = \sum_{i=1}^{N} \lambda_i Z\,(s_i) \qquad (5.5)$$

Where $Z'(s_0)$ is the estimated value at s_0; $Z(s_i)$ is the observed value at point s_i; N is the sample size; λ_i are the weights chosen for the point s_i.

In order to choose weight is needed to satisfy the following statistical conditions:

a. unbiasedness

$$E\{Z'(s_0) - Z(s_0)\} = 0 \quad (5.6)$$

b. minimum variance

$$var\{Z'(s_0) - Z(s_0)\} = minumum \quad (5.7)$$

According to Journel and Huijbregts (1978), the minimisation of Equation (4.7) that is subject to the constraint of Equation (5.6), using the Lagrange multiplier (μ), results in the following UK system:

$$\begin{cases} \sum_{j=1}^{N} \lambda_j \gamma(s_i, s_j) + \sum_{l=1}^{K} \mu_l f_l(s_i) = \gamma(s_j, s_0) & i = 1,2,3,\dots,N \\ \sum_{i=1}^{N} \lambda_i f_l(s_i) = f_l(s_0) & l = 1,2,3,\dots\dots,k \end{cases} \quad (5.8)$$

Where:

$\gamma(s_i, s_j)$ is the semivariogram between two points s_i and s_j; μ_l is the Lagrange multiplier associated with the lth unbiased condition.

The optimum weights λ_i can be obtained by solving these equations simultaneously. For the calculation of λ-s, a variogram which is a measure of spatial continuity of the data, is required (Kastelec and Košmelj, 2002). The variance of this estimation is given in the following equation (Kumar, 2007):

$$\sigma_k^2(s_0) = \sum_{i=1}^{N} \lambda_j \gamma(s_i, s_0) + \sum_{l=1}^{k} \mu_l f_l(s_0) \quad (5.9)$$

In literature the universal kriging with co-variables is the most applied method to interpolate monthly, seasonal and annual precipitation and temperature data in region with complex topography and high variation in densities and elevational distribution of climate stations (Bois et al., 2018; Beguería et al., 2018; Stahl et al., 2006). In Italy elevation, latitude and longitude are the main predictors (Gentilucci et al., 2018; Secci et al., 2010). In northern Italy, an increase of precipitation and decrease of temperature with elevation and a

decrease of rainfall and temperature with distance to the shoreline are expected results, because of the presence of the Mediterranean Sea. In this study, the distance to the shoreline was applied as fourth predictor to improve the quality of the interpolation. In figure 11 is reported, as example, the comparison between the interpolation of precipitation, maximum and minimum temperature performed with all the predictors (elevation, longitude, latitude and distance to the shoreline), and without the distance to shoreline for the year 2015. Figure 11 has evidenced that the interpolations performed with all the predictors are more detailed instead of those made with only elevation, latitude and longitude. Marked differences are observed for the maximum and minimum temperature. For instance, throughout the easter coast the interpolation without the distance to the shoreline has detected a homogeneous annual maximum temperature of 21°C. While a graduate decrease of the maximum temperature (between 20°C and 24°C) with the distance to the shore line was recorded by the interpolation with all the predictors. Same results are figured out for the minimum temperature. Figure 11 has evidenced that for the interpolation with all the predictors the eastern coast records higher rates of precipitation (and decrease with the distance to the shore line) instead of the interpolation with only elevation and latitude and longitude as auxiliary variables, where a more homogeneous area was observed.

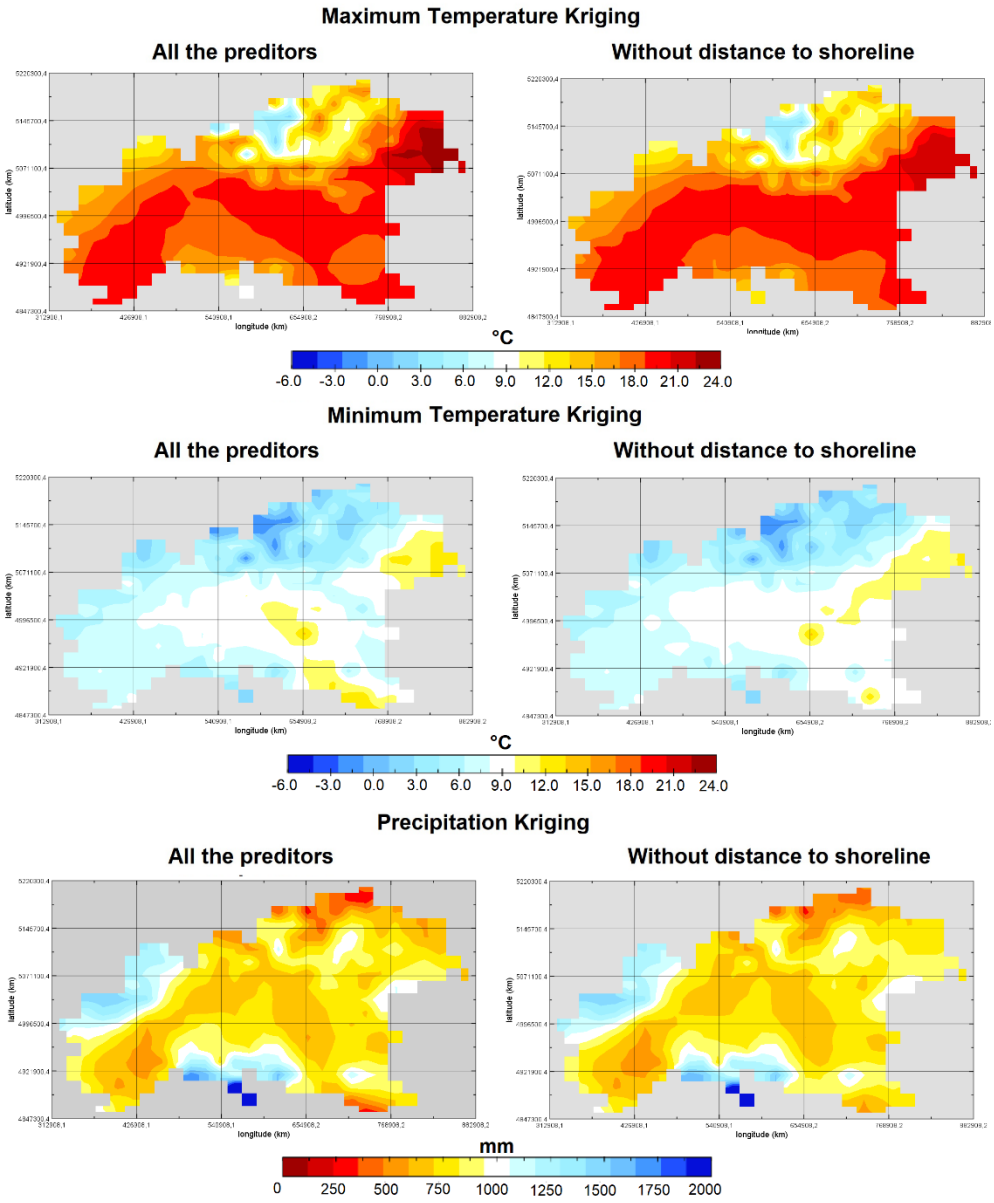

Figure 9: Comparison between the interpolation of precipitation, maximum and minimum temperature performed with all the predictors (elevation, longitude, latitude and distance to the shoreline), and without the distance to shoreline, for the year 2015.

Finally, to assess predictive accuracy, predicted values were compared with observed values in the validation dataset. The grid layers were validated using

a jackknife resampling procedure. This was based on withholding single observatories in turn from the network, making estimates based on interpolation from the remaining observatories, and calculating the difference between the predicted and observed values for each observatory that was withheld (Phillips et al., 1992). First for each gridded layer for the variables analysed, the Mean Absolute Error (MAE) was computed to determine overall magnitude of error:

$$MAE = \frac{1}{n}\sum_{i=1}^{n} | (P_i - O_i) | \quad (5.10)$$

where n is the number of samples; P_i is the predicted climatic value; O_i is the observed precipitation and temperature values.

Second the agreement Index D was calculated. Index D is a relative and bounded measure of model validity, and it scales with the magnitude of the variables, retaining mean information and not amplifying outliers (Willmott, 1982). A D value = 1 corresponds to a perfect match between estimates and the observed data:

$$D = 1 - \frac{\sum_{i=1}^{n}(O_i - P_i)^2}{\sum_{i=1}^{n}(|(P_i - O)| + |(O_i - P)|)^2} \quad (5.11)$$

where O_i is the observation value; P_i is the forecast value; O is the average observation values; P is the average forecast values.

All geostatistical operations were carried out using the R package gstat (Pebesma and Gräler, 2018).

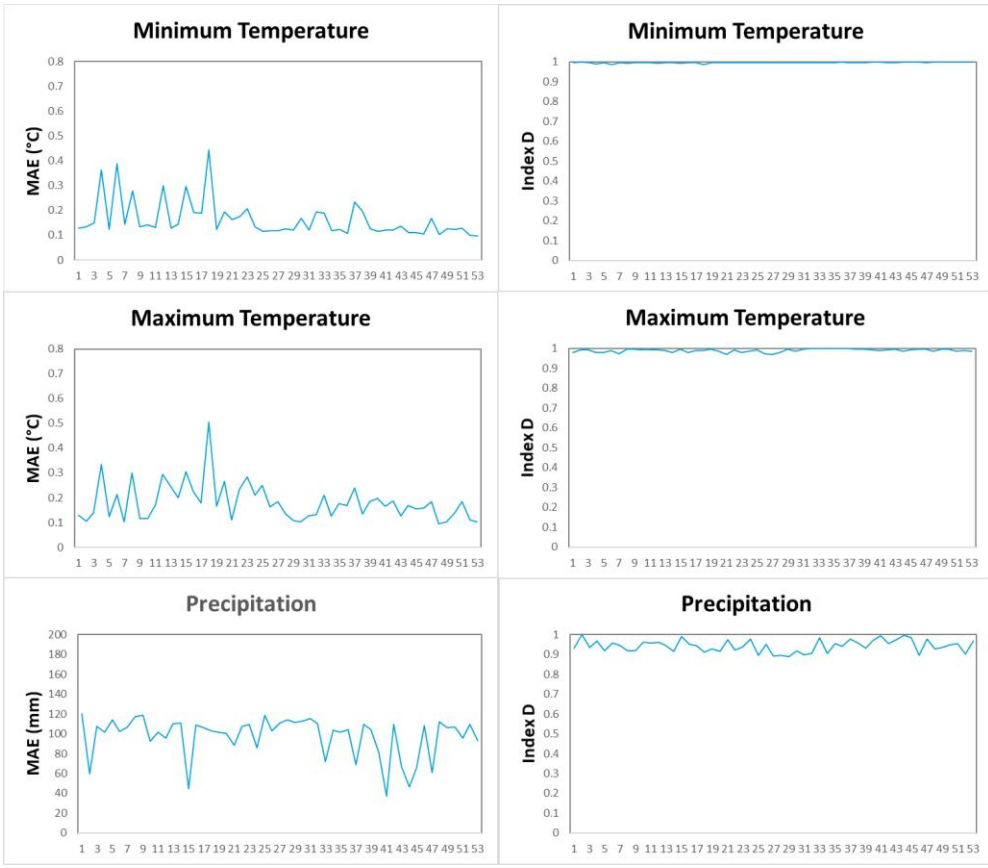

Figure 12: Mean Standard Error (MAE) and agreement index D calculated for minimum temperature, maximum temperature and precipitation. Y axes are the years from 1965 to 2017 for 53 years

Figure 12 show the MAE and index D plot obtained for minimum temperature, maximum temperature and precipitation. As expected, given the availability of data and the complexity of the northern Italy territory, the agreement between the observed and predicted data is much better for maximum and minimum temperature. In this regard, agreement index D values are close to 0, and no more than 0.5°C of MAE are observed for temperatures. For precipitation D values are very high, ranging between 0.9 and 1, while the mean absolute error ranges between a maximum of 120 mm and e minimum of 40 mm.

5.2. Evapotranspiration observation in historical series and projection models

The evapotranspiration (ET) provides a link between energy and water balance in the hydrological cycle. ET is defined as the transfer of liquid water to the atmosphere as water vapor from bare soil and water bodies such as rivers and lakes (evaporation), as well as vegetated surfaces through plants' leaves (transpiration) (Allen et al., 1998). ET is a critical component of the water and energy balance of climate-soil-vegetation interactions and can account for a water loss of about 90% in arid regions (Lu et al., 2019).

The ET is divided in reference (or potential) evapotranspiration (ET_0), and actual evapotranspiration (E_a). The ET_a is the quantity of water that is transferred as water vapor to the atmosphere from an evaporating surface (Wiesner, 1970) under real conditions (e.g. water availability, vegetation type, physiological mechanisms, climate), whereas ET_0 represents the atmospheric evaporative demand (AED) of a reference surface (generally a grass crop having specific characteristics), and it is assumed that water supply from the land is unlimited (Allen et al., 1998). ET_0 expresses the evaporating power of the atmosphere at a specific location and time of the year and it allows for spatial and temporal comparisons, independent of different land cover types and temporal coverage changes (Katerji and Rana, 2011). The only factors affecting ET_0 are climatic parameters (radiation, air temperature, surface pressure, wind speed and relative humidity). Consequently, ET_0 is a climatic parameter and can be computed from weather data.

In literature the Thornthwaite, the Penman-Monteith and the Hargraves equation are the three most used methods to estimate evapotranspiration

Thornthwaite

The most simple and straightforward method to estimate the potential evapotranspiration is the Thornthwaite. The Thornthwaite equation is a temperature-based method that uses only mean monthly temperature and latitude of the site to estimate potential evapotranspiration. Thornthwaite equation is as follows (Thornthwaite, 1948):

$$PET = 16(10T_a/I)^a \qquad (5.12)$$

Where: PET is the Potential Evapotranspiration, mm/month (month of 30 days

each and 12 hours day time); T is the mean temperature (°C); I is the annual or seasonal heat index (summation of 12 values of monthly heat indices); a is an empirical exponent (a=0.675 x 10-6/3 -0.771 x 10-4[2 + 0.1792 x 10-1/+ 0.49239)

This method is the subject of many criticisms. Generally, the Thornthwaite method underestimates the potential evapotranspiration in areas of continental climate (Marcos-Garcia et al., 2017; Trajkovic, 2005). For example, it considers that PET is null when the temperature is near zero.

Penman-Monteith

The International Commission for Irrigation (ICID), the Food and Agriculture Organization of the United Nations (FAO), and the American Society of Civil Engineers (ASCE) have adopted the Penman–Monteith (PM) method (Allen et al., 1998) as the standard method for computing daily ET_0 from climate data. The PM method is widely used because it is a physically-based approach that can be used globally, and has been widely tested (Itenfisu et al., 2000). The main disadvantage of the PM method is the large amount of data involved. The equation uses standard climatological records of solar radiation (sunshine), air temperature, humidity and wind speed. The Penman-Monteith equation is given as (Allen et al. 1998):

$$ET_0 = \frac{0.408\Delta(R_n - G) + \gamma \frac{900}{T+273} u_2 (e_s - e_a)}{\Delta + \gamma(1 + 0.34u_2)} \quad (5.13)$$

Where ET_0 is crop reference ET ($mmday^{-1}$); R_n is net radiation at the crop surface ($MJ\ m^{-2}day^{-1}$); G is soil heat flux density ($MJ^{m-2}\ day^{-1}$); T is air temperature at 2 m height (°C); u_2 is the wind speed at 2 m height (ms^{-1}); $e_s - e_a$ is saturation vapor pressure deficit (kPa); Δ is slope vapor pressure curve ($kPa\ °C^{-1}$).

The PM equation is generally recommended as the standard method for estimating ET_0. In fact, the PM method is the most worldwide accurate under all types of climatic conditions, and many studies have used the PM equation in applications related to climatology, hydrology, agriculture and ecology. Such as in France (Mjejra et al., 2014; Chaouche et al., 2010), in Slovenia (Maček et al., 2018), in Romania (Croitoru et al., 2013), in Israel (Cohen et al., 2002), in Spain (Tomas-Burguera et al., 2020), in Italy (Vergni and Todisco, 2011), and in Great Britain (Prudhomme and Williamson, 2013).

Hargreaves

The Hargreaves equation (HG, Hargreaves and Samani, 1985) is one of the most widely used simple ET_0 equation for daily or monthly ET_0. The HG method requires mean temperature (T) and solar radiation (Rs) data and it is based on the following expression:

$$ET_0 = R_e \cdot H_a(T + 17.8) \cdot \Delta T^{H_e} \quad (5.14)$$

Where H_a and H_e are empirical standard parameters. The solar radiation, R_e, is expressed in $mm \cdot d^{-1}$. T is the mean temperature ((Tmax + Tmin)/2 °C) and ΔT is the difference between Tmax and Tmin.

This method is used for the estimation of ET_0 in several regions of the Mediterranean Basin, such as in Spain (García-Garízabal et al., 2014), in Greece (Kitsara et al., 2013), in Italy (Pavanelli and Capra, 2014; Capra et al., 2013; Matzneller et al., 2010), in Turkey (Citakoglu et al., 2014), and in Portugal (Valverde et al., 2015). Among the various methods, compared with the PM equation, the Hargreaves (HG) equation provided the best results, at both the annual and seasonal scales. This equation has been suggested to be the best alternative where data are scarce (Alexandris and Petkovic, 2008). Therefore, Vicente-Serrano et al., (2014) recommended the use of the HG equation to determine average ET_0 values in the Mediterranean region, where data availability is limited. In fact, there were no significant spatial differences in the performance of this equation in either humid or dry climatic area**.**

In this study, due to the only availability of daily precipitation and temperature data for both historical series and GCM/RCM couples, the Hargreaves equation was applied to estimate the reference evapotranspiration ET_0

5.3. Drought analysis

Monitoring drought requires a variety of indicators and indices. Drought indices are quantitative measures that characterize all four meteorological, agricultural, hydrological, and socioeconomic drought types by assimilating data from one or several variables (indicators) such as precipitation and evapotranspiration into a single numerical value. The nature of drought indices reflects different events and conditions; they can reflect the climate dryness anomalies (mainly based on precipitation) or correspond to delayed

agricultural and hydrological impacts such as soil moisture loss or lowered reservoir levels. Some indices are currently used for the development of weekly grid-based drought condition maps (Zargar et al., 2011). The most common indicators of drought used in Europe are the Standardised Precipitation Index (SPI) and the Standardised Precipitation Evapotranspiration Index (SPEI) indices.

5.3.1. Standardised Precipitation Index (SPI)

It is commonly accepted that drought is a multi-scalar phenomenon. The Standardised Precipitation Index (SPI, McKee et al., 1993) is a popular meteorological drought index, and it is solely based on precipitation data. It classifies precipitation with its multiyear average. SPI overcomes the discrepancies resulting from using a non-standardized distribution by transforming the distribution of the precipitation record to a normal distribution. For this, a rainfall time series is transformed so that it can be described by a statistical gamma distribution, and further transformed into a standardised normal distribution. The mean is then set to zero and values above zero indicate wet periods and values below zero indicate dry periods. An important aspect of SPI is its ability to calculate drought events at different time scales (1, 3, 6, 12, 24 and 36 months). Because over several time periods precipitation deficit gradually affects different water resources (e.g., stream flow, groundwater, and snowpack). In this regard the index can be used to describe the four types of drought, and the classification of the values range from very wet to very dry drought conditions.

5.3.2. Standardised Precipitation Evapotranspiration Index (SPEI)

Standardised Precipitation Evapotranspiration Index (SPEI, Vicente-Serrano et al., 2010) is a multiscalar drought index designed to consider both precipitation and potential evapotranspiration (ET_0). It is based on the climatic water balance, calculated as the difference between precipitation and the atmospheric evaporative demand. Like the SPI, the SPEI can measure drought severity according to its intensity and duration, and can identify the onset and end of drought episodes. The SPEI allows comparison of drought severity through time and space, since it can be calculated over a wide range of climates, as can the SPI.

5.3.3. Past and future drought investigation

Past (1965-2017), near future (2020-2049) and fare future (2070-2099) northern Italy droughts were investigated. The two drought indices, SPEI and SPI, were applied at a weekly scale to the gridded atmospheric evaporative demand, precipitation and temperature data obtained by both the historical series and future projection models couples (Med-CORDEX and Euro-CORDEX). The SPEI-CRAN Package was used for the investigation of both indices (Beguería and Vicente- Serrano, 2017). To be able to detect and characterise all the possible drought events, SPEI and SPI were estimated at 12-, 24-, and 36-month scales. Once the two indices were calculated, SPEI and SPI global series were derived for each cell grid and the main drought events were identified based on three parameters:

- Drought events classification by mean of threshold. For this purpose, McKee et al. (1993) classified drought episodes in four different classes, mild, moderate, severe and extreme. In this study drought episodes with at least 10 years of returning period were investigated, focusing on severe and extreme episodes (Table 9).
- Percentage of area interested. A drought conditions, as defined by index values, should affect more than ¼ of the study area (Gonzalez-Hidalgo et al., 2018).
- Drought duration. A drought event is defined by McKee et al. (1993) as a period where the drought index is continuously negative and the drought event reaches a value of -1.0 or less. The drought begins when the drought index falls below zero and ends with the positive value of the index. To avoid the over detection of events, the minimum drought length of 3 consecutive weeks was considered.

Table 9: Classification of drought episodes in two class of events: severe and extreme, where R is the observed SPEI or SPI value

Class event	Range
Severe	$-1.65 \leq R < -1.28$
Extreme	$R < -1.65$

For the 1965-2017 period, each drought episode was characterized by detecting the starting and ending weeks, the duration (number of consecutive weeks), the magnitude (considered as the index value reached), percentage of area affected.

For near future (2020-2049) and far future (2070-2099) periods according with the RCP 4.5 and 8.5, the main drought episodes characterisation was focused on the detection of the total number of severe and extreme event, temporal duration, and percentage of affected area.

To compare each class of events, calculated at different time scales by the SPEI and SPI, a bubble plot was applied (Ouzeau et al., 2016). The bubble plot highlights the different outcomes obtained, respectively, with SPEI and SPI, comparing severe and extreme drought episode duration (x axis), with magnitude on the y axis (SPI or SPEI value), and percentage of area under drought (bubble size).

5.3.4. Past and future drought trend analysis

Because the drought analysis has a crucial importance for planning and management of water resources, possible significant changes (or trends) over time should be detected.

The concept of trend represents long-term smooth variations. The identification and estimation of long-term trend was a real challenge for the statisticians. The main problem is not statistical or mathematical but originates from the fact that the trend is a latent (non- observable) component and its definition as a long-term smooth movement is statistically vague. In literature there is a great number of methods applied in the trend analysis that include both descriptive analyses and statistical tests (Mudelsee et al. 2019; Madsen et al. 2014).

The temporal evolution of past (1965-2017) near future (2020-2049) and far future (2070-2099) drought episodes was checked using the Mann-Kendall test (MK, Mann, 1945, Kendall 1976). The Mann-Kendall is a rank-based non-parametric test for detecting monotonic trend in the time series. This test is preferable to others (Pettitt, Wald–Wolfowitz, etc.), because it has been widely used in several papers concerning drought in Italy (Buttafuoco et al., 2015) and in the other Mediterranean areas (Merino et al., 2015); thus, could let a comparison on the data. The slopes of the trends were calculated by Sen's slope estimator (Sen, 1968). The Sen’s slope estimator is preferred to the linear least square that is more vulnerable to gross error of data and has a

confidential interval more sensitive to the non-normality of the distributions. The statistical significance was assessed at 95% (0.05). All the trend analysis was developed using scripts with the R open source software (R Development Core Team 2011).

5.3.5. Past and future drought spatial evolution

The Spatial variability of drought events is highly complex on a regional scale. This has been demonstrated in several regions of the world (Song et al. 2014; Capra and Scicolone 2012). In particular it has been suggested that the spatial drought patterns may differ in relation with the drought indices applied. In fact, different indices may give rise to more diverse patterns (Gonzalez-Hidalgo et al., 2018). The methodologies applied to the historical series and GCM/RCM couples are described in the following subsections

5.3.5.1. Historical series

The spatial behaviour of the main drought events in the northern Italy in the 1965-2017 period was investigated. In detail the spatial prorogation gradients of two study cases with the latitude and longitude was analysed in deep comparing the spatial gradient with the circulation patterns. This last analysis for the historical series is especially interesting, because, in the Po Valley, more than 50% of total freshwater resources are used in agriculture, whereas water availability is becoming scarcer due to over-exploitation, salinization and long periods drought (Antonellini et al., 2008).

5.3.5.2. Future projection models

The main goal of the Paris agreement (COP21) is to hold global warming well below 2°C and to pursue efforts to limit to 1.5°C above preindustrial temperature (UNFCCC 2015). Actually, global temperature warming is about 1.0 °C above pre-industrial levels. This increase has severely impacted human livelihoods, social economies, and natural systems. Furthermore, if the current trajectory of greenhouse emissions continues, we could end the 21th century with more than 3 °C global mean temperature (GMT) rise (Sanford et al. 2014). Hence, +2 and +3 °C global mean temperature increase are important milestones, not only for mitigation but also to understand the expected impacts of drought. If the World will warm by 2 and +3°C, many vulnerable countries

and regions would be critically interested. With regard to the political and socioeconomic achievability of these goals, it is important to quantify how drought risk changes for these two warming targets and whether there are significant differences between them (Donnelly et al., 2017).

The spatial impacts of +2 and +3°C global warming before the preindustrial levels on future drought episodes in the northern Italy were investigated. From the 12 maximum and minimum temperature and 12 precipitation GCM-RCM couples, the mean models for respectively +2 °C and for +3°C of global mean temperature raise were obtained. Subsequently the SPEI and SPI drought indices were applied at the two global mean GCM-RCM couples and the main severe and extreme future drought events were detected by mean of the same procedure described in the section "**5.3.3. Past and future drought investigation**". In this regards the spatial behaviour of drought duration (expressed as the number of consecutive weeks) passing from a global temperature increase of +2°C to +3°C above preindustrial levels was analysed.

CHAPTER 6: RESULTS

This chapter shows firstly the 1965-2017 droughts obtained from the historical series, secondly near (2020-2049) and far (2070-2099) future drought episodes detected form the future projection models. To reduce the number of graphs and tables are often showed values or graphics summaries and the most representative images of what has been obtained from the calculations.

6.1. Historical series

In this section the results of the droughts characterisation performed on the historical series recorded at the ground in the norther Italy for the 1965-2017 period are reported. Therefore, the main drought events are displayed, and their spatial and temporal evolution is investigated.

6.1.1. Drought detection and indices comparison

In this section the results of the drought characterisation performed on the historical series in the norther Italy for the 1965-2017 are reported. Therefore, the main drought events are displayed, and their temporal and spatial evolution is investigated. Moreover, the main drought triggering factor were investigated, comparing the results obtained for the two drought indices, SPEI and SPI.

6.1.1.1. Main drought events

The main events recorded in the north of Italy for the 1965-2017 period were analysed using the two drought indices, SPEI and SPI, on a 12-month time scale. Drought episode must have a minimum duration of 3 consecutive weeks, involve at list the 25% of the norther Italy and the index values have to be below or equal the -1.82 threshold. In this regard for each drought event the starting and ending weeks, the duration expressed in consecutive weeks are analysed. To understand the spatial evolution of the identified drought

events the prorogation gradients were also investigated and reported in Table 10.

Table 10: Main drought episodes observed in the 1961-2017 period by SPEI and SPI. For each detected event are reported the propagation gradient, starting week and ending week and duration (number of weeks).

Gradient	SPEI	Duration	SPI	Duration
EW	9/Nov/1983-23/Feb/1984	15	9/Nov/1983-16/Feb/1984	14
EW	16/Jan/1989-23/Jul/1987	26	9/Jan/1989-1/Jul/1987	24
EW	9/Apr/1990-9/Feb/1991	41	23/Apr/1990-9/Nov/1990	27
SN	9/Oct/1997-23/Sep/1998	44	16/Oct/1997-1/Sep/1998	43
SN	9/Oct/2002-23/May/2002	20	9/Jan/2002-16/May/2002	18
EW	9/Aug/2003-23/Apr/2004	35	16Sep/2003-1/Mar/2004	23
SN	1/Mar/2007-9/Apr/2008	54	1/Oct/2006-9/Apr/2008	74
SN	23/Dec/2011-16/Nov/2012	47	23/Dec/2011-16/Nov/2012	47
SN	23/May/2017-23/Dec/2017	29	9/May/2017-23/Dec/2017	31

The analysis has figured out that nine major drought events affected the northern Italy in the 1965–2017 period. The results have figured out that according with SPEI the first drought episode, characterised by a magnitude below -1.82, is recorded in 1983, with 15 consecutive weeks under drought (November 9, 1983–February 23, 1984). Before 2000s other three more episodes were observed: in 1987 with 25 weeks, this event mainly involved the central-western part of the northern Italy with SPEI values between -1.4 and -1.8 for the cities of Turin (Piedmont), Milan (Lombardy) and Genoa (Liguria); in1990 the central part of northern Italy was interested by 41 weeks of drought and the SPEI index recorded for the cities of Turin and Milan values between -1.4 and -2.0; the third event was observed in 1997 and mostly

interested the central-western part of the northern with 44 weeks, the mainly involved cities were Turin (Piedmont), Milan (Lombardy) and Venice (Veneto) with SPEI values from -1.4 and -2.2. After 2000s droughts become more frequent and was characterised by longer events. Remarkable are the episodes of: 2003 with 35 consecutive weeks (August 9, 2003- April 23, 2004). This event interested the whole northern Italy, in particular, the most affected cities were Bologna (Emilia-Romagna), Turin (Piedmont), Milan (Lombardy) and Trieste (Friuli-Venezia Giulia) with peak of the SPEI index of -2.7; the two longest events in 2008 (March 1, 2007-April 9, 2008) with 54 weeks and 2011 (December 23, 2011- November 16, 2012) with 47 weeks interested the whole study area. The main cities involved where Genoa (Liguria), Bologna (Emilia-Romagna) with SPEI values below -2.0 in 2008, while for 2011 also for Venice (Veneto) the SPEI index was below -2.0; the last event was recorded in 2017 with 29 weeks (May 23, 2017-December 23, 2017), and the lowest values of the SPEI index (from -1.4 and -2.0) were observed in Turin (Piedmont), Milan (Lombardy), Bologna (Emilia-Romagna) and Genoa (Liguria).

The drought characterisation figured out also a strong agreement between the episodes recorded by the two indices, SPEI and SPI. In fact, for the greatest part of the events a maximum difference of 2/3 weeks was observed with a tendency of overestimation for the SPEI index. Except for few episodes, in fact, table 10 shows that two drought events recorded the highest difference between SPEI and SPI. The first one was in 1990, lasting for 41 consecutive weeks according to SPEI (April 9, 1990–February 9, 1991), whereas SPI highlighted a drought event of 27 weeks with a similar starting date (April 23, 1990), but finishing earlier on November 9, 1990. The second drought episode was recorded in 2007, specifically March 1, 2007–April 9, 2008 for SPEI, lasting 54 weeks, whereas SPI observed a longer episode also in 2006 (starting date October 1, 2006) and finishing on April 9, 2008.

To inquire the factors that have brought to these differences of lengths in the two investigated period (1990-1991 and 2006-2008) the seasonal precipitation and potential evapotranspiration (ET_0) in the study period were analysed and plotted in figure 13.
Figure13 highlights that, for the first episode (1990-1991), at the beginning of summer 1990, the north Italy was affected by a precipitation deficit with 208.2 mm instead of the seasonal average of 255.8 mm of the reference period 1970–2001. Subsequently, since winter 1991, the drought episode was exacerbated

by potential evaporation values of 51.2 mm/weeks, 9.4 mm/weeks above the normal. This has suggested that in the last weeks of the event, the main triggering factor that influenced drought in northern Italy was a potential evapotranspiration above the normal, and for this reason the SPEI index has detected a longer drought event instead of the SPI.
While for the second events underlined (2006-2008) figure 13 shows that, in contrast to the 1990-1991 event, the drought episode in the north Italy was generated in 2007 by a precipitation deficit recorded at the beginning of winter 2006, with 160.6 mm instead of the winter average of 190.2 mm of the reference period 1970–2001. Subsequently during spring 2007, potential evapotranspiration values (82.9 mm/weeks) above the normal of 10.7 mm/weeks acted as a triggering factor of the drought episode through to April 2008. This has defined that due to the precipitation deficit of the first weeks, the SPI index has identified a 20 weeks earlier drought event. Moreover, the SPEI index usually provides early starting weeks, giving rise to longer drought events.

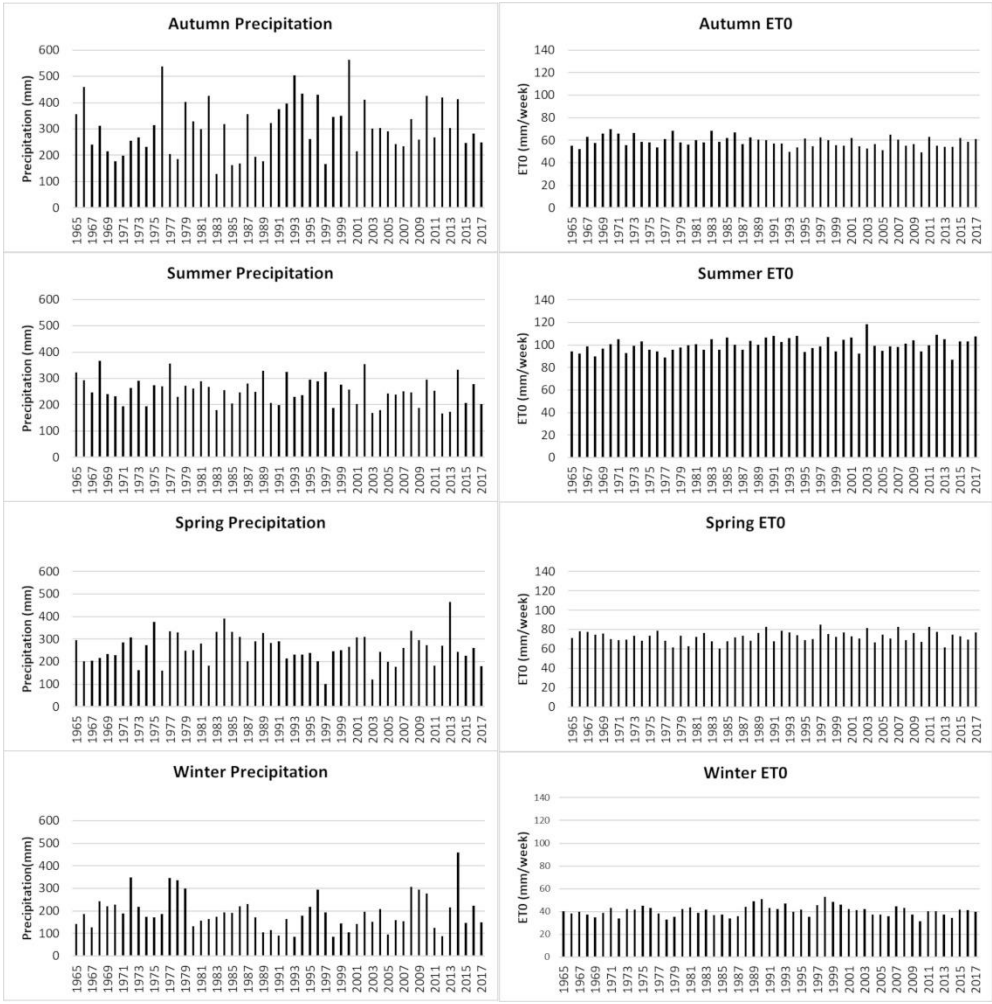

Figure13: In figure are reported in the left part the seasonal precipitation and in the right part the seasonal potential evapotranspiration (ET0) recorded in Po plain in the common period 1965–2017.

Table 10 also points out the two different propagation gradients observed in northern Italy: east to west and south to north. Detailed analysis is provided in the following section **6.1.2. Spatial propagation of drought**

6.1.1.2. Drought events comparison

The characterisation of droughts in the norther Italy was performed by mean of the investigation of two drought classes: severe which includes all the events with the index values between -1.82 and -1.65, and extreme that are all the episodes with the index values below -1.65.

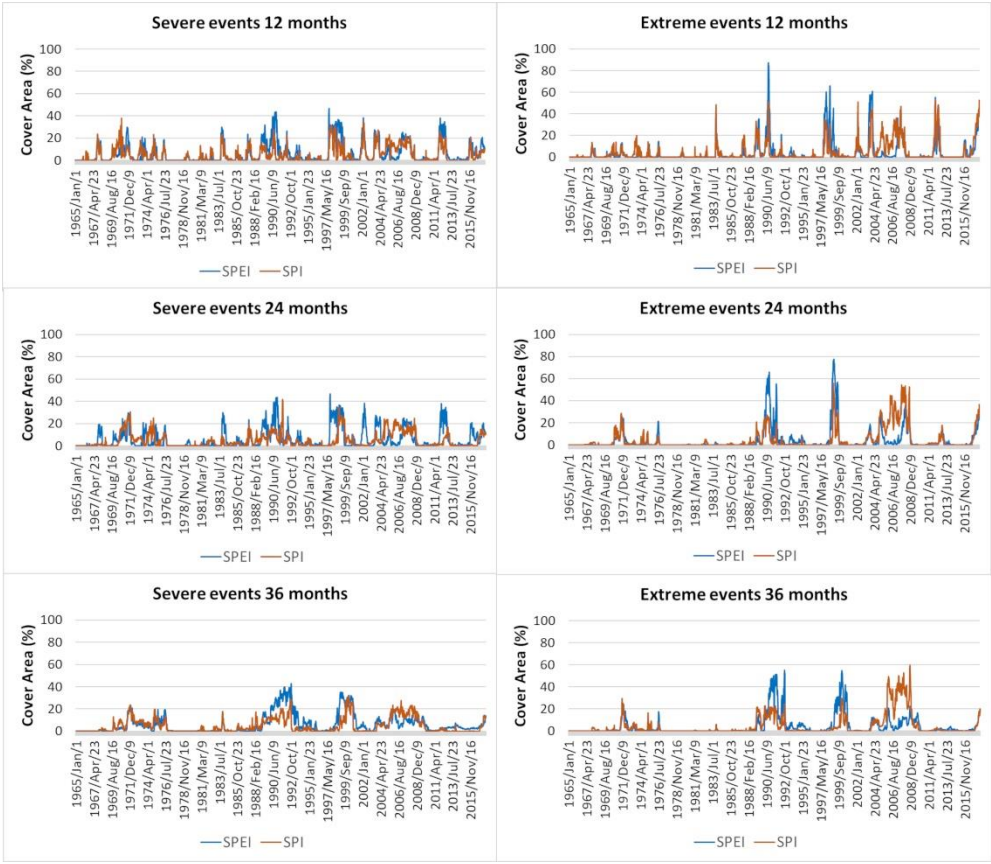

Figure 14: Evolution of the land affected by drought events at a 12, 24, and 36 month time scale for severe and extreme. The blue line is the land portion individuated by the SPEI and the orange is the one observed by the SPI index.

The effectiveness of the two drought indices in identifying historical severe and extreme drought events was tested comparing the percentage of total land affected by SPI and SPEI droughts, including both thresholds (Figure 14).

Obviously, detection of the surface area differs as a function of the threshold, with the weakest ones being higher, but there were also some differences between SPI and SPEI for the three timescales analysed.

Basically, the two indices detected the same events; however, they show different patterns in percentage of affected area, particularly between severe and extreme episodes. For drought at 12 months, Figure 14 shows that the majority of severe events reach threshold of 25% of the affected area, with a maximum of 42% and 44% in 1990 and 1997. While for extreme episodes, the number of events exceeding 25% are lower, but represent over 50% of the area under drought.

Figure 14 shows, again marked dissimilarities between SPEI and SPI records for the extreme event observed in 1990-1991 and 2006-2008. Therefore, in the previous section figure 13 has showed that during the last weeks (December 1, 1990-February 9, 1990) of the 1990-1991 drought event, the main triggering factor was a potential evapotranspiration above the normal. Figure 14 has confirmed this outcome, in fact on December 9, 1990 SPEI has identified a maximum percentage of area under drought of 81%, instead of the 60% of the SPI. Similar outcomes were reached also for the second event (2006-2008). In fact, figure 14 has evidenced that in the first weeks (October 1, 2006-March 1, 2007) the main drought triggering fact was a precipitation deficit. This has brought to a drought episode of 74 weeks for SPI, instead of 54 weeks for SPEI. This situation on October 1, 2006-March 1, 2007 is displayed in figure 14 with a percentage of area under drought of 2% recorded by SPEI, instead of the 37% of the SPI index.

However, figure 14 shows that on 24-month scales results are similar to those of 12-months. Whereas on the 36-month scale, unlike the 12-months, fewer events exceeded the 25% spatial threshold, and in particular, for the extreme events, the comparison highlighted the fact that peaks of severity have fallen to less than 50% of the study area. However, the relationship between timescales is far from simple: some episodes on the 12-month scale were not identified on the 24- or 36-month scales (Figure 14)

Differences in magnitude, length and percentage of area under drought between SPEI and SPI was also tested by means of the bubble plot. The bubble plot allows to compare the main severe and extreme SPEI and SPI drought events at 12-, 24- and 36-months (Figure 15). Each bubble represents the drought duration (x axis), magnitude (y axis) and percentage of area under

drought (size of the bubble). According with the previous results, figure 15 shows that, for both severe and extreme drought events, more episodes observed at 12-months scales were not detected at 24 and 36-month scales, and at long time scales, drought episodes become longer. For instance, according with extreme SPEI events, the mean length at 12-month was 15 weeks, at 24-months was 22 weeks and at 36-months was 33 weeks. A different behaviour between SPEI and SPI was also detected in episode length. In fact, the bubble plot (Figure 15) displays a good accordance between SPEI and SPI, but slight underestimation of the SPI length was detected. In fact, at 12-months for the SPI index, except for a few episodes, the mean length recorded is approximately 8 weeks for severe episodes and 12 weeks for extreme ones. While SPEI identified severe drought events with mean length of 10 consecutive weeks and extreme episodes of 15 consecutive weeks.

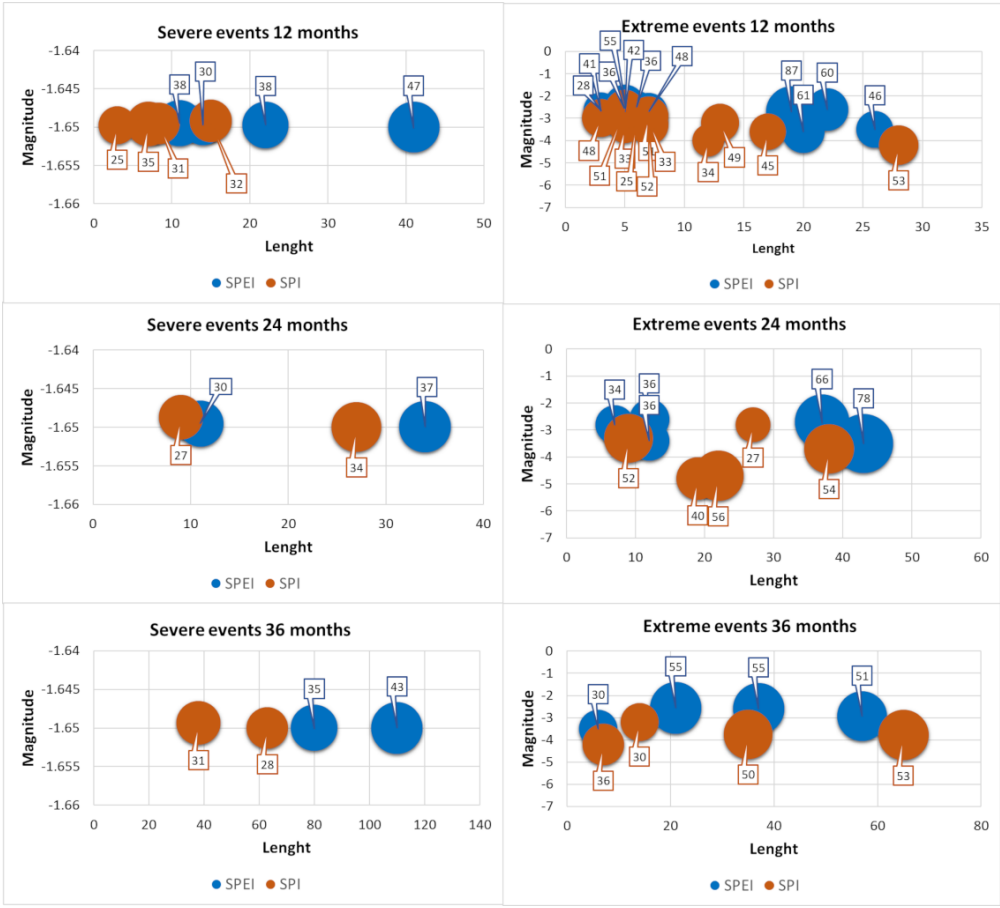

Figure 15: Comparison of the main drought episodes (severe and extreme) calculated by means of SPEI and SPI at 12, 24, and 36 months. Each bubble gives the duration (x), magnitude (y), and percentage of area under drought (bubble size). Blue colour is used for SPEI, whereas orange for SPI.

Finally, the last step of the comparison between the two indices, SPE and SPI, for severe and extreme episodes at 12, 24, and 36 months was performed observing the difference of percentage of total land surface under drought recorded by SPEI and SPI (Figure 16). Positive values indicate a larger area of drought according to the SPEI and vice versa. Figure 16 indicates different behaviour between the two indices, which is quite clear for the extreme episodes. In fact, Figure 16 shows that 2000 should be a turning point, in fact since 2000, SPI has detected longer and more severe drought episodes than

the SPEI. While before 2000 SPI events used to observe drought events that interest a larger area instead SPEI.

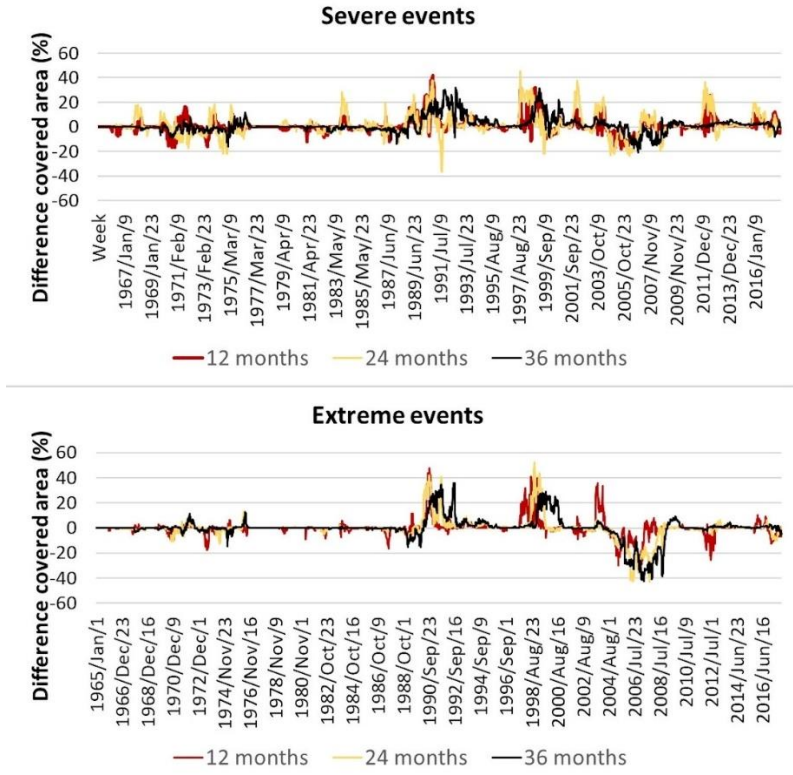

Figure 16: Difference of land affected by severe and extreme drought between SPEI and SPI. The red colour represents the temporal scale of 12 months, the orange one is for 24 months, and the black one is for 36 months.

In order to be able to fix a precise year of turning point, in table 11 is reported an extract of the sequential Mann-Kendall test applied on the SPEI and SPI difference series at 12 months.

Table 11: Sequential Mann-Kendall test applied on the SPEI and SPI difference series at 12 months. Where PROG is the progressive row Kendall's normalized tau's, RETR is the retrograde e row Kendall's normalized tau's, and TP indicate at what indices of the original timeseries the PROG and RETR cross, i.e. TRUE at potential trend turning points.

YEAR	PROG	RETR	TP
2001	2.46	1.13	FALSE
2002	2.75	0.55	FALSE
2003	2.93	0	TRUE
2004	3.02	-0.61	FALSE
2005	3.09	-1.12	FALSE
2006	3.14	-1.68	FALSE
2007	2.83	-2.18	FALSE
2008	2.28	-2.25	FALSE
2009	1.75	-1.98	FALSE
2010	1.27	-1.4	FALSE
2011	0.86	-0.71	FALSE
2012	1.1	0	FALSE
2013	1.09	-0.37	FALSE
2014	0.93	0	FALSE
2015	1.04	0.37	FALSE
2016	1.31	1.22	FALSE
2017	1.45	0.33	FALSE

Table 11 shows that for the year 2003 the sequential Mann-Kendall test identified a turning point (TP column). This is in agreement with the results obtained comparing SPEI and SPI. Thus, two different behaviour of the two drought indices was observed since the detection of the main drought events with the identification of the 1990-1991 and 2006-2008 drought events, where the greatest difference between SPEI and SPI were underlined.

6.1.2. Spatial propagation of drought

The analysis of the major drought episodes, displayed in the previous section **6.1.1.1. Main drought event** highlighted that two different gradients interested the northern Italy. The first one is east to west, and the second one is south to north (Table 10). These two gradients were recognized in a specific

sequence of charts over the analysed period. From 1983 to 1991, the main propagation gradient was EW, then until 2017, SN predominated except for 2003. To Follow the two main drought events that are characterised by a East to West and South to North propagation gradient.

Drought event August 9,2003-April 23, 2004

The major episode observed under an east–west propagation gradient was on August 9, 2003–April 23, 2004 lasting for 35 consecutive weeks (Figure 17), an event generated in the north-eastern sector, close to the Carnican and Julian Alps.

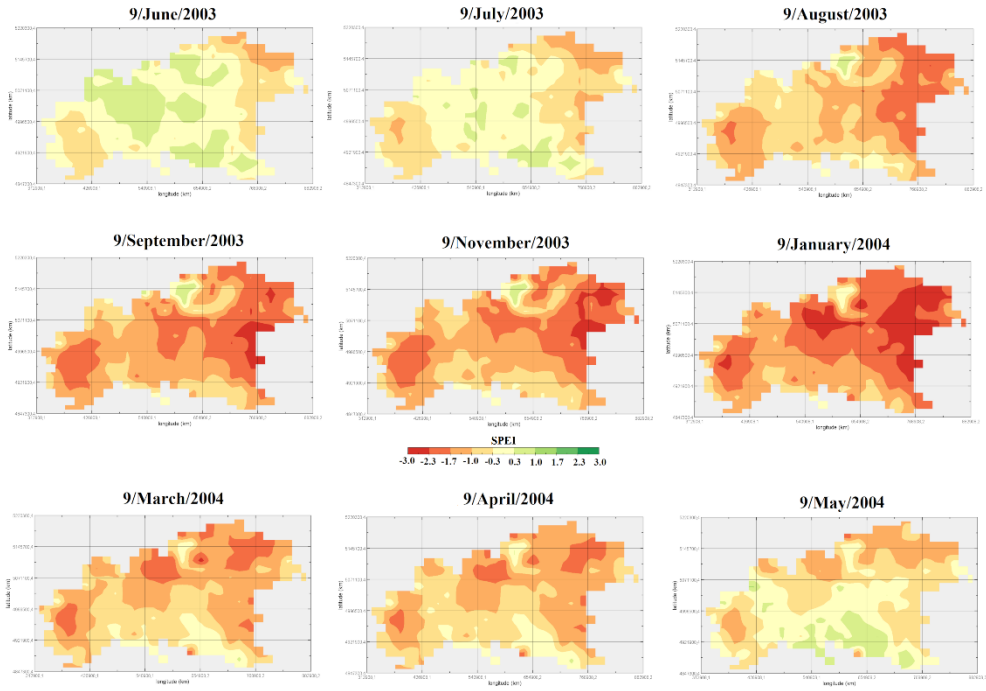

Figure 17: Spatial and temporal evolution of the drought event observed in the August 9, 2003–April 23, 2004 period.

The temporal evolution of this event, has showed that it was generated in August 9, 2003 in the eastern part of the study area, and SPEI values between

-2.0 and -2.5 were recorded in Trieste (Friuli-Venezia Giulia). Subsequently figure 16 shows a westward evolution of drought and in January 2004 the cities of Trieste (Friuli-Venezia Giulia), Milan (Lombardy), Bologna (Emilia-Romagna) and Turin (Piedmont) were characterised by SPEI values between -1.4 and -2.3. The spatial evolution of the drought also showed clear asymmetry between the northern (Alpine chain) and southern (Apennine chain) part of the study area. In fact, during the 35 weeks of drought, the southern part of the study area recorded SPEI values close to zero (0 and −0.8), and the city of Genoa, the capital of Liguria, recorded for the whole period SPEI values between –0.3 and .1.2. This suggests that the southern sector of Italy was undergoing a slight precipitation deficit. Whereas the northern part was interested by severe drought conditions with SPEI values between −3 and −1.5, except for the Valtellina valley, where a water surplus was recorded with SPEI values between 0 and 1.5. The analysis of extreme drought event reported in Table 12 has pointed out that the greatest part of the drought event should be classified as extreme, in fact from August 16, 2003 to April 24, 2004 an extreme event of 27 consecutive weeks was recorded. This event was characterised by a SPEI value of -3 and an average of area under drought of 70%. The episode was also analysed observing the temporal evolution of the percentage of area under drought (Figure 18). Figure 18, shows that the maximum of percentage of area under drought was reached on February 9, 2004 with 80% and the absolute minimum SPEI values was -3.6.

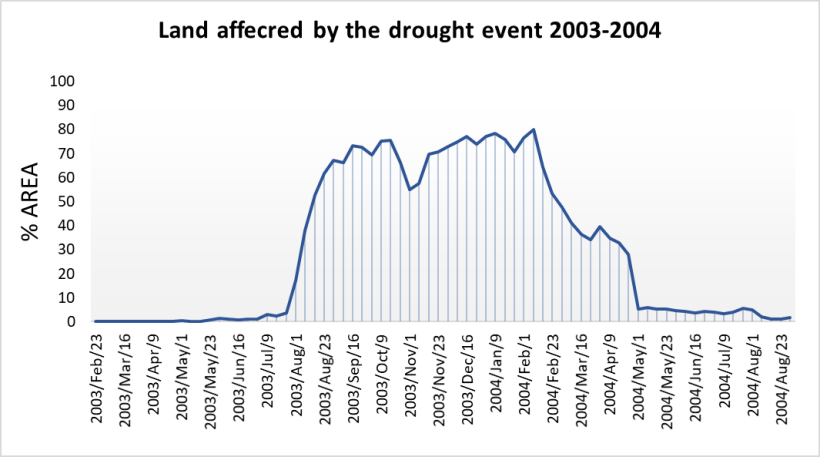

Figure 18: Temporal evolution of the percentage of land covered by the drought episode recorded in August 9,2003-April 23, 2004.

Drought event December 23, 2011-October 16, 2012

The second major episode was identified from December 23, 2011 to October 16, 2012, lasting for 47 consecutive weeks (Figure 19).

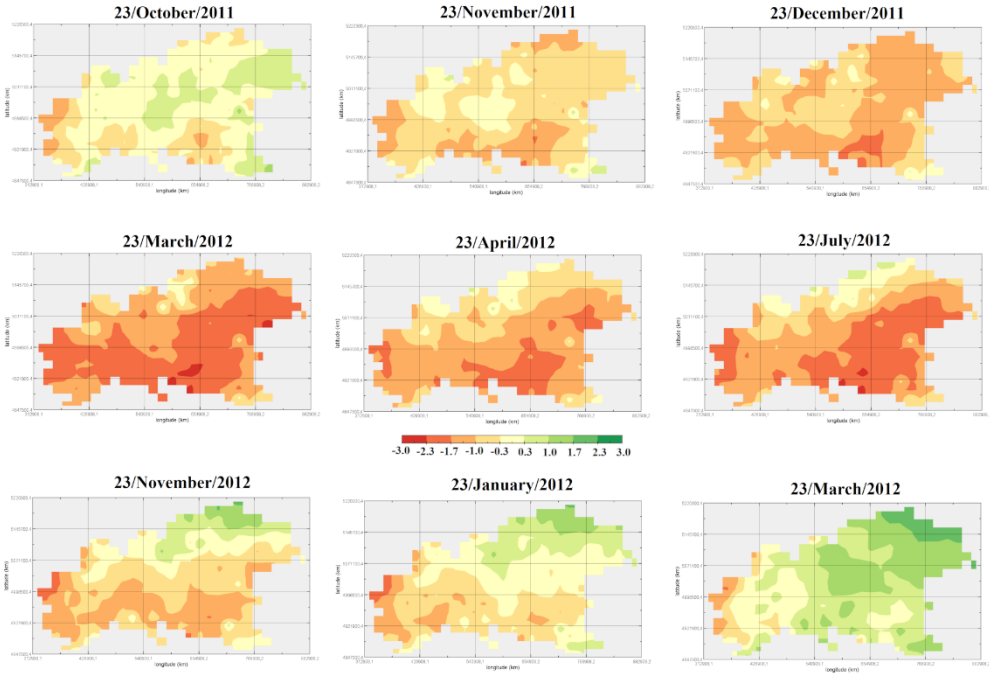

Figure 19: Spatial and temporal evolution of the drought event observed in the December 23, 2011–October 16, 2012 period.

The spatial evolution of drought runs in a south to north gradient. On December 23, 2011, a SPEI value between −3 and −2.3 was recorded in the greatest part of the south (Apennines chain) with 25% of the area under drought, in fact in the cities of Genova (Liguria) and Bologna (Emilia-Romagna) SPEI values were between -1.7 and -2.5. Whereas in the north, no drought condition was detected (SPEI close to 0). Subsequently on March 2012 the greatest part of the study area was interested by drought with SPEI values between -1.4 and -2.7 for the cities of Genoa (Liguria), Bologna (Emilia-Romagna), Trieste (Friuli-Venezia Giulia) and Venice (Veneto). Differently from the previous analysed event, in this case the drought evolution was characterised by two extreme events evidenced by table 12. In

fact, the south to north evolution was evident during the two drought extremes reached on March 9, 2012–April 9, 2012 and on July 16, 2012–September 1, 2012, that mainly interest the south-eastern sector of the study area. Figure 19 shows that, the northern part of the study area acts as a barrier, suggesting that northern Europe did not experience drought conditions. In particular, the two extreme events were short (5 weeks for the first and 7 weeks the second), and they respectively involved 71% and 61% of the northern Italy territory. As the previous event, the episode was also analysed by analysing the temporal evolution of the percentage of area under drought (Figure 20). Figure 20 shows that on March 23, 2012 the first drought peak was reached with a magnitude of -2.4 and 78% of area under drought. While the second one was recorded on July 23, 2012 with magnitude of −2.7 and 68% of the study area was touched by drought. A third peak was observed on November 1, 2012 with 50% of area under drought, but the extreme event analysis did not bring it to light, because this was 1 week lasting event.

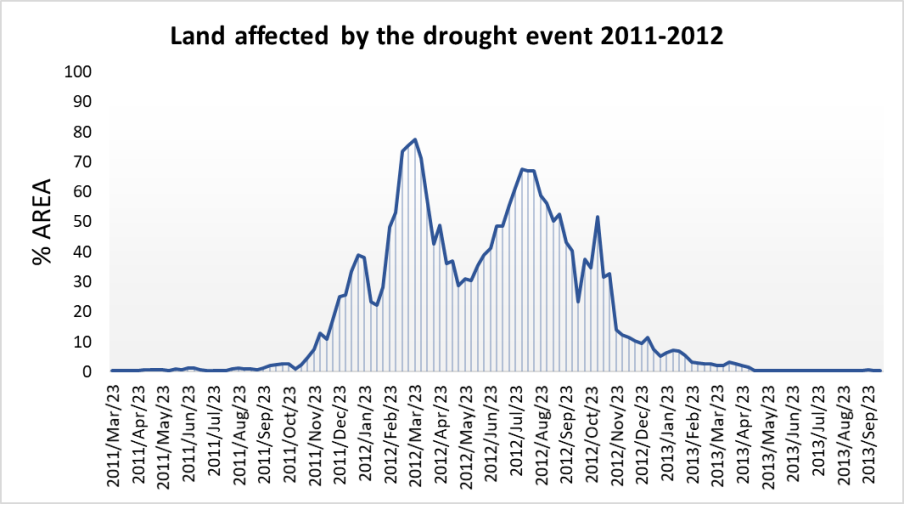

Figure 20: Temporal evolution of the percentage of land covered by the drought episode recorded in December 23, 2011-October 16, 2012.

Table 12: Characterization of extreme drought episodes observed in the 1961–2017 period by SPEI and SPI, calculated at 12 months. For each detected event are reported the propagation gradient, starting week and ending week, and duration length.

SPEI				SPI			
Period	**Length**	**Magni**	**Area**	**Period**	**Length**	**Magni**	**Area**
1983/Nov/23-1983/Dec/9	3	-2.6	41	1983/Nov/23-1983/Dec/9	3	-3.1	49
1989/Feb/1-1989/Feb/16	3	-2.7	29	1989/Jan/23-1989/Feb/23	5	-3.4	33
1989/May/16-1989/Jun/23	6	-2.5	36	1989/May/23-1989/Jun/23	5	-2.9	25
1990/Jul/9-1990/Nov/23	19	-2.7	84	1990/Aug/16-1990/Oct/9	8	-2.9	51
1997/Nov/16-1998/Apr/1	19	-2.8	60	1998/Jan/1-1998/Apr/1	13	-4.1	34
1998/Jun/23-1998/Sep/9	11	-3.9	66	1998/Aug/1-1998/Aug/23	4	-3.5	30
2002/Mar/23-2002/Apr/23	5	-2.7	42	2002/Mar/23-2002/Apr/23	5	-2.6	51
2003/Aug/16-2004/Mar/1	27	-3	70	2003/Oct/9-2004/Feb/9	17	-3.7	44
2007/Aug/9-2007/Oct/16	10	-2.6	36	2007/Aug/9-2007/Oct/16	10	-2.9	33
2012/Mar/9-2012/Apr/9	5	-2.4	71	2012/Feb/23-2012/Apr/9	7	-3.3	51
2012/Jul/16-2012/Sep/1	7	-2.7	61	2012/Jun/1-2012/Sep/23	16	-3.3	48
2017/Aug/1-2017/Dec/23	20	-3.5	46	2017/Jun/9-2017/Dec/23	27	-4.3	51

6.1.3. Drought trends

The drought spatial trend and its statistical significance were calculated on SPEI and SPI at 12-, 24- and 36- months by mean of the Mann-Kendall test. The results obtained for all the timescales showed the same behaviour. For this reason, in figure 21 are represented the spatial trend and its statistical significance (p-value 95%) for the 12 months SPEI and SPI. The comparison between SPEI and SPI results has highlighted that SPEI negative trends are more intense than SPI. In detail figure 21 shows that in the norther Italy the

western and south-western sectors documented marked negative trends of the two drought indices, instead of the eastern part.

For SPEI 12-months the analysis has detected that in the 1965-2017 period negative trends involved 55% of the study area, and the lowest values were recorded in the western and south western part (Figure21). In fact, in proximity of the main mountain chain (Western Alps and Maritime Alps) a maximum decrease of the index between -3 and -2 was recorded. The analysis has also figured out that all the negative trends recorded in these sectors are statistical significative, with p-values below or equal to 0.05. Figure 21 shows that in the other parts of the northern Italy drought trends are no statistical significative and close to zero, except for small portions in the north and north-eastern area were positive and significative trends are identified.

For SPI 12-months, figure 21 shows that, instead of SPEI results, negative trends are also recorded in the southern and north eastern part of the study area, with 70% of the northern Italy involved. The most of these sectors did not recorded statistical significance trends, expect for the central-western portion of the Po Pain where a statistical significance trend of the SPI value of -2 was identified. According with SPEI, in the north eastern sectors positive or close to zero no significative trends were detected, except for a northern part, at the border with the Po Plain where positive (-2 and +3) and statistically significative trends were recorded.

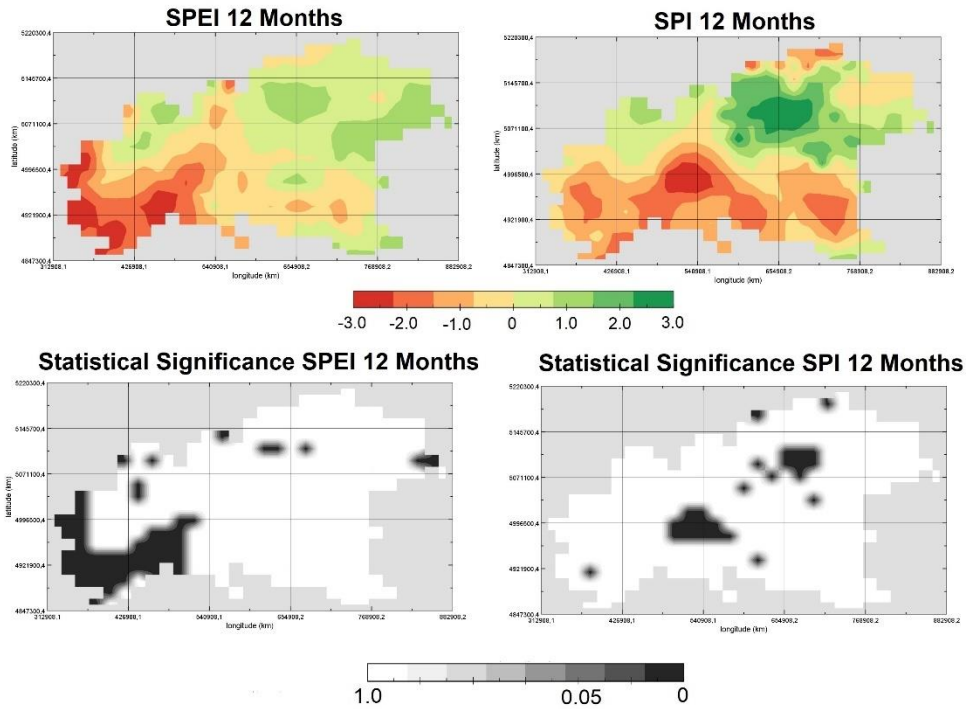

Figure 21: Spatial distribution and statistical significance of the 12-month SPEI and SPI trends for the 1965-2017 period in northern Italy.

6.2. Future projection models

In this section the results of the drought characterisation performed on the EURO-CORDEX and MED-CORDEX RCM-GCM couples in the norther Italy for the main near (2020-2049) and far (2070-2099) future periods are reported for the RCP 4.5 and 8.5. Therefore, the main future drought events are displayed, and their temporal and spatial evolution is investigated. Moreover, severe and extreme future drought events were analysed in case of a global warming of +2 or +3 °C above preindustrial levels

6.2.1. Future drought characteristics

The model validation procedure (previously described in section **4.3. Models validation**) has underlined that among the GCM/RCM couples, the EC-EARTH-RACMO22E and MPI-ESM -CCLM4 for both the RCP 4.5 and 8.5

are the less reliable for the northern Italy. In fact they provided the worse comparisons, between data recorded at the ground a projected by the models with the highest Root Mean Square Error (RMSE) in the extreme event class

The main near (2020-2049) and far (2070-2099) future 30-yr periods as identified by SPEI and SPI at the 12-month time scale, for RCP 4.5 and RCP 8.5 were identified. Likewise, the analysis performed on the 1965-2017 period, drought episodes were identified by mean of SPEI and SPI indices and must follow three parameters: have a minimum length of 3 consecutive weeks, involve at list the 25% of the norther Italy and fall into two different event classes, severe and extreme. In this regard for each 30-y period the number of the main future events, the duration and the percentage of area involved were investigated. In figure 22 the plain-coloured histograms represent the SPEI results, while the dotted pattern marks the SPI outcomes. For each combination of RCM and GMC, the figure reports the total number, the mean percentage of affected area, and the mean duration of the drought events for the considered 30-yr period.

A good agreement between the SPEI and SPI results is observed, especially for the number of drought events. In fact, figure 22 indicates that in most cases both indicators identify the same number of episodes, with the highest differences observed for the less reliable model couples (EC-EARTH-RACMO22E and MPI-ESM -CCLM4). For RCP 4.5 in the period 2020-2049 (near future), SPEI identified 5 to 7 extreme drought episodes, while SPI detected 4 to 6 extreme drought events. For the far future (2070-2099), the number of drought episodes will increase for the majority of the reliable model couples with 6 to 8 events for SPEI and 5 to 7 episodes for SPI. The results for RCP 8.5 revealed that SPEI identify between 5 and 8 extreme drought events in the near future, with a further increase for the 30 years in the far future (7 to 9). Analogously SPI recorded 5 to 8 events for the first 30-y period and a slight increase will be expected for the far future with 6 to 9 events.

Looking at the percentage of area affected by drought, SPI provided lower values than SPEI (Figure 22). In both scenarios SPEI detected drought events that are spatially more extended than those identified by SPI. In particular, for RCP 8.5 this difference becomes marked for the two couples EC-EARTH-HIRHAM5 and HadGEM2-CCLM4. Overall, the drought characterisation provided by SPEI indicated that for the concentration pathway RCP 4.5 in the 2020-2049 period, the maximum percentage of area interested by an extreme

drought event will range between a minimum of 37% in CM5-ALADIN52 to a maximum of 49% in HadGEM2-RACMO22. A further increase of drought-affected area is expected for the last thirty years of the century, with a maximum of 55% simulated by the couple HadGEM2-RACMO22E. The highest increment is provided by the model couple CM5-ALADIN52, with +12% of area affected by drought (Figure 22). An increase of the spatial extent of individual drought events will also be observed in the 2070-2099 period, with a maximum of 68% of interested area during a single episode as simulated by HadGEM2-RACMO22 for the RCP 4.5 scenario. Comparing the two scenarios, the percentage of area interested by drought episodes is even larger in RCP 8.5: in the near future this percentage will range between 49% and 55% for respectively CM5-ALADIN52 and HadGEM2-RACMO22E.

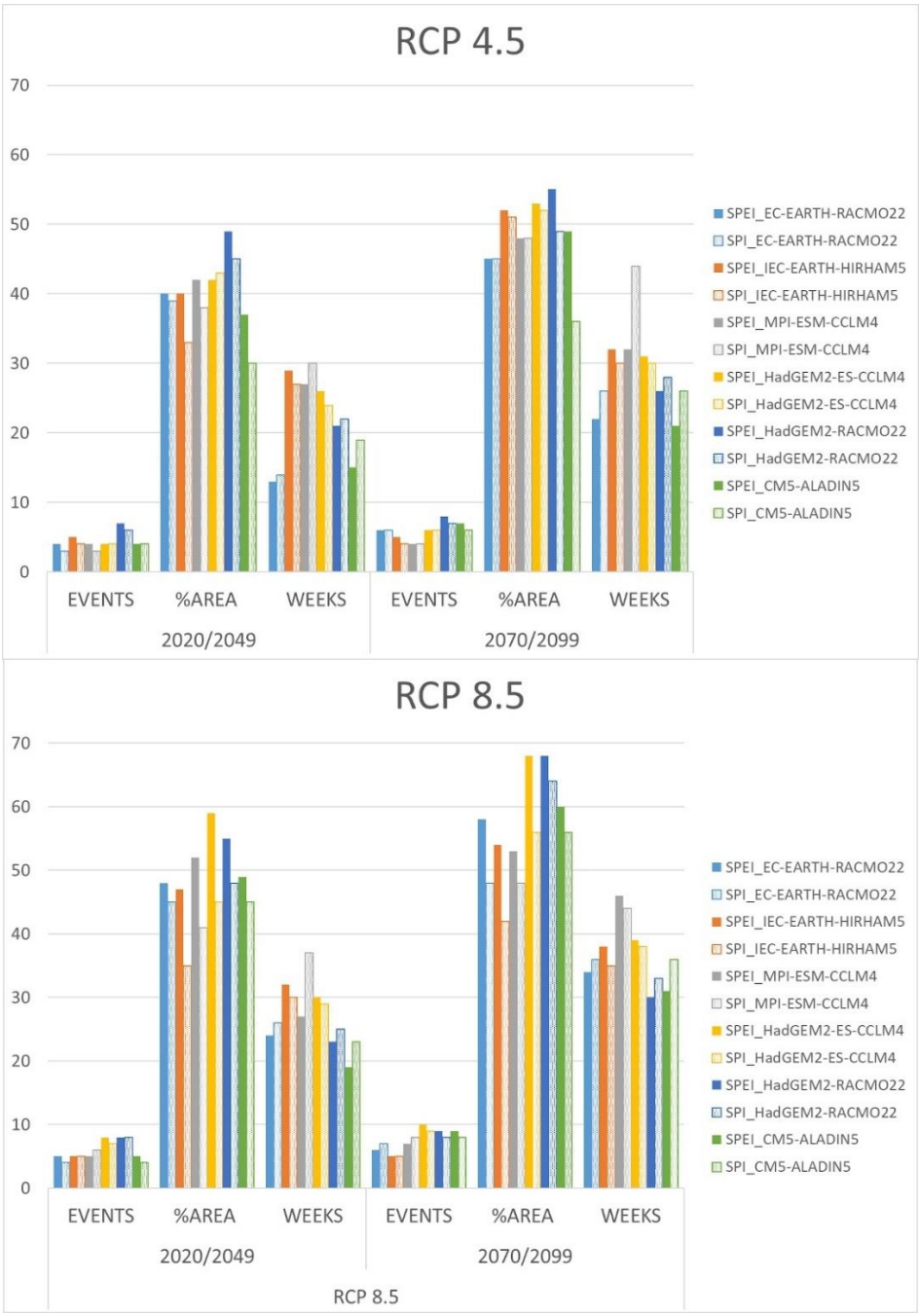

Figure 22: Number of drought events, mean percentage of area affected by drought and mean number of consecutive drought weeks expected for the near (2020-2049) and far future (2070-2099). Colors identify different models couples as indicated in the legend. The plain-coloured histogram represents 12-month SPEI results, and the dotted pattern indicates 12-month SPI outcomes.

For the maximum duration of the main drought events, SPI and SPEI behaved differently across model couples. For EC-EARTH-HIRHAM5 and HadGEM2-ES-CCLM4, SPEI detected a longer duration than SPI, and vice-versa for HadGEM2-RACMO22E and CM5-ALADIN52. The largest difference is recorded by CM5-ALADIN52 for both RCPs, with SPI indicating events that are 4-5 weeks longer than for SPEI. The drought analysis based on SPEI indicates, for the period 2020-2049 in the RCP 4.5 scenario, a maximum duration of a drought event ranging between 15 consecutive weeks for the CM5-ALADIN52 pair and 29 weeks for EC-EARTH-HIRHAM5 (figure 22). A further increase in the duration of drought events is expected for the last 30 years of the century: for the period 2070-2099 the maximum duration will be between 21 and 32 weeks, respectively estimated by CM5-ALADIN52 and EC-EARTH-HIRHAM5. The RCP 8.5 scenario reveals more severe drought events, both in terms of affected area and continuous duration. For the near future, in RCP 8.5 the drought duration is expected to be 3 to 4 weeks longer for CM5-ALADIN52 and EC-EARTH-HIRHAM5. The drought duration will further increase for the period 2070-2099, with a maximum increase of 12 consecutive weeks as simulated by CM5-ALADIN52 (figure 22).

Overall, the analysis has indicated that the SPEI and SPI detect the same drought events, with somehow different results in the percentage of affected area and drought duration.

The last step of the comparison, for the near and far future, of the SPEI and SPI results on the percentage of drought affected area calculated at 12-, 24- and 36-month time scale is performed. Because clearer outcomes are gained for the extreme events, in figures 23 and 24 are reported the SPEI and SPI extreme event comparison for the four reliable model couples under respectively RCP 4.5 and RCP 8.5. In figures positive values stand for SPEI episodes that are more extended than SPI. Unlike the 1965-2017 period, figure 23 shows that for both near and far future the comparison did not evidenced a clear behaviour. In fact, in 2020-2049, for all the GMCs/RCMs couples there is a tendency of SPEI to detect more severe drought events in terms of spatial extent, especially towards the end of the period. In particular this becomes more marked for the couples EC-EARTH-HIRHAM5 and CM5-ALADIN52 where since the 2030s positive values of the plots are identified suggesting that the main triggering factor that will drive droughts in the near future will be a potential evapotranspiration above the normal. While for 2070-2099, the

difference between SPEI and SPI is more variable, and was not possible detect a period of overestimation and underestimation of the two indices.

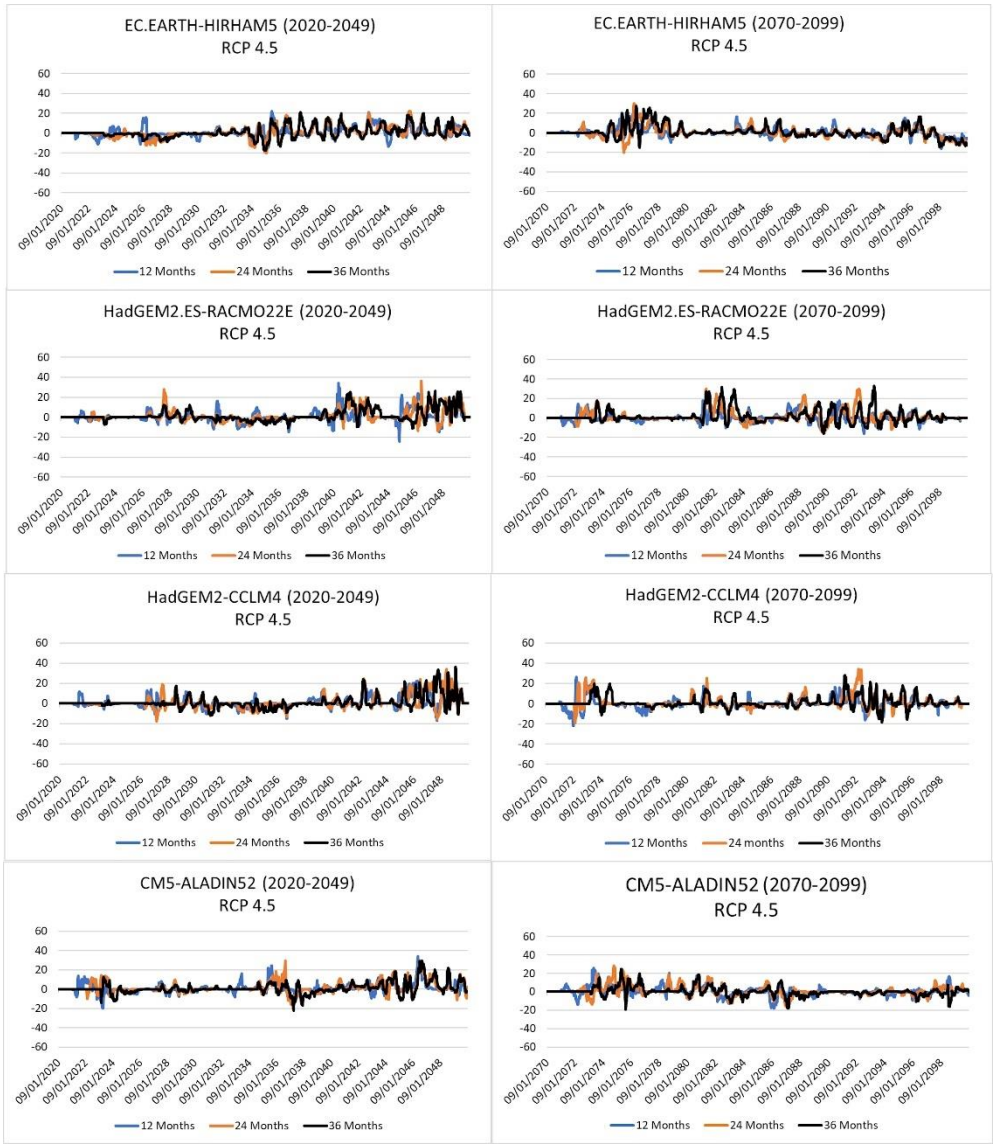

Figure 23: Difference in the percentage of area affected by intense drought events as estimated by SPEI and SPI for RC 4.5, as a function of time. Left panels are for the near future (2020-2049) and right panels for the far future (2070-2099). Model couples are indicated in the legends. The blue lines stand for a temporal aggregation scale of 12 months, orange is for 24 months, and black is for 36 months.

Figure 24 shows that for the RCP 8.5 the comparison on the percentage of drought affected area identified a tendency of SPEI overestimation for the 30 years period 2020-2049, suggesting that the main triggering factor will be the potential evapotranspiration above the normal. This is marked for the EC-EARTH-HIRHAM5 couple. While for the other three couples the plots show that for the greatest part of the near future SPEI and SPI will record events equally spatial distributed, and for shorts periods (i.e. 2040-2050 for CM5-ALADIN52 or 2020-2030 for HadGEM2-CCLM4 and HadGEM2-RACMO22) SPEI will detect more severe drought events in terms of spatial extent. While for the far future period (2070-2099) a not clear situation of overestimation and underestimation of the two indices was again observed.

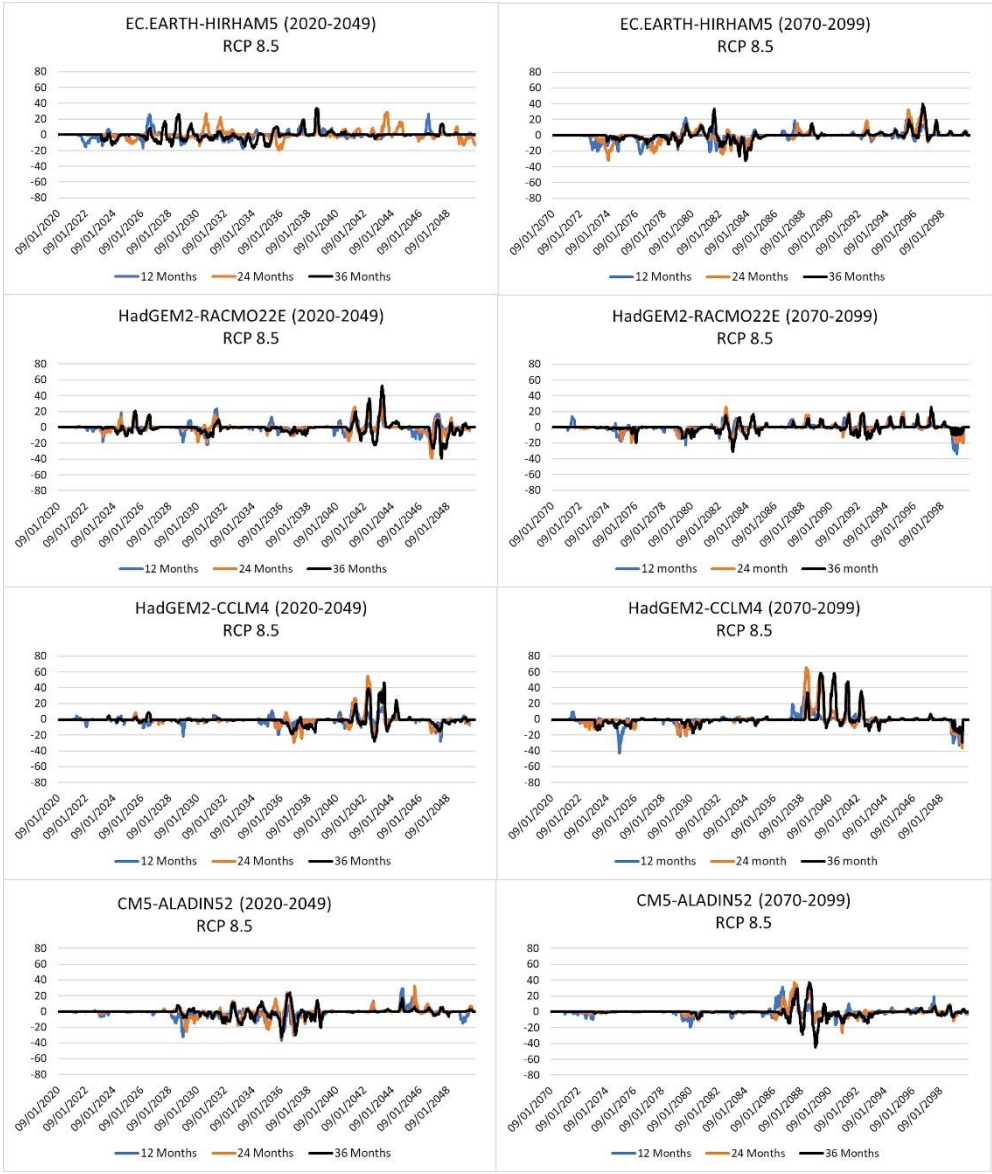

Figure 24: Difference in the percentage of area affected by intense drought events as estimated by SPEI and SPI for RC 8.5, as a function of time. Left panels are for the near future (2020-2049) and right panels for the far future (2070-2099). Model couples are indicated in the legends. The blue lines stand for a temporal aggregation scale of 12 months, orange is for 24 months, and black is for 36 months.

6.2.2. Drought trends

The analysis of the most intense drought events identified an increase of severity increasing in the 2070-2099 period, in terms of both duration and percentage of drought-affected area.

In this regard the spatial distribution of the two drought indices was investigated in order to detect which areas of the northern Italy will be mostly interested by a drought severity increase. Figures 25 and 26 report the 12-month SPEI and SPI trends and their statistical significance in the 2020-2100 period for RCP 4.5, for the four most reliable model couples. While figures 27 and 28 report the trend analysis for the RCP 8.5 for SPEI and SPI respectively.

For the SPEI RCP 4.5 (figure 25), HadGEM2-CCLM4, HadGEM2-RACMO22 and CM5-ALADIN52 showed a significant intensification of droughts along the Alpine chain (northern part of the study area). In this area, the drought index is expected to decrease between -1.2 and -2.4 with respectively 27%, 25%, 29% of area interested. In the other parts of northern Italy, three model couples indicate no significant trends for the 2020-2100 period, while EC-EARTH-HIRHAM5 estimates a significant increase of droughts also in the central portion (North of the Po Plain) with 56% of area under drought.

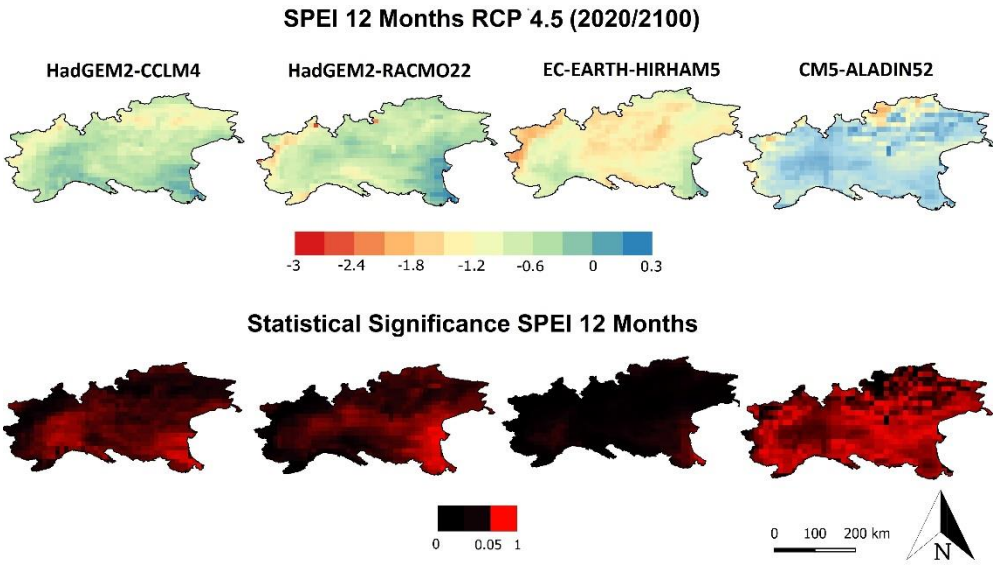

Figure 25: Spatial distribution and statistical significance of the 12-month SPEI trends for the 2020-2100 period in northern Italy for RCP 4.5. The four most reliable model couples are considered.

While for the SPI RCP 4.5, figure 26 shows that SPI used to detected fewer negative trends instead of SPEI, in particular for all the reliable GCM/RCM couples the positive trend are not statically significative. For HadGEM2-CCLM4, HadGEM2-RACMO22 and EC-EARTH-HIRAM5, the only statistically significant trends are observed in the western part of the study area, in proximity of the Piedmont region, with respectively 20%, 11% and 7% of area interested. Therefore, in this sector a decrease of SPI values between -1.2 and -1.8 is expected.

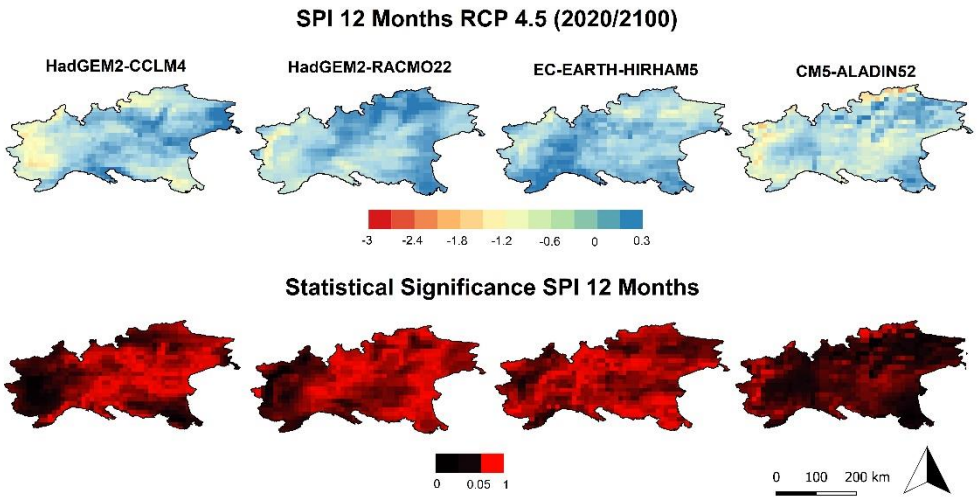

Figure 25 Spatial distribution and statistical significance of the 12-month SPI trends for the 2020-2100 period in northern Italy for RCP 4.5. The four most reliable model couples are considered.

For SPEI RCP 8.5, figure 27 reveals that the models estimate a dramatic increase of drought severity. For HadGEM2-CCLM4, HadGEM2-RACMO22, EC-EARTH-HIRAM5 and CM5-ALADIN52 the analysis showed significant negative trends, which becomes especially intense in the Alps with values between -1.8 and -3. Specially for HadGEM2-CCLM4, HadGEM2-RACMO22 negative significant trend are estimated for the whole study area.

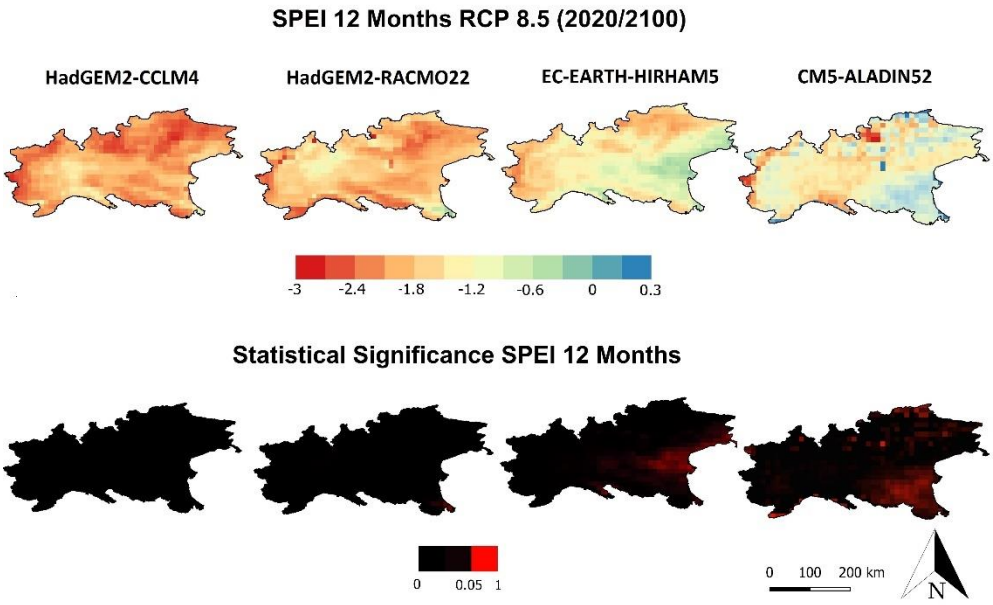

Figure 26: Spatial distribution and statistical significance of the 12-month SPEI trends for the 2020-2100 period in northern Italy for RCP 8.5. The four most reliable model couples are considered.

While for SPI RCP 8.5, figure 28 showed a more critical situation instead of the scenario RCP4.5, but unlike the results obtained for SPEI, not the whole study area will be interested by a drought intensification. In fact, the four reliable models couples, estimated a significative increase of drought severity (-1.8 and -2.4) in two different part of the study area. The wester sector, along the Occidental Alps, and the central part of the Po Plain with a total percentage of area under drought of 52%, 45%, 72% and 69% respectively.

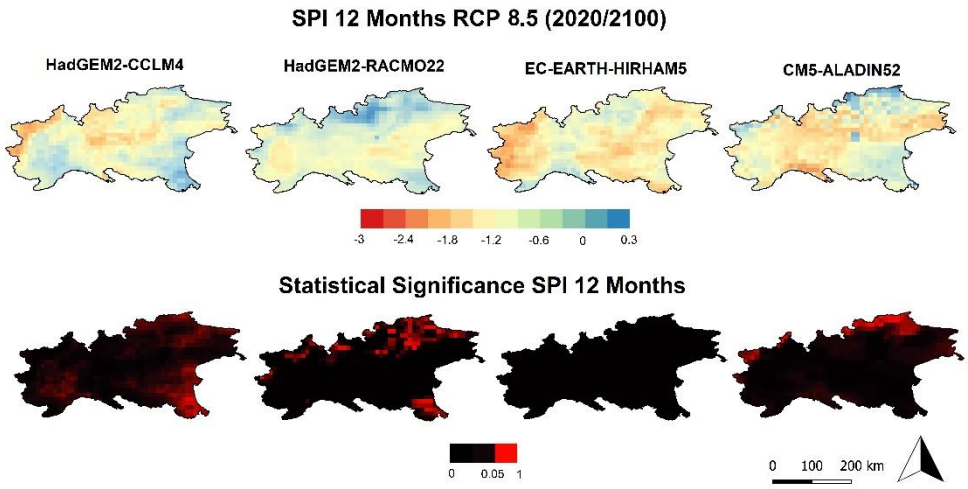

Figure 28: Spatial distribution and statistical significance of the 12-month SPiI trends for the 2020-2100 period in northern Italy for RCP 8.5. The four most reliable model couples are considered.

6.2.3. Drought spatial propagation

Finally, the change in the spatial extent of drought episodes was then investigated considering how droughts develop in case of a global warming of +2 or +3 °C above preindustrial levels, in keeping with the recent IPCC reports. Figures 29 and 30 shows the spatial extent of respectively severe and extreme drought events according to SPEI and SPI at 12-months. For severe drought episodes (Figure 29), SPEI detected more spatially extended events. Both indicators reveal that drought events at +2°C of global temperature increase will be homogenously distributed in the study area, with durations between 5 to 15 consecutive weeks. In a few sectors along the Alps, droughts with a duration of 20 weeks are present. Moving to the +3°C temperature warming, no relevant increase of severe drought events is observed.

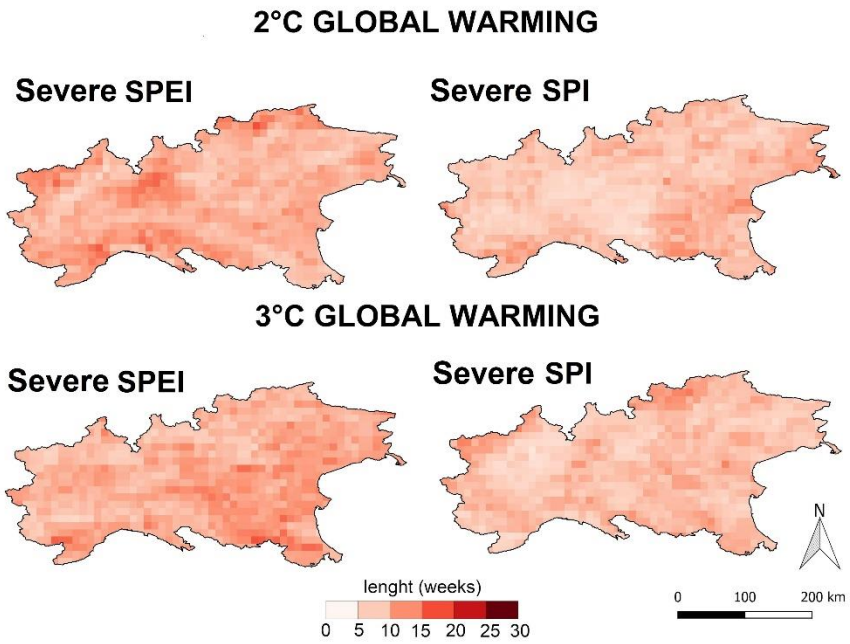

Figure 29: Spatial distribution (in consecutive weeks) of drought duration for heavy events, computed from SPI and SPEI. The upper plots refer to a global warming of +2 °C, and the lower plots to a warming of +3 °C.

On the contrary, extreme drought episodes show a strong increase. In the whole study area, an increase of drought duration is expected, reaching 10-30 consecutive weeks. In particular figure 30 shows that for a +2°C global warming the sector that will be mostly interested by the longest drought events are the Alps with duration of also 30 consecutive weeks. While, for a +3 °C global a clear north to south prorogation gradient is evidenced, in fact, the southern portion of the Po Plain is expected to experience severe drought events with duration of 30 consecutive weeks, while for the Alps the duration will decrease at 10-20 consecutive weeks.

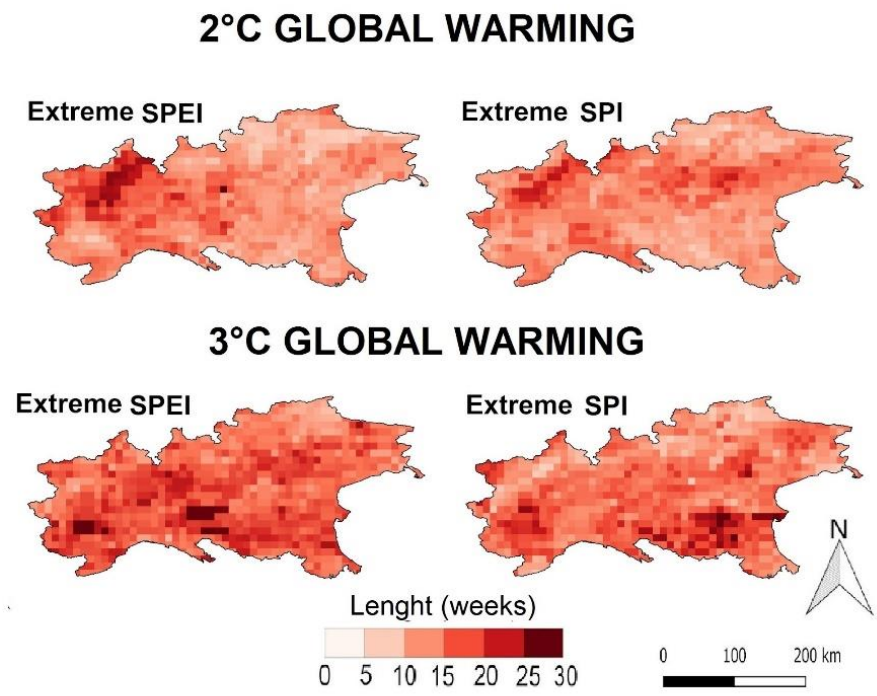

Figure 30: Spatial distribution (in consecutive weeks) of drought duration for severe events, computed from SPI and SPEI. The upper plots refer to a global warming of +2 °C, and the lower plots to a warming of +3 °C.

CHAPTER 7: DISCUSSION

The present study gives a novel contribution to the assessment of the temporal and spatial variability of drought conditions in northern Italy since 1965, focusing the attention on three study periods, past (1965-2017), near future (2020-2049) and far future (2070-2099).

The work allowed the creation of two different database for the northern Italy.

- For the 1965-2017 period, the database is made up 88 of historical daily temperature and precipitation ground series from the SCIA (National System for the Collection, Processing and Dissemination of Climatic Data of Environmental Interest) database.
- For the two periods 2020-2049 and 2070-2099, the database is made up of 12 daily temperature and precipitation ensembles at spatial resolution of 0.11 degree (12 km) from the RCMs RACMO22E, HIRHAM5, CCLM4 and ALADIN52, driven by the EC-EARTH, MPI-ESM, HadGEM2 and CM5 GMCs.

The need of high quality, continuous and homogeneous records lead to retain 88 time series recorded at the ground that have been quality controlled, reconstructed and homogenised in order to identify and correct the erroneous values for the past period (1965-2017). While for the near future (2020-2049) and far future (2070-2099) the performance of the 12 models couples was tested by comparison against models-ground observations for weak, mean, heavy and extreme events.

Because is well known in literature that drought episodes are hard to quantify and identify in terms of onset, end, duration and magnitude (Wilhite, 2000). The study proposed to use two drought indices, the Standardised Precipitation Index (SPI) and the Standardised Precipitation Evapotranspiration Index (SPEI), to analyse for the first time in the international literature, past and future drought episodes in a region apparently rich in water resources. In fact, even if northern Italy completely falls into the Mediterranean Basin, it could be considered as a borderline Mediterranean climate region, mainly characterised by a temperate climate (Cfa and Cf, Fratianni and Acquaotta, 2017).

The main drought events were identified following three parameters: the minimum duration must be of 3 consecutive weeks, they have to interest at least 25% of the northern Italy, and the events were classified in severe and extreme following the indices thresholds. In this regard the main past and future drought episodes were characterised in term of starting and ending data, duration in weeks, magnitude and percentage of area under drought. The trends and spatial prorogation were also investigated.

The aspects of the study for the three sub-periods are described in greater detail below.

7.1. Past (1965-2017) drought events

As explained in the previous sub-chapter in this study the main drought episodes in northern Italy during the 1965-2017 period have been detected and characterised.

7.1.1. Drought analysis and indices comparison

The study has showed that even if drought events were investigated in northern Italy since the 1965, the first main event was recorded in 1983, with 15 consecutive weeks of duration for the SPEI-12 months, and the episodes increased since 2001. In their studies, Hoerling et al. (2012) and Gudmundsson and Seneviratne (2015) stated that the whole Mediterranean Basin experienced an intensification of drought over the two last decades. This could be related to a migration of the North Atlantic Oscillation from the North Atlantic to more northerly regions (200–300 hPa) in recent years. This migration reflects higher than average surface temperatures in the Mediterranean (Wallace and Gutzler, 1981). In particular, remarkable are the events observed in 2003, 2012 and 2017 with a duration between 29 and 47 consecutive weeks. Tomasino et al. (2004) and Marchina et al. (2019) observed that the drought events of 2003 and 2017 have led to an important shortage of the Po River, with a 95% reduction of the water inflow recorded at the station Pontelagoscuro, in the middle of the Po Plain. Therefore, as consequence of these drought events, the industrial crops resulted to be moderately negatively hit by the drought. As regards fruit cultivations an important increase of price was experienced due to the reduction the

quantities. Lastly, as concerns cereals, the changes in production and price due to the drought have been positive but small, and so the effects observed for this group of crops are quite limited (Musolino et al., 2017).

The study has figured out the importance of the application of multiple indices, in fact, Bachmair et al., (2016) and Svoboda et al., (2016) assumed that monitoring drought requires a variety of indicators and indices, calculated at different time scales. The application of SPEI and SPI indices has demonstrated that drought episodes are highly complex. In fact, even if agreement was found between the episodes recorded by SPEI and SPI indices, the events of 1990 and 2007 recorded a large difference between the two indicators. Particularly in 2007, drought impacted several parts of Europe, and the SPI suggested that, in the northern Plain, the drought episode started in 2006 with a precipitation deficit and subsequently evolved in spring 2007 because of a potential evapotranspiration demand above the normal. Sepulcre-Canto et al. (2012) reported that, due to the deficient winter precipitation, the Po River had reached a historically low level, and the Italian government declared a state of emergency in April 2007. Herceg (2012) in his study identified the 2007 drought episode as being one of the major drought events during 1971–2010 in south-eastern Europe.

Detection of weekly severe and extreme drought events at different time scales was also performed. The classification into two drought event classes means that they may depend on different controlling factors. Trenberth et al. (2013) studied the various drought. triggering factors on a global scale. In this regard, the characterization of the main severe and extreme drought episodes highlighted that, in the northern Italy, the triggering factors could have changed over time, and the study found two different behaviours. Before 2003, drought events seem to be mostly related with an evaporative. demand above the expected. This is consistent with the temperature trend increase detected by Toreti et al. (2010) in the period 1961–2006 and Acquaotta et al. (2015) in the period 1961–2010. However, after 2003, the predominant triggering factor seems to be precipitation, but not in the expected way. In fact, most recent research has identified no significant trend in precipitation in northern Italy (Fratianni and Acquaotta, 2017). Nevertheless, a detailed analysis in rainfall distribution by Baronetti et al. (2018) and Acquaotta et al. (2019a) identified changes in the intraannual distribution of precipitation recently, more specifically an increase in the length of period characterized by consecutive days without precipitation; also more intense extreme episodes were

experienced, suggesting that after 2003 the main triggering factor is the change in temporal distribution of rainfall. These results would agree also with the previous comment about affected area before and after 2003 according to SPEI and SPI, respectively.

7.1.2. Major drought events and spatial propagation

The results of the main extreme drought episodes showed high complexity at regional scale (Capra and Scicolone, 2012), and the two different propagation gradients suggested that different factors can affect the onset and evolution of these events particularly related to teleconnection patterns observed in the Mediterranean basin (Raymond et al., 2018).

The August 9, 2003–April 23, 2004 drought period was characterized by a persistent anticyclonic situation with exceptionally few cyclonic days throughout the summer of 2003 (Fink et al., 2004). Previous studies by Rebetez et al. (2006) and Mues et al. (2012) showed that extreme drought conditions were recorded in most of central and western Europe. The climatic conditions comparison between 2003 and the baseline (1961–1990) highlighted the fact that the north of Italy was one of the driest regions, as from August 2003 to April 2004, every month recorded precipitation rates lower than the baseline, with the exception of October 2003 and January 2004. The potential evapotranspiration was clearly above normal during summer 2003 and did not decrease until the end of the year. Regarding temperature, summer 2003 was exceptionally hot and the minimum and maximum temperatures were 4°C higher than the baseline. During the drought event, an east–west propagation gradient was detected, and presumably, temperature played an important role as a triggering factor. Indeed, the same spatial evolution was observed by Zaitchik et al. (2006) for the heat wave recorded during the drought period. This episode was also characterized by hours of sunshine above the annual average, and the air humidity was below normal. García-Herrera et al. (2010) stressed that the heat wave registered in 2003 was the result of several anomalous conditions occurring during winter and summer 2003. In fact, between February 2003 and April 2003, a large, persistent negative precipitation anomaly was recorded between Scandinavia and Europe, and a large positive temperature anomaly at the surface was observed between the British Isles and Scandinavia. These were the effects from a strong positive phase of the East Atlantic teleconnection pattern. The

heat wave that led to a late summer drought episode in 2003 had a strong influence on regional hydrology.

The second significant drought episode occurred from December 23–November 16, 2011. This event affected countries in south-west Europe, especially the Iberian Peninsula, south of France and north Italy. Unlike 2003, the affected countries received less precipitation than expected, in addition to a moderate temperature and positive evapotranspiration anomaly, which led to a severe drought episode (Spinoni et al., 2015). The rainfall analysis proposed by EDO (2012) showed that this drought episode was characterized by a precipitation deficit that started in winter 2011, and lasted until spring 2012, affecting southwest to northwest regions. In April 2012, the highest positive precipitation anomaly was recorded in north Italy; however, since January 2011, the wettest part was England. The observed south–north drought propagation gradient in comparison with the precipitation analysis proposed by EDO showed that, during 2012, the precipitation deficit may have acted as factor triggering drought. The episode caused a serious soil moisture deficit in the north of Italy, due to failure of the water supply rather than high evapotranspiration values. Recent reanalysis carried out by the Climatic Research Unit (http://www.cru.uea.ac.uk/) on several circulation patterns demonstrated that the strong precipitation anomaly recorded in 2012 was probably linked to two teleconnection patterns commonly found in the Mediterranean basin. The first is the Western Mediterranean Oscillations (WeMO) (Martin-Vide and Lopez-Bustins, 2006). The second is the Upper-Level Mediterranean Oscillation index (ULMOi), which is a combination of the Balearic Sea and Libya/Egypt windows. Both the indices identified a negative phase in 2012 (Redolat et al., 2018) giving rise to a ridge above the Mediterranean area, causing high pressure in southern Europe and low-pressure in the north.

7.1.3. Drought trend

The trend analysis on drought evets has figured out a similar spatial distribution for both the SPEI and SPI indices. As concern SPEI, the Occidental Alps were interested by the greatest drought intensification. Even if in this area high precipitation rates are still recorded (Brunetti et al., 2018), since the early 80s, a slight decrease of liquid precipitation amount was observed (Fratianni et al., 2015). Moreover, the trend analysis has also

evidenced that SPEI has detected negative drought trend more intense than SPI, suggesting that in the Occidental Alps the main drought triggering factor should be a potential evapotranspiration above the normal, due to an important temperature increase (Acquaotta et al., 2015) in the last decades, which interested also the thickness of the permafrost (Pogliotti et al, 2015).

As concern the SPI index, the study has figured out, that unlike the SPEI, the central part of the Po Plain has experienced the highest drought increase. As evidenced by Baronetti et al. (2018) and Acquaotta et al. (2019a), the Po Plain recently, was interested by changes in the intraannual distribution of precipitation (increase in the length of dry periods and more intense extreme episodes), suggesting that in this area the main triggering factor should be related with precipitation deficit.

7.2. Near future (2020-2049) and past future (2070-2099) drought events

Drought events expected in northern Italy for the near (2020-2049) and far future (2070-2099) were investigated using SPEI and SPI. To this end, 12 GCMs/RCMs combinations from MED-CORDEX and EURO-CORDEX with spatial resolution of 0.11 degrees were collected and analysed for the RCP 4.5 and RCP 8.5 emission scenarios

7.2.1. Drought events comparison

Concerning the future drought evolution, the results indicated an increase of drought severity passing from the near future to the far future. This positive trend is mainly seen in the percentage of affected area and in drought duration. The increase is more marked for RCP 8.5, with 68% of northern Italy affected by a single extreme drought and a maximum of 33 consecutive drought weeks for the 2070-2099 period.

These drought changes, started at the end of the twentieth century, in fact the comparison of the results obtained for the past situation in northern Italy (1965-2017) with the near future results (2020-2049) in the RCP 4.5 scenario indicates that the positive trend continues in the future and it is mainly seen in the percentage of affected area, with a maximum of +11% of drought-affected

area projected by the HadGEM2-RACMO22 couple. For RCP 8.5, the drought conditions in northern Italy will be even more severe, with an increase that will interest both the number of events and the percentage of area under drought, for instance +4 episodes and +17 % dry area from the HadGEM2-RACMO22 model couple. These results are consistent with those detected in other studies using different approaches. In fact, Hertig and Tramblay (2017), Quintana-Seguí et al., (2016) and Dubrovský et al. (2014) found that future projections showed more probable and severe drought events for the whole Mediterranean basin, with a marked increase in the duration of dry spells.

Accordingly with the results obtained from the actual condition (1965-2017), the application of two different drought indices has proved to be a good solution to best characterise future drought events, in fact even if both indices were able to detect the same drought events, marked differences were highlighted in the percentage of drought-affected area as estimated by SPEI and SPI. The variance between the two indices showed that, as already observed for the past condition, future drought events may depend on different triggering factors. The analysis of the main severe and extreme drought episodes in northern Italy, figured out that two possible triggering factors can act over the years. During the 2020-2049 period, the largest part of the GCMs/RCMs couples for both the RCP 4.5 and 8.5 evidenced that drought episodes seem to be most related with an above-normal evaporative demand. This finding is consistent with the results of Marcos-Garcia et al. (2017), suggesting that the increase of temperature will play the most important role in drought episodes, particularly for the RCP 8.5 simulations, in the first half of this century.

On the contrary, for the later part of the century, both the RCP 4.5 and 8.5 showed a not clear predominance of the potential evapotranspiration as triggering factor rather than precipitation deficit. Guiot and Cramer (2016) showed that Mediterranean ecosystems are sensitive not only to warming but also to changes in water availability. In particular Raymond et al. (2018) demonstrated in his study that in the Mediterranean rainy days will decrease in winter, which contributes to the drying process of the basin. Even if past variations in precipitation and their projections for the future are spatially more heterogeneous than temperature fields, for most scenarios, the changes in both fields will combine to reduce water availability and trigger losses of Mediterranean ecosystems and their biodiversity during the coming decades. Furthermore, Merkenschlage and Hertig (2020) and Brogli et al. (2019)

reported, for this later period, that precipitation quantiles are expected to decrease in the whole Mediterranean area, where more extended dry periods and extreme precipitation episodes will be experienced, also as a consequence of drier conditions during summer. In winter, circulation changes associated with a geopotential height anomaly are estimated to be the main cause of dry conditions (Seager et al. 2019). Along these lines, Polade et al. (2017) showed that winter precipitation decrease will range between 10 and 35% in the whole basin in the last part of the century, compared to the 1960–1989 period.

7.2.2. Drought trends

In the national and international literature, the temporal evolution of past and future droughts in northern Italy has not been already studied in detail. On the other hand, several studies were devoted to the analysis of the spatial and temporal distribution of precipitation in the northern Italy, focusing on the Po Plain (Baronetti et al. 2018; Brunetti et al. 2018). These works figured out that the rainiest and snowiest area is along the Alps (Terzago et al. 2013, Fratianni and Acquaotta 2017). High amounts of precipitation were found also by Parodi et al. (2017) along the Maritime Alps owing to mesoscale convective systems generated on the sea. The analysis of future drought trends performed on the two drought indices has showed significant results for the SPEI 12-months index. Evidencing that the rainiest sectors of northern Italy will experience an increase of drought severity in the RCP 4.5 scenario. This has confirmed what previously observed for the actual condition (1965-2017), and by Gandolfi et al. (2019) suggesting that the Alpine chain is highly susceptible to droughts increase. For RCP 8.5, the whole study area will be affected by more severe drought events.

7.2.3. Drought spatial prorogation

For a +2°C increase of global temperature, the analysis has suggested that extreme drought episodes will be characterised by very long dry spells along the mountain ranges (Alps). According to the trend analysis, the Alpine chain, instead of the Po Plain, will be the sector that is mostly affected by more severe and longer drought events. This implies potentially severe impacts on permafrost degradation, influencing surface water quality, erosion and slope instability (Colombo et al., 2019). For a +3 °C increase of global temperatures, a North-to-South gradient of dry spells is identified, and the Po Plain will

become more severely affected by extremely long drought events. Long dry periods have a marked impact on agriculture: as consequence of a large number of consecutive dry days, there can be a high reduction of crop growth, depending on the species, and a mortality increase. In particular wheat, barley and oat production are strongly influenced by long dry spells in winter (Raymond et al. 2019). The North-to-South gradient observed in northern Italy is indeed present in the whole Mediterranean basin (Quintana-Seguí et al., 2016).

The Mediterranean basin climate is determined by the interaction between large scale circulations, mid-latitude and sub-tropical processes (Mariotti and Dell'Aquila, 2012). As already evidenced for the study period 1965-2017, the in northern Italy drought episodes are mostly influenced by the North Atlantic Oscillation (NAO), the Mediterranean Oscillation (MO) and the Western Mediterranean Oscillation (WeMO), in fact two drought propagation gradients (North-to-South and East-to-West) were detected. The North-to-South drought gradient for the twenty-first century is probably the result of a stronger positive phase of NAO and MO, leading to drier conditions over most of the Mediterranean basin. Demuzere et al. (2009) and Vicente-Serrano et al. (2011) showed that the positive phase of NAO and MO for the twenty-first is simulated also by GCMs. Santos et al. (2007) estimated a future extension of the NAO's southern centre of action through the eastern part of the Mediterranean Basin, implying an intensification of NAO in southern Europe. This difference between the positive and negative phase of NAO can explain the future North-to-South drought gradient and the decrease of precipitation expected for the last decades of the century. Finally, Beranová and Kyselý (2016) showed that most RCMs simulate a positive change of the NAO index and a negative change of the WeMO index. Most RCMs indicate that, also in the future, the spatial links between circulation indices and precipitation deficit will be similar to those observed in the 1961-1990 period. This suggests that in the Mediterranean basin the two indices will both play a role in affecting future precipitation.

CHAPTHER 8: CONCLUSION AND FUTURE RESEARCH

8.1. Conclusion

This work analysed, for the first time the properties of drought episodes in in the past (1965-2017) near (2020-2049) and far (2070-2099) future for northern Italy, a crucial region from the point of view of water resources.

In this regard historical ground series over the northern Italy belonging the SCIA database were collected and Euro-CORDEX and Med-CORDEX GCMs/RCMs couples at spatial resolution of 0.11 degrees (12 km2) were analysed for the RCP 4.5 and RCP 8.5 concentration pathways. To increase the results reliability, ground series were quality checked, reconstructed and homogenised. While on the GCMs/RCMs couples the validation was performed, revealing that the couples EC-EARTH-HIRHAM5, HadGEM2-CCLM4, HadGEM2-RACMO22 and CM5-ALADIN52 perform best for northern Italy.

The results showed that although northern Italy is historically rich in water resources. Several drought episodes were detected since 1983 and will continue and increase in the twenty-first century. In fact, most GCMs/RCMs couples indicated an increase of drought severity, in terms of duration and percentage of drought-affected area, especially for the RCP 8.5 and for the later part of the century. In particular, the trend analysis has figured out that actually the Alpine chain (a water tower for the surrounding area) is significantly affected by increasing of drought conditions, and this intensification will continue in near future and far future, until the end of the twenty-first century.

The study also emphasizes the importance of applying multiple indices, and the comparison brought to light several drought triggering factors acting over the years. In fact, for the 1965-2017 period, a positive evapotranspiration anomaly seems to have been the main trigger in the period before the 2003, whereas after 2003, droughts could be mostly related to precipitation because of changes in their annual distribution. While for the near future (2020-2049) and far future (2070-2099) a positive evapotranspiration anomaly appears to be the main drought-triggering factor for the first part of the century, while in

the last thirty years, even if water demand will continue to increase because of rising temperatures, for both the RCP 4.5 and 8.5 is not clear if the potential evapotranspiration above the normal or the precipitation deficit will be the main triggering factor.

Finally, this study contributes to understand better drought episodes, pointing out that although the triggering factors changed over time, circulation patterns also influenced the occurrence of drought events. In particular, in 2003, a link with the positive phase of the East Atlantic teleconnection pattern detected an east to west drought propagation gradient. While in 2012, the south to north spatial evolution of drought was the result of a link with the negative phase of two teleconnection patterns in the Mediterranean basin: Western Mediterranean Oscillations and Upper-Level Mediterranean Oscillation. Moreover, the intensification of the latters circulation patterns is expected to bring more severe drought episodes in the southern part of the study area, even for the end of the century, detecting a north-to-south drought propagation gradient moving from +2°C to +3°C of global warming above preindustrial level.

8.2. Climate change strategies

Over 75% of the population of the European and the Mediterranean regions lives in urban areas, and this percentage is expected to grow to 82% by 2050. The agglomeration of people, assets and economic activity makes cities particularly vulnerable, and thus priority areas for climate change impact assessment (Shi et., al 2016). Recent decades have seen record-breaking heat extremes worldwide (Guerriero et al., 2018).

This has resulted in the proliferation of adaptation and mitigation measures that are useful in facing changing conditions and new risks and enabling communities to adapt and respond to rapid-worldwide-climate-change issues (Fazey et al., 2018). In particular the European Union is active in the climate change challenge as demonstrated by its engagement in leading global efforts to drive the transition towards a low-carbon economy and to prevent and limit the consequences of climate change. In fact, climate change and related impacts can increase territorial vulnerability and produce deep socio-economic imbalances over the whole Europe with high damage costs (Fischer and Schär, 2010). In these regards, the European Union has committed itself to limit global average temperature increase to less than 2°C compared to pre-industrial levels signing the Kyoto Protocol agreement in 1998 and setting

ambitious long-term goals as cutting greenhouse gas emissions by 80–95% by 2050 compared to 1990 levels.

Nowadays, according to the European Commission guidelines, the majority of the EU Member States have defined and implemented comprehensive adaptation strategies, identifying suited measures and interventions to reduce the impacts of climate change on the most vulnerable sectors. The first adaptation strategy in Europe was developed in Finland in 2005. Nowadays about 76% of the European countries have adopted a National Adaptation Strategy (NAS) and 61% have developed a National Action plan (NAP). Twenty-two web platforms are also available all over Europe, eight of which (Austria, Denmark, Finland, Germany, Norway, Sweden, Switzerland and UK) are more inclusive and directly connected to the implementation of a national adaptation strategy and/or action plan (Pietrapertosa et al., 2018)

Concerning Italy, the NAS was issued in 2015, while the draft of the NAP was submitted to public consultation in 2017. The NAS in Italy has been thoroughly based on the involvement of stakeholders and decision makers and on the principle of preferring mainstreaming adaptation across existing policies to introducing new policies focused exclusively on adaptation. Also in Italy, the construction of NAS started from the definition and identification of potentially vulnerable sectors and special cases were identified due to specific physical and geographical vulnerabilities, i.e. mountain areas (Alps and Apennines) and the Po river basin, due to its critical role on the national level (Table 13).

Table 13: Vulnerable sectors considered by the Italian NAS (NAS 2014)

Physical Environment	**Human health and ecosystems:**	**Energy, agriculture and fishery**	**Critical infrastructures**	**Special cases**
Water resources (quantity and quality) Desertification, land degradation and droughts Hydro-geologic risk	Human health Terrestrial ecosystems Marine ecosystems Inner water ecosystems Forestry	Agriculture and food production Aquaculture and fishery Energy Coastal zones Tourism Urban and metropolitan centres	Cultural heritage Transport	Mountain areas (Alps and Apennines) Po river basin

Taking note of the geographical diversity of Italy, the NAP provides some synthetic reports dealing with macro-climatic regions identified within the country which are consistent with expected variations in temperature and connected phenomena as well as impacts of climate change classified as threats and opportunities (i.e. negative and positive ones) for each of the macro-regions under investigation and for each of the socio-economic sectors identified. Each identified impact has been assigned a level of intensity, ranging from low to high.

NAP is a tool for supporting the implementation of NAS. It provides a set of adaptation actions in order to mitigate and take advantage from climate change for the most vulnerable sectors already identified with NAS. Four are the main targets:

- contain the vulnerability of natural, social and economic systems to climate change impacts;
- increase the systems' own adaptive capacity;
- increase the exploitation of opportunities;
- support the vertical integration and coordination of actions at different levels.

The greatest part of the main cities of northern Italy developed their Sustainable Energy Action Plan (SEAP) aimed to achieve the objective of reducing CO_2 emissions by a minimum of 20% by the year 2020. Mainly through the promotion of energy efficiency and the use of renewable energy sources in a local authority's territory (Pietrapertosa et al, 2019).

Among them, remarkable is Bologna (Emilia- Romagna region), was the first Italian city, to provide for some concrete local measures, in order to make the city more resilient and able to meet the climate change challenges. The Plan identifies three macro-factors of vulnerability (Drought and water scarcity; heat waves in urban areas; and extreme rain events and hydrogeological risk) and set some strategies and a set of objectives. It describes the actions necessary to achieve them, in a time-frame set at 2025, distinguishing those of responsibility of the Municipality from those that see the involvement of other subjects, and consequently adapting the level of detail of envisaged actions (Boeri et al., 2018).

Padua (Veneto), drafted also an adaptation plan in 2016 and was the only Italian city to use a methodology built from those already existing at the international level. The most detected effects due to climate changes in Padua are the floods and heat islands. Actions are planned to adapt to these risks, in order to mitigate and compensate the effects of land consumption. The plan emphasizes the importance of soil protection, promoting the reuse of already urbanized soils (existing urban fabric). In particular is empathised the creation of many multifunctional green areas which, in addition to absorbing large amounts of CO2, allow greater water absorption (Zucaro and Morosini, 2018).

The capital of Ligura (Genoa), in the recent years was interested by several devastating extreme events, such as the floods of 2011 and 2014 (Acquaotta et al., 2019c). From 2019, the Genoa is officially the first city in Europe to activate collaboration with DRMKC technicians (Disaster Risk Management Knowledge Center) of the Joint Research Center of the European Commission. This collaboration was born to develop prevention policies and to prepare changes needed according to the current and future risk scenarios (Pirlone et al., 2020).

8.3. Future research

From the work developed by this dissertation, several prospective study fields have emerged.

Satellite data

The first thing required to extend this work is to improve the reliability of drought estimation, focusing on satellite data. In Chapter 2, drought is classified into four types: meteorological, agricultural, hydrological and socioeconomic. This classification acknowledges that a range of factors, including topography, antecedent conditions, vegetation type, and land use, work together to determine the consequences of precipitation shortfalls, and that a deficit of a given magnitude will not affect all landscapes in the same way. However, in reality, it can be difficult to neatly classify a drought event into a single category.

Historically, drought is monitored and classified from frameworks based on ground stations, by mean of drought indices. For instance, in this work the Standardised Precipitation Evapotranspiration Index and the Standardised Precipitation Index were applied. However, in regions with a complex topography, drought indices should be integrated with remote sensing data, collected from different satellite such as MODIS (Moderate Resolution Imaging Spectroradiometer), Landsat8 and, the European optical imaging satellite, Sentinel-2 In this regards, remote sensing can be a very useful tool, since it provides continuous and consistent observations of relevant variables linked to ecosystem status and the hydrologic cycle (Rhee and Im, 2017).

A suite of remotely-sensed indices already exist, each with different emphasis. For instance, the Precipitation Condition Index (PCI), the Temperature Condition Index (TCI) and the Land Surface Temperature (LST), are commonly used remote sensing drought indexes that have a clear climatological perspective (García-León et al., 2019).

Recently, the availability of remote sensing data and surface-atmosphere models has allowed for the development of global actual evapotranspiration (Eta) products (Zhang et al. 2016). Similarly, drought indices have been developed based on the evapotranspiration deficit, mainly to analyse natural vegetation and crop stress; for instance, Anderson et al. (2011), Yao et al.

(2010) and Mu et al. (2011) developed different normalized drought indices, such as the the Evapotranspiration Deficit Index (EDI) and the Evaporative Stress Index (ESI) by means of observational meteorological data and space-based products to estimate evapotranspiration deficit.

It would be interesting to see in the same studied places, how the characterisation of the main drought event will be improved integrating in the methodology satellite-based drought indices.

Water resources

The following research is based in the characterisation of the main past and expected drought event in northern Italy. An effect of the global change on environmental conditions in the Mediterranean regions is the increasing uncertainty in water resource availability and has significant hydrological implications. To assess the possible consequences of climate change for the future availability of water resources in vulnerable regions, such as northern Italy, it is necessary to understand the relationships between climate variability and the occurrence of hydrological droughts. This complexity highlights the need for a more detailed analysis of how streamflow responds to climate fluctuations at various time scales.

In Italy, national and international analyses have been done in this direction, revealing a prominent hydrological response to precipitation deficits at short time scales in basins and in particular these studies were restricted to small river basins located in central and southern Italy (Maccioni et al., 2015; Valigi et al., 2016), lacking a broad spatial perspective which would allow comparability and an easier interpretation of the results.

Because the northern Italy is crossed by the Po River, making this region one of the most productive areas in Italy. One of the possible required things to improve this work is to monitor the hydrological response of the river to meteorological drought conditions, to better understand, detect, predict and mitigate the effects of climate change.

Early warning system

Climate change early warning system are emerging and lessons from extant hazard warning systems might prove instructive if warnings about extreme climate change become necessary. Prospects for effective social response can be improved by skilful early warning, but experience with current natural hazard warning systems indicates that effectiveness is not determined just by predictive accuracy; many other factors play into warnings usefulness, especially lead time and the available social response set. It is too early to start issuing warnings of severe and/or abrupt climate change, but not too early to sort out how the threat might be evaluated and communicated as knowledge improves or, worse, if a threatening climate event becomes likely (Travis 2013, Pulwarty and Sivakumar 2014). In the Po river basin an early warning system, called "DEWS-Po: Drought Early Warning System for the Po River" has been developed to manage at a first-time flood's events, and afterwards it was upgraded with skillnesses and tools to enable its use along with drought events. The DEWS-PO is operation since 2009 and mainly involves monitoring of meteorological and hydrological droughts (Acácio et al., 2013).

References

Acácio, V., Andreu, J., Assimacopoulos, D., Bifulco, C., di Carli, A., Dias, S., Kampragou, E., Monteagudo, D.H., Rego, F., Seidl, I., Vasiliou, E. and Walters, W. (2013). Review of current drought monitoring systems and identification of (further) monitoring requirements. DROUGHT-R&SPI Technical Report, 6.

Acquaotta, F., Baronetti, A., Bentivenga, M., Fratianni, S. and Piccarreta, M. (2019a) Estimation of rainfall erosivity in Piedmont (north-West Italy) by using 10-minute fixed-interval rainfall. Időjárás, 123(1), 1–18. Doi: 10.28974/idojaras. 2019.1.1.

Acquaotta, F., Fratianni, S., Aguilar, E. and Fortin, G. (2019b) Influence of instrumentation on long temperature time series. Climatic Change, 156, 1–20. Doi: 10.1007/s10584-019-02545-z.

Acquaotta, F., Faccini, F., Fratianni, S., Paliaga, G., Sacchini, A. and Vilìmek V. (2019c) Increased flash flooding in Genoa Metropolitan Area: a combination of climate changes and soil consumption? Meteorology and Atmospheric Physics, 131(4), 1099-1110. Doi: 10.1007/s00703-018-0623-4

Acquaotta, F., Faccini, F., Fratianni, S., Paliaga, G. and Sacchini, A. (2018) Rainfall intensity in the Genoa Metropolitan Area (Northern Mediterranean): secular variations and consequences. Weather, 73(11), 356-362. Doi: 10.1002/wea.3208Acquaotta, F, Fratianni, S, Venema, V. (2016) Assessment of parallel precipitation measurements networks in Piedmont, Italy. Internationa Journal of Climatology, 36(12), 3963-3974. Doi: 10.1002/joc.4606.

Acquaotta, F., Fratianni, S. and Garzena, D. (2015) Temperature changes in the North-Western Italian Alps from 1961 to 2010. Theoretical and Applied Climatology, 122(3–4), 619–634. Doi: 10.1007/s00704-014-1316-7.

Aguilar, E., Peterson, T.C., Obando, P.R., Frutos, R., Retana, J.A., Solera, M., Soley, J., Garcia, I.G., Araujo, R.M. and Santos, A.R. (2005) Changes in precipitation and temperature extremes in Central America and northern South America 1961–2003. Journal of Geophysical Reswangearch: Atmospheres, 110(D23107), 1–15. Doi: 10.1029/2005JD006119.

Alexandersson, H. (1986) A homogeneity test applied to precipitation data. Journal of Climatology, 6, 661–675.

Alexandris, S., Stricevic, R. and Petkovic, S. (2008) Comparative analysis of reference evapotranspiration from the surface of rainfed grass in central Serbia, calculated by six empirical methods against the Penman-Monteith formula. European Water, 21(22), 17-28.

Alfio, M.R., Balacco, G., Parisi, A., Totaro, V. and Fidelibus, M.D. (2020) Drought Index as Indicator of Salinization of the Salento Aquifer (Southern Italy). Water, 12(7), 1927. Doi: 10.3390/w12071927.

Allen, R.G., Pereira, L.S., Raes, D. and Smith, M. (1998) Crop evapotranspiration. Guidelines for computing crop water requirements. FAO irrigation and drainage paper, 56, 227 pp.

Andreu, J., Ferrer-Polo, J., Pérez, M.A. and Solera, A. (2009) Decision support system for drought planning and management in the Jucar river basin, Spain. In 18th World IMACS/MODSIM Congress, Cairns, Australia, Vol. 1317.

Antonellini, M., Mollema, P., Giambastiani, B., Bishop, K., Caruso, L., Minchio, A., Pellegrini, L., Sabia, M., Ulazzi, E. and Gabbianelli, G. (2008) Salt water intrusion in the coastal aquifer of the southern Po plain, Italy. Hydrogeology Journal, 16(8), 1541–1556. Doi: 10.1007/s10040-008-0319-9.

Bachmair, S., Stahl, K., Collins, K., Hannaford, J., Acreman, M., Svoboda, M., Knutson, C., Smith, K.H., Wall, N., Fuchs, B., Crossman, N. D. and Overton, I.C. (2016) Drought indicators revisited: the need for a wider consideration of environment and society. WIREs Water, 3(4), 516-536. Doi:10.1002/wat2.1154.

Baronetti, A., Acquaotta, F. and Fratianni, S. (2018) Rainfall variability from a dense rain gauge network in north-West Italy. Climate Research, 75(3), 201–213. Doi: 10.3354/ cr01517.

Bartolini, C. (2010) Outline of Italy's Geomorphology. Journal of the Virtual Explorer, Electronic Edition, ISSN 1441-8142, 36(22), 1-17. In: (Eds.) Marco Beltrando, Angelo Peccerillo, Massimo Mattei, Sandro Conticelli, and Carlo Doglioni, The Geology of Italy: tectonics and life along plate margins. Doi: 10.3809/jvirtex.2010.00216.

Beguería, S., Serrano-Notivoli, R. and Tomas-Burguera, M. (2018). Computation of rainfall erosivity from daily precipitation amounts. Science of The Total Environment, 637, 359-373. Doi: 10.1016/j.scitotenv.2018.04.400

Beguería, S. and Vicente-Serrano, S.M. (2017) SPEI: Calculation of the Standardised Precipitation-Evapotranspiration Index, R package version 1.7. R Foundation for Statistical Computing, Vienna, Austria, 16 pp

Bellprat, O., Kotlarski, S., Lüthi, D. and Schär, C. (2012) Exploring Perturbed Physics Ensembles in a Regional Climate Model. Journal of Climate 25(13):4582-4599. Doi: 10.1175/JCLI-D-11-00275.1.

Beranová, R. and Kyselý, J. (2016) Links between circulation indices and precipitation in the Mediterranean in an ensemble of regional climate models. Theoretical and applied climatology, 123(3-4), 693-701. Doi: 10.1007/s00704-015-1381-6.

Boeri, A., Fini, G., Gaspari, J., Gianfrate, V. and Longo, D. (2018) Bologna resilient city: from the adaptation plan to local actions. TECHNE-Journal of Technology for Architecture and Environment, 193-202. Doi: 10.13128/Techne-22103.

Bois, B., Joly, D., Quénol, H., Pieri, P., Gaudillère, J. P., Guyon, D., ... & Van Leeuwen, C. (2018). Temperature-based zoning of the Bordeaux wine region. Oeno One, 52(4).

Brinckmann, S., Krähenmann, S. and Bissolli, P. (2016) High-resolution daily gridded datasets of air temperature and wind speed for Europe. Earth System Science Data, 8, 491–516. Doi: 10.5194/essd-8-491-2016.

Brogli, R., Sørland, S.L., Kröner, N. and Schär, C. (2019) Causes of future Mediterranean precipitation decline depend on the season. Environmental Research Letters, 14(11), 114017. Doi: 10.1088/1748-9326/ab4438.

Browning, J.M. and Schneider C. (2017) SNHT: Standard Normal Homogeneity Test. R package version 1.0.5.

Brunetti, M., Bertolini, A., Soldati, M. and Maugeri, M. (2018) High-resolution analysis of 1-day extreme precipitation in a wet area centered over eastern Liguria, Italy. Theoretical and Applied Climatology, 135, 341–353. Doi: 10.1007/s00704-018-2380-1.

Bucchignani, E., Montesarchio, M., Zollo, A.L. and Mercogliano, P. (2016) High-resolution climate simulations with COSMO-CLM over Italy: performance evaluation and climate projections for the 21st century. International Journal of Climatology, 36: 735-756. Doi: 10.1002/joc.4379.

Buttafuoco, G., Caloiero, T. and Coscarelli, R. (2015). Analyses of drought events in Calabria (southern Italy) using standardized precipitation index. Water Resources Management, 29(2), 557-573. Doi: 10.1007/s11269-014-0842-5.

Capra, A., Consoli, S. and Scicolone, B. (2013). Long-term climatic variability in Calabria and effects on drought and agrometeorological parameters. Water Resources Management, 27(2), 601-617.

Capra, A. and Scicolone, B. (2012) Spatiotemporal variability of drought on a short-medium timescale in the Calabria region (southern Italy). Theoretical and Applied Climatology, 110(3), 471–488. Doi: 10.1007/s00704-012-0720-0.

Carrera-Hernández, J.J. and Gaskin, S.J. (2007) Spatio temporal analysis of daily precipitation and temperature in the Basin of Mexico. Journal of Hydrology, 336(3–4),231–249. Doi: 10.1016/j.jhydrol.2006.12.021.

Castaldini, D., Marchetti, M., Norini, G., Vandelli, V. and Zuluaga Vélez, M.C. (2019) Geomorphology of the central Po Plain, Northern Italy. Journal of Maps, 15(2), 780-787. Doi: 10.1080/17445647.2019.1673222.

Chaouche, K., Neppel, L., Dieulin, C., Pujol, N., Ladouche, B., Martin, E., Salas, D. and Caballero, Y. (2010). Analyses of precipitation, temperature and evapotranspiration in a French Mediterranean region in the context of climate change. Comptes Rendus Geoscience, 342(3), 234-243. Doi:

10.1016/j.crte.2010.02.001Christensen, J.H., Carter, T.R., Rummukainen, M. and Amanatidis, G. (2007) Evaluating the performance and utility of regional climate models: the PRUDENCE project, Climatic Change, 81, 1–6. Doi: 10.1007/s10584-006-9211-6.

Citakoglu, H., Cobaner, M., Haktanir, T. and Kisi, O. (2014). Estimation of monthly mean reference evapotranspiration in Turkey. Water resources management, 28(1), 99-113. Doi: 10.1007/s11269-013-0474-1

Cohen, S., Ianetz, A. and Stanhill, G. (2002). Evaporative climate changes at bet Dagan, Israel, 1964–1998. Agricultural and Forest Meteorology, 111(2), 83-91. Doi: 10.1016/S0168-1923(02)00016-3

Colombo, N., Salerno, F., Martin, M., Malandrino, M., Giardino, M., Serra, E., Godone, D., Said-Pullicino, D., Fratianni, S., Paro, L., Tartari, G and Freppaz, M. (2019) Influence of permafrost, rock and ice glaciers on chemistry of high-elevation ponds (NW Italian Alps). Science of The Total Environment, 685, 886-901. Doi: 10.1016/j.scitotenv.2019.06.233.

Cook, E.R., Seager, R., Cane, M.A. and Stahle, D.W. (2007). North American drought: Reconstructions, causes, and consequences. Earth-Sciences Reviews, 81(1-2), 93-134. doi.org/10.1016/j.earscirev.2006.12.002

Courault, D. and Monestiez, P. (1999) Spatial interpolation of air temperature according to atmospheric circulation patterns in southeast France. International Journal of Climatologym 378:365–378. Doi: 10.1002/(SICI)1097-0088(19990330)19:4<365::AID-JOC369>3.0.CO;2-E.

Critto, A., Torresan, S., Ronco, P., Zennaro, F., Santini, M., Trabucco, A., and Marcomini, A. (2016) Assessing hydrological drought risk for the irrigation sector in future climate scenarios: lessons learned from the Apulia case study (Italy). EGUGA, EPSC2016-7813.

Croitoru, A. E., Piticar, A., Dragotă, C. S. and Burada, D. C. (2013). Recent changes in reference evapotranspiration in Romania. Global and Planetary Change, 111, 127-136. Doi: 10.1016/j.gloplacha.2013.09.004

Daubenmire, R.F. (1943) Vegetational Zonation in the Rocky Mountains. Botanical Review. 9 (6),325–393. Doi:10.1007/BF02872481.

Demuzere, M., Werner, M., van Lipzig, N.P.M. and Roeckner, E. (2009) An analysis of present and future ECHAM5 pressure fields using a classification of circulation patterns. International Journal Climatology 29:1796–1810. Doi.org/10.1002/joc.1821.

Desiato, F., Fioravanti, G., Fraschetti, P., Perconti, W. and Piervitali, E. (2015) Il clima futuro in Italia: analisi delle proiezioni dei modelli regionali (The future climate in Italy: analysis of the Regional model projections). The Italian National Institute

for Environmental Protection and Research (ISPRA), Stato dell'Ambiente, 58. In Italian. ISBN: 978-88-448-0723-8.

Desiato, F., Lena, F. and Toreti, A. (2007). SCIA: a system for a better knowledge of the Italian climate. Bollettino di Geofisica Teorica ed Applicata, 48(3), 351-358.

Diffenbaugh, N.S. and Giorgi, F. (2012). Climate change hotspots in the CMIP5 global climate model ensemble. Climatic Change, 114(3-4), 813–822. Doi: 10.1007/s10584-012-0570-x.

Diodato, N., Fratianni, S. and Bellocchi, G. (2020) Reconstruction of snow days based on monthly climate indicators in the Swiss pre-alpine region. Regional Environmental Change, 20, 55. Doi: 10.1007/s10113-020-01639-0

Domonkos, P. and Coll, J. (2017) Homogenisation of temperature and precipitation time series with ACMANT3: method description and efficiency tests. International Journal of Climatology, 37(4), 1910-1921. Doi: 10.1002/joc.4822.

Donnelly, C., Greuell, W., Andersson, J., Gerten, D., Pisacane, G., Roudier, P., and Ludwig, F. (2017) Impacts of climate change on European hydrology at 1.5, 2 and 3 degrees mean global warming above preindustrial level. Climatic Change, 143(1-2), 13-26. Doi: 10.1007/s10584-017-1971-7.

Drumond, A., Gimeno, L., Nieto, R., Trigo, R.M. and VicenteSerrano, S.M. (2017) Drought episodes in the climatological sinks of the Mediterranean moisture source: the role of moisture transport. Global and Planetary Change, 151, 4–14. Doi: 10.1016/j.gloplacha.2016.12.004.

Dubreuil, V., (1997) La sécheresse dans la France de l'Ouest : une contrainte climatique trop souvent oubliée. Science et changements planétaires / Sécheresse, 8(1):47-55.

Dubrovský, M., Hayes, M., Duce, P., Trnka, M., Svoboda, M. and Zara, P. (2014) Multi-GCM projections of future drought and climate variability indicators for the Mediterranean region. Regional Environmental Change, 14(5), 1907-1919. Doi: 10.1007/s10113-013-0562-z.

EDO (2012). Drought News March 2012. European Drought Observatory. Available at: http://edo.jrc.ec.europa.eu/documents/ news/EDODroughtNews201203.pdf

EEA (European Environmental Agency, 2010) Mapping the impacts of natural hazards and technological accidents in Europe, An overview of the last decade. EEA Technical report, No. 13/2010, Copenhagen, Brussels.

Fazey, I., Carmen, E., Chapin III, F.S., Ross, H., Rao-Williams, J., Lyon, C., Connon, I.L.C.,Searle, K. and Knox, K. (2018) Community resilience for a 1.5 C world. Current Opinion in Environmental Sustainability, 31, 30-40. Doi: 10.1016/j.cosust.2017.12.006Fazzini, M., Fratianni, S., Biancotti, A. and Billi, P. (2004) Skiability conditions in several skiing complexes on Piedmontese and

Dolomitic alps. Meteorologische Zeitschrift, 13(3), 253-258. Doi:10.1127/0941-2948/2004/0013-0253

Fink, A., Brucher, T., Kruger, A., Leckebusch, G., Pinto, J. and Ulbrich, U. (2004) The 2003 European summer heatwaves and drought—synoptic diagnosis and impacts. Weather, 59 (2009–2216), 209–216. Doi: 10.1256/wea.73.04.

Fiori E, Ferraris L, Molini L, Siccardi F, Kranzlmueller D, Parodi A (2017) Triggering and evolution of a deep convective system in the Mediterranean Sea: modelling and observations at a very fine scale. Q J Roy Meteor Soc 143(703):927–941. https://doi.org/10.1002/qj.2977

Fischer, E.M., Rajczak, J. and Schär, C. (2012) Changes in European summer temperature variability revisited. Geophysical Research Letters, 39(12), 1970. Doi:10.1029/2012GL052730.

Fischer, E. M. and Schär, C. (2010). Consistent geographical patterns of changes in high-impact European heatwaves. Nature Geoscience, 3(6), 398-403.

Flato, G., Marotzke, J., Abiodun, B., Braconnot, P., Chou, S. C., Collins, W., Cox, P., Driouech, F., Emori, S., Eyring, V., Forest, C., Gleckler, P., Guilyardi, E., Jakob, C., Kattsov, V., Reason, C. and Rummukainen, M. (2013) Evaluation of Climate Models, in: Climate Change: The Physical Science Basis. Contribution of Working Group I to the Fifth Assessment Report of the Intergovernmental Panel on Climate Change, edited by: Stocker, T. F., Qin, D., Plattner, G.-K., Tignor, M., Allen, S. K., Boschung, J., Nauels, A., Xia, Y., Bex, V. and Midgley, P. M. (2013), Cambridge University Press, Cambridge, UK and New York, NY, USA.

Fratianni, S. and Acquaotta, F. (2017) The climate of Italy. In: Soldati, M. and Marchetti, M. (Eds.) Landscapes and Landforms of Italy. World Geomorphological Landscapes. Cham: Springer. Doi: 10.1007/978-3-319-26194-2_4.

Fratianni, S., Terzago, S., Acquaotta, F., Faletto, M., Garzena, D., Prola, C. and Secondo, B. (2015) How snow and its physical properties change in a changing climate alpine context? Engineering geology for society and territory—climate change and engineering geology, vol 1. Springer, Switzerland, pp 57–60. Doi: 10.1007/978-3-319-09300-0_11.

Fratianni, S., Cassardo, C. and Cremonini, R. (2009) Climatic characterization of Foehn episodes in Piedmont, Italy. Geografia Fisica e Dinamica Quaternaria 32:5–22. ISSN 0391-9838.

Gandolfi, C., Facchi, A., Crespi, A., Rienzner, M. and Maugeri, M. (2019) Drought Variability and Trend Over the Lombardy Plain from Meteorological Station Records. In International Mid-Term Conference of the Italian Association of Agricultural Engineering (pp. 39-47). Charm: Springer.

García-Garizábal, I., Causapé, J., Abrahao, R. and Merchan, D. (2014). Impact of climate change on Mediterranean irrigation demand: historical dynamics of climate and future projections. Water resources management, 28(5), 1449-1462. Doi: 10.1007/s11269-014-0565-7.

García-Herrera, R., Garrido-Perez, J.M., Barriopedro, D., Ordóñez, C., Vicente-Serrano, S.M., Nieto, R., Gimeno, L., Sorí, R. and Yiou, P. (2019) The European 2016/17 drought, Journal of Climate, 32, 3169–3187. Doi.org/10.1175/JCLI-D-18-0331.1.

García-Herrera, R., Díaz, J., Trigo, R.M., Luterbacher, J. and Fischer, E.M. (2010) A review of the European summer heat wave of 2003. Critical Reviews in Environmental Science and Technology, 40(4), 267. Doi: 10.1080/10643380802238137.

García-León, D., Contreras, S. and Hunink, J. (2019) Comparison of meteorological and satellite-based drought indices as yield predictors of Spanish cereals. Agricultural Water Management, 213, 388-396. Doi: 10.1016/j.agwat.2018.10.030.

Gentilucci, M., Barbieri, M. and Burt, P. (2018). Climatic variations in Macerata province (Central Italy). Water, 10(8), 1104. Doi: 10.3390/w10081104

Gerber, N. and Mirzabaev, A. (2017). Benefits of action and costs of inaction: Drought mitigation and preparedness – a literature review (No. 1). WMO, Geneva, Switzerland and GWP, Stockholm, Sweden.

Giorgi, F., Jones, C. and Asrar, G.R. (2009) Addressing climate information needs at the regional level: the CORDEX framework. World Meteorological Organization (WMO) Bulletin, 58(3), 175, 2009. ISNN: 0042-9767.

González-Hidalgo, J.C., Vicente-Serrano, S.M., Peña-Angulo, D., Salinas, C., Tomas-Burguera, M. and Beguería, S. (2018) Highresolution spatio-temporal analyses of drought episodes in the western Mediterranean basin (Spanish mainland, Iberian Peninsula). Acta Geophysica, 66, 81–392. Doi: 10.1007/s11600-018-0138-x.

Gudmundsson, L. and Seneviratne, S.I. (2015) European drought trends. Proceedings of the International Association of Hydrological Sciences, 369, 75–79. Doi: 10.5194/piahs-369-75-2015.

Guenzi, D., Acquaotta, F., Garzena, D., Baronetti, A. and Fratianni, S. (2019) An algorithm for daily temperature comparison: co. temp-comparing series of temperature. Earth Science Informatics, 1–6. Doi: 10.1007/s12145-019-00414-y.

Guenzi, D., Acquaotta, F., Garzena, D. and Fratianni, S. (2017) CoRain: a free and open source software for rain series comparison. Earth Science Informatics, 10(3), 405–416. Doi: 10.1007/s12145-017-0301-y.

Guerreiro, S.B., Dawson, R.J., Kilsby, C., Lewis, E. and Ford, A. (2018) Future heat-waves, droughts and floods in 571 European cities. Environmental Research Letters, 13(3), 034009. Doi: 10.1088/1748-9326/aaaad3.

Guiot, J. and Cramer, W. (2016) Climate change: The 2015 Paris Agreement thresholds and Mediterranean basin ecosystems. Science, 354(6311), 465-468. Doi: 10.1126/science.aah5015.

Guo, Y., Huang, S., Huang, Q., Wang, H., Fang, W., Yang, Y. and Wang, L. (2019) Assessing socioeconomic drought based on an improved Multivariate Standardized Reliability and Resilience Index. Journal of Hydrology, 568, 904-918. Doi: 10.1016/j.jhydrol.2018.11.055.

Hagemann, S., Machenhauer, B., Jones, R., Christensen, O. B., Déqué, M., Jacob, D. and Vidale, P. L. (2004) Evaluation of water and energy budgets in regional climate models applied over Europe, Climate Dynamics, 23, 547–567. Doi: 10.1007/s00382-004-0444-7.

Hanks, R.R. (2011) Encyclopedia of geography terms, themes, and concepts. Santa Barbara, CA: ABC-CLIO.

Hargreaves, G.H. and Samani, Z.A. (1985) Reference crop evapotranspiration from temperature. Applied Engineering in Agriculture, 1, 96–99.

Hartmann, D.L., Klein Tank, A.M.G., Rusticucci, M., Alexander, L.V., Brönnimann, S., Charabi, Y., Dentener, F.J., Dlugokencky, E.J., Easterling, D.R., Kaplan, A. and Zhai, P.M. (2013) Observations: Atmosphere and surface In Stocker T.F., Qin D., Plattner G.-K., Tignor M., Allen S.K., Boschung J., et al. (Eds.), Climate change: The physical science basis. Contribution of working group I to the fifth assessment report of the intergovernmental panel on climate change Cambridge, England; New York, NY: Cambridge University Press, 159–254.

Hayes, M., Svoboda, M., Wall, N. and Widhalm, M. (2011) The Lincoln declaration on drought indices: universal meteorological drought index recommended. Bulletin of the American Meteorological Society, 92(4), 485-488. Doi: 10.1175/2010BAMS3103.1.

Herceg, A. (2012) The Palfai drought index. In: Gregoricˇ, G. (Ed.) Drought Management Centre for South-East Europe (DMCSEE) – Summary of the result of the project. Ljubljana, Slovenia: Slovenian Environmental Agency, pp. 17–22.

Hertig, E. and Tramblay, Y. (2017) Regional downscaling of Mediterranean droughts under past and future climatic conditions. Global and Planetary Change, 151, 36-48. Doi: 10.1016/j.gloplacha.2016.10.015.

Hoerling, M., Eischeid, J., Perlwitz, J., Quan, X., Zhang, T. and Pegion, P. (2012) On the increased frequency of Mediterranean drought. Journal of Climate, 25(6), 2146–2161. Doi: 10.1175/JCLI-D-11-00296.1.

Hunter, R.D. and Meentemeyer, R.K. (2005) Climatologically aided mapping of daily precipitation and temperature. Journal of Applied Meteorology, 44(10),1501–1510. Doi: 10.1175/JAM2295.1.

Isaaks, E. and Srivastava, R. (1989) An Introduction to Applied Geostatistics. Oxford University Press Inc., New York, 561 pp.

Itenfisu, D., Elliott, R.L., Allen, R.G. and Walter, I.A. (2000) Comparison of reference evapotranspiration calculations across a range of climates. In National irrigation symposium. Proceedings of the 4th Decennial Symposium, Phoenix, Arizona, USA, November 14-16, 2000. (pp. 216-227). American Society of Agricultural Engineers.

Jacob, D., Petersen, J., Eggert, B., Alias, A., Christensen, O. B., Bouwer, L. M., Braun, A., Colette, A., Déqué, M., Georgievski, G., Georgopoulou, E., Gobiet, A., Menut, L., Nikulin, G., Haensler, A., Hempelmann, N., Jones, C., Keuler, K., Kovats, S., Kröner, N., Kotlarski, S., Kriegsmann, A., Martin, E., van Meijgaard, E., Moseley, C., Pfeifer, S., Preuschmann, S., Radermacher, C., Radtke, K., Rechid, D., Rounsevell, M., Samuelsson, P., Somot, S., Soussana, J.-F., Teichmann, C., Valentini, R., Vautard, R., Weber, B. and Yiou, P. (2014) EURO-CORDEX: new high-resolution climate change projections for European impact research. Regional Environmental Change, 14, 563-578. Doi: 10.1007/s10113-013-0499-2.

Jimenez-Munoz, J. C., Mattar, C., Barichivich, J., Santamaría-Artigas, A., Takahashi, K., Malhi, Y., Sobrino, J.A. and van der Schrier G. (2016) Record-breaking warming and extreme drought in the Amazon rainforest during the course of El Nino 2015–2016. Scientific Reports 6, 1–12. Doi: 10.1038/srep33130.

Journel, A.G. and Huijbregts, C.J. (1978) Mining Geostatistics. Academic Press, London, UK, 600 pp.

Kastelec, D. and Košmelj, K. (2002) Spatial interpolation of mean yearly precipitation using universal kriging. In: Mrvar, A. and Ferligoj, A. (eds) Developments in Statistics, FDV, Ljubljana, Slovenia, 149-162 pp.

Katerji, N. and Rana, G. (2011) Crop reference evapotranspiration: a discussion of the concept, analysis of the process and validation. Water resources management, 25(6), 1581-1600. Doi: 10.1007/s11269-010-9762-1.

Kendall, M.G. (1976) Rank Auto Correlation Methods. 4th Edn., Griffin, Oxford.

Keyantash, J. and Dracup, J.A. (2002) The quantification of drought: an evaluation of drought indices. Bulletin of the American Meteorological Society, 83(8), 1167-1180. Doi: 10.1175/1520-0477-83.8.1167.

Kitsara, G., Papaioannou, G., Papathanasiou, A. and Retalis, A. (2013). Dimming/brightening in Athens: Trends in sunshine duration, cloud cover and reference evapotranspiration. Water resources management, 27(6), 1623-1633.

Kotlarski, S., Keuler, K., Christensen, O., Colette, A., Déqué, M., Gobiet, A., Goergen, K., Jacob, D., Lüthi, D., van Meijgaard, E., Nikulin, G., Schär, C., Teichmann, C., Vautard, R., Warrach-Sagi, K. and Wulfmeyer, V. (2014) Regional climate modeling on European scales: a joint standard evaluation of the EURO-CORDEX RCM ensemble. Geoscientific Model Development, 7, 1297-1333. Doi:10.5194/gmd-7-1297-2014.

Kumar, V. (2007) Optimal contour mapping of groundwater levels using universal kriging – a case study. Hydrological Sciences Journal, 52 (5), 1038-1050. Doi: 10.1623/hysj.52.5.1038.

Lamy, C. and Dubreuil, V. (2013) Impact potentiel du changement climatique sur les sécheresses pédologiques en Bretagne au 21eme siècle. Climatologie, 10,107-121.

Lloyd-Hughes, B. (2014). The impracticality of a universal drought definition. Theoretical and Applied Climatology, 117(3-4), 607-611. Doi: 10.1007/s00704-013-1025-7.

Loucks, D.P. and Gladwell J.S. (1999). Sustainability Criteria for Water Resource Systems, Cambridge: Cambridge University Press.

Lu, Z., Zhao, Y., Wei, Y., Feng, Q. and Xie J. (2019). Differences among Evapotranspiration Products Affect Water Resources and Ecosystem Management in an Australian Catchment. Remote Sensing, 11: 958. Doi: 10.3390/rs11080958.

Luterbacher, J., Dietrich, D., Xoplaki, E., Grosjean, M. and Wanner, H. (2004) European seasonal and annual temperature variability, trends, and extremes since 1500. Science, 303, 1499–1503. Doi: 10.1126/science.1093877.

Maccioni, P., Kossida, M., Brocca, L. and Moramarco, T. (2015) Assessment of the drought hazard in the Tiber River basin in central Italy and a comparison of new and commonly used meteorological indicators. Journal of Hydrologic Engineering, 20 (8), 1–11. Doi: 10.1016/(ASCE)HE. 1.

Maček, U., Bezak, N. and Šraj, M. (2018). Reference evapotranspiration changes in Slovenia, Europe. Agricultural and forest meteorology, 260, 183-192. Doi: 10.1016/j.agrformet.2018.06.014

Madsen, H., Lawrence, D., Lang, M., Martinkova, M. and Kjeldsen, T.R. (2014). Review of trend analysis and climate change projections of extreme precipitation and floods in Europe. Journal of Hydrology, 519, 3634-3650. Doi: 10.1016/j.jhydrol.2014.11.003.

Magno, R., Angeli, L., Chiesi, M. and Pasqui, M. (2014) Prototype of a drought monitoring and forecasting system for the Tuscany region. Advances in Science and Research, 11, 7-10. Doi:10.5194/asr-11-7-2014.

Mann, H.B.,1945. Nonparametric tests against trend, Econometrica. 13, 245–259.

Maraun, D., Widmann, M., Gutiérrez, J. M., Kotlarski, S., Chandler, R. E., Hertig, E., Wibig, J., Huth, R. and Wilcke, R.A.I. (2015) VALUE: A framework to validate downscaling approaches for climate change studies. Earth's Future, 3: 1–14. Doi: 10.1002/2014EF000259.

Marchina, C., Natali, C. and Bianchini, G. (2019) The Po River water isotopes during the drought condition of the year 2017. Water, 11(1), 150. Doi: 10.3390/w11010150.

Marchina, C., Natali, C., Fazzini, M., Fusetti, M., Tassinari, R. and Bianchini, G. (2017) Extremely dry and warm conditions in northern Italy during the year 2015: effects on the Po river water. Rendiconti Lincei, 28(2), 281–290. Doi: 10.1007/s12210-017-0596-0.

Marcos-Garcia, P., Lopez-Nicolas, A. and Pulido-Velazquez, M. (2017) Combined use of relative drought indices to analyze climate change impact on meteorological and hydrological droughts in a Mediterranean basin. Journal of Hydrology, 554, 292-305. Doi: 10.1016/j.jhydrol.2017.09.028.

Mariotti, A. and Dell'Aquila, A. (2012) Decadal climate variability in the Mediterranean region: roles of large-scale forcings and regional processes. Climate Dynamics, 38(5-6), 1129-1145. Doi: 10.1007/s00382-011-1056-7.

Martin-Vide, J. and Lopez-Bustins, J.A. (2006) The western Mediterranean oscillation and rainfall in the Iberian peninsula. International Journal of Climatology, 26, 1455–1475. Doi: 10.1002/joc.1388.

Masih, I., Maskey, S., Mussá, F.E.F. and Trambauer, P. (2014) A review of droughts on the African continent: A geospatial and long-term perspective. Hydrology and Earth System Sciences, 18, 3635-3649. Doi:10.5194/hess-18-3635-2014.

Matzneller, P., Ventura, F., Gaspari, N. and Pisa, P.R. (2010). Analysis of climatic trends in data from the agrometeorological station of Bologna-Cadriano, Italy (1952–2007). Climatic change, 100(3-4), 717-731. Doi: 10.1007/s10584-009-9686-z

McKee, T.B.N., Doesken, J. and Kleist, J. (1993) The relationship of drought frequency and duration to timescales. In: Proceedings of the Eighth Conference on Applied Climatology. Boston: American Meteorological Society, pp. 179–184.

Mearns, L.O., Gutowski, W.J., Jones, R., Leung, L.-Y., McGinnis, S., Nunes, A. M. B. and Qian, Y. (2009) A regional climate change assessment program for North America, EOS, 90, 311–312. Doi: 10.1029/2009EO360002.

Merino, A., López, L., Hermida, L., Sánchez, J. L., García-Ortega, E., Gascón, E. and Fernández-González, S. (2015). Identification of drought phases in a 110-year record from Western Mediterranean basin: Trends, anomalies and periodicity analysis for Iberian Peninsula. Global and Planetary Change, 133, 96-108. Doi: 10.1016/j.gloplacha.2015.08.007.

Merkenschlager, C. and Hertig, E. (2020) Seasonal assessments of future precipitation extremes in the Mediterranean area considering nonstationarities in predictor-predictand relationships. Climate Research, 80(1), 19-42. Doi: 10.3354/cr01590.

Milovanović, B., Schuster, P., Radovanović, M., Vakanjac, V. R. and Schneider, C. (2017) Spatial and temporal variability of precipitation in Serbia for the period 1961–2010. Theoretical and Applied Climatology, 130(1-2), 687-700. Doi: /10.1007/s00704-017-2118-5.

Mishra, A.K. and Singh, V.P. (2010) A review of drought concepts. Journal of hydrology, 391(1-2), 202-216. Doi: 10.1016/j.jhydrol.2010.07.012.

Mjejra, M., Dubreuil, V. and Henia, L. (2015) Suivi de la sécheresse agro-climatique à partir du déficit d'évaporation dans le bassin versant de la Mejerda (Tunisie). 28éme colloque de l'Association Internationale de Climatologie. Liège-Belgique.

Mu, Q., Zhao, M and Running, S.W. (2011) Improvements to a MODIS global terrestrial evapotranspiration algorithm. Remote Sensing of Environment, 115: 1781-1800. Doi: 10.1016/j.rse.2011.02.019

Mudelsee, M. (2019) Trend analysis of climate time series: A review of methods. Earth-Science Reviews, 190, 310-322. Doi: 10.1016/j.earscirev.2018.12.005.

Mues, A., Manders, A., Schaap, M., Kerschbaumer, A., Stern, R. and Builtjes, P. (2012) Impact of the extreme meteorological conditions during the summer 2003 in Europe on particulate matter concentrations. Atmospheric Environment, 55, 377–391. Doi: 10.1016/j.atmosenv.2012.03.002.

Musolino, D., De Carli, A. and Massarutto, A. (2017) Evaluation of socio-economic impact of drought events: the case of Po river basin. European Countryside, 9(1), 163-176. Doi: 10.1515/euco-2017-0010.

Nagy, L. and Grabherr, G. (2009) The Biology of Alpine Habitats: Biology of Habitats. New York: Oxford University Press, 28–50 pp. ISBN 978-0-19-856703-5.

Osborn, T., Barichivich, J., Harris, I., van der Schrier, G. and Jones, P. (2017) Monitoring global drought using the self-calibrating Palmer Drought Severity Index. Bulletin of the American Meteorological Society, 98(8), S32-S33. Doi: 10.1175/2017BAMSStateoftheClimate.1.

Ouzeau, G., Soubeyroux, J.M., Schneider, M., Vautard, R. and Planton, S. (2016) Heat waves analysis over France in present and future climate: application of a new method on the EUROCORDEX ensemble. Climate Services, 4, 1–12. Doi: 10.1016/j.cliser.2016.09.002.

Palmer, W.C. (1965) Meteorological drought (Vol. 45). US Department of Commerce, Weather Bureau, 58 pp.

Parodi, A., Ferraris, L., Gallus, W., Maugeri, M., Molini, L., Siccardi, F., and Boni, G. (2017) Ensemble cloud- resolving modelling of a historic backbuilding mesoscale convective system over Liguria: the San Fruttuoso case of 1915. Climate of the Past,13, 455–472. Doi: 10.5194/cp-13-455-2017.

Pavanelli, D. and Capra, A. (2014). Climate change and human impacts on hydroclimatic variability in the Reno River catchment, Northern Italy. CLEAN–Soil, Air, Water, 42(5), 535-545. Doi: 10.1002/clen.201300213.

Pebesma, E. and Gräler, B. (2018) Introduction to Spatio-Temporal Variography. Münster: Institute for Geoinformatics University of Münster, 1–11 pp.

Pebesma, E.J. (2012) Spacetime: spatio-temporal data in R. Journal of Statistical Software, 51(7),1–30. Doi: 10.18637/jss.v051.i07.

Pebesma, E.J. (2004) Multivariable geostatistics in S: the gstat package. Computers & Geosciences, 30(7), 683–691. https://doi.org/10.1016/j.cageo.2004.03.012.

Pedrotti, F. 2018. Climate gradients and biodiversity in mountains of Italy. Cham: Springer International Publishing. Doi: 10.1007/978-3-319-67967-9.

Pereira, L.S., Oweis T. and Zairi A. (2002) Irrigation management under water scarcity. Agricultural Water Management, 57(3), 175-206. doi.org/10.1016/S0378-3774(02)00075-6.

Perini, L., Salvati, L., Zitti, M. and Bajocco, S. (2011) A proposal for a meteorological index of climate change impact. Italian Journal of. Agrometeorology, 1, 17-24.

Phillips, D.L., Dolph, J. and Marks, D. (1992) A comparison of geostatistical procedures for spatial analysis of precipitation in mountainous terrain. Agricultural Meteorology, 58, 119–141. Doi: 10.1016/0168-1923(92)90114-J.

Piccarreta, M., Capolongo, D. and Boenzi, F. (2004) Trend analysis of precipitation and drought in Basilicata from 1923 to 2000 within a southern Italy context. International Journal of Climatology, 24(7), 907-922. Doi:10.1002/joc.1038.

Pietrapertosa, F., Salvia, M., Hurtado, S. D. G., d'Alonzo, V., Church, J. M., Geneletti, D., Musco, F. and Reckien, D. (2019). Urban climate change mitigation and adaptation planning: are Italian cities ready?. Cities, 91, 93-105. Doi: 10.1016/j.cities.2018.11.009.

Pietrapertosa, F., Khokhlov, V., Salvia, M. and Cosmi, C. (2018) Climate change adaptation policies and plans: A survey in 11 South East European countries. Renewable and Sustainable Energy Reviews, 81, 3041-3050. Doi: 10.1016/j.rser.2017.06.116.

Pinna, M. and Vittorini, S., (1985) Contributo alla determinazione dei regimi pluviometrici in Italia. Memorie della Società Geografica Italiana, 39,147-168.

Pinna, M. (1978) L'atmosfera e il clima. UTET, Torino, 478 pp.

Pirlone, F., Spadaro, I. and Candia, S. (2020) More Resilient Cities to Face Higher Risks. The Case of Genoa. Sustainability, 12(12), 4825. Doi:10.3390/su12124825.

Pogliotti, P., Guglielmin, M., Cremonese, E., Morra di Cella, U., Filippa, G., Pellet, C. and Hauck, C. (2015) Warming permafrost and active layer variability at Cime Bianche, Western European Alps. The Cryosphere, 9(2), 647-661. Doi: 10.5194/tc-9-647-2015.

Polade, S.D., Gershunov, A., Cayan, D.R., Dettinger, M.D. and Pierce, D.W. (2017) Precipitation in a warming world: Assessing projected hydro-climate changes in California and other Mediterranean climate regions. Nature communications, 7, 10783. Doi: 10.1038/s41598-017-11285-y.

Prudhomme, C. and Williamson, J. (2013). Derivation of RCM-driven potential evapotranspiration for hydrological climate change impact analysis in Great Britain: a comparison of methods and associated uncertainty in future projections. Hydrology and Earth System Sciences, 17(4), 1365-1377. Doi:10.5194/hess-17-1365-2013

Pulwarty, R.S. and Sivakumar, M.V.K. (2014) Information systems in a changing climate: Early warnings and drought risk management, Weather and Climate Extremes, 3, 14-21. Doi:10.1016/j.wace.2014.03.005.

Quintana-Seguí, P., Martin, E., Sánchez, E., Zribi, M., Vennetier, M., Vicente-Serrano, S. and Vidal, J.-P. (2016) Sub-chapter 1.3.3. Drought: observed trends, future projections. In The Mediterranean region under climate change (pp. 123–131). Doi: 10.4000/books.irdeditions.23157.

R Development Core Team (2011) R: A Language and Environment for Statistical Computing. R Foundation for Statistical Computing, Vienna, Austria. ISBN 3-900051-07-0.

Raäisaänen, J. (2007) How reliable are climate models?. Tellus A: Dynamic Meteorology and Oceanography, 59(1), 2-29.

Raymond, F., Ullmann, A., Tramblay, Y., Drobinski, P. and Camberlin, P. (2019) Evolution of Mediterranean extreme dry spells during the wet season under climate change. Regional Environmental Change, 1-13. Doi: 10.1007/s10113-019-01526-3.

Raymond, F.A., Ullmann, A., Camberlin, P., Oueslati, B. and Drobinski, P. (2018) Atmospheric conditions and weather regimes associated with extreme winter dry spells over the Mediterranean basin. Climate Dynamics, 50(11–12), 4437–4453. Doi: 10.1007/s00382-017-3884-6.

Raymond, F.A., Ullmann, P., Camberlin, P., Drobinski, C. and Chateau Smith, C. (2016). Extreme dry spell detection and climatology over the Mediterranean Basin during the wet season. Geophysical Research Letters, 43, 7196–7204. Doi: 10.1002/2016GL069758.

Rebetez, M., Mayer, H., Dupont, O., Schindler, D., Gartner, K., Kropp, J.P. and Menzel, A. (2006) Heat and drought 2003 in Europe: a climate synthesis. Annals of Forest Science, 63(6), 569–577. Doi: 10.1051/forest:2006043.

Redolat, D., Monjo, R., Lopez-Bustins, J.A. and Martin-Vide, J. (2018) Upper-level Mediterranean oscillation index and seasonal variability of rainfall and temperature. Theoretical and Applied Climatology, 134(3–4), 1059–1077. Doi: 10. 1007/s00704-018-2424-6.

Ren, L., Arkin, P., Smith, T.M. and Shen, S.S. (2013) Global precipitation trends in 1900–2005 from a reconstruction and coupled model simulations. Journal of Geophysical Research: Atmospheres, 118(4), 1679-1689. Doi: 10.1002/jgrd.50212.

Renza, D., Martinez, E., Arquero, A. and Sanchez, J. (2010) Drought estimation maps by means of multidate Landsat fused images. In 30th EARSeL Symposium: Remote Sensing and Geoinformation, Education, and Natural and Cultural Heritage, vol. 30.

Rhee, J. and Im, J. (2017) Meteorological drought forecasting for ungauged areas based on machine learning: Using longrange climate forecast and remote sensing data. Agricultural and Forest Meteorology, 237, 105-122. Doi: 10.1016/j.agrformet.2017.02.011.

Russia Beyond, 2016 Moscow's July Heat Wave Breaks 137-year Record (2016) Available online at: https://www.rbth.com/news/2016/08/01/moscows-july-heat-wave-breaks-137-year-record_617081 (last accessed on 13.06.2020).

Ruti, P., Somot, S., Giorgi, F., Dubois, C., Flaounas, E., Obermann, A., Dell'Aquila, A., Pisacane, G., Harzallah, A., Lombardi, E., Ahrens, B., Akhtar, N., Alias, A., Arsouze, T., Raznar, R., Bastin, S., Bartholy, J., Béranger, K., Beuvier, J., Bouffies-Cloche, S., Brauch, J., Cabos, W., Calmanti, S., Calvet, J.C., Carillo, A., Conte, D., Coppola, E., Djurdjevic, V., Drobinski, P., Elizalde, A., Gaertner, M., Galan, P., Gallardo, C., Gualdi, S., Goncalves, M., Jorba, O., Jorda, G., Lheveder, B., Lebeaupin-Brossier, C., Li, L., Liguori, G., Lionello, P., Macias-Moy, D., Onol, B., Rajkovic, B., Ramage, K., Sevault, F., Sannino, G., Struglia, M.V., Sanna, A., Torma, C. and Vervatis, V. (2015) MED-CORDEX initiative for Mediterranean climate studies. Bulletin of the American Meteorological Society. Doi: 10.1175/BAMS-D-14-00176.1.

Sacchini, A., Ferraris, F., Faccini, F. and Firpo, M. (2012). Environmental climatic maps of Liguria (Italy). Journal of Maps, 8(3), 199-207. Doi: 0.1080/17445647.2012.703901

Salter. C., Hobbs, J. andWheeler, J. (2005) Essentials of World Regional Geography 2nd Edition, New York: Harcourt Brace, 464–465. ISBN 13: 9780030322716.

Sanford, T., Frumhoff, P.C., Luers, A. and Gulledge, J. (2014) The climate policy narrative for a dangerously warming world. Nature Climate Change, 4(3), 164-166. Doi: 10.1038/nclimate2148.

Science News California drought worst in at least 1,200 years (2014) Available online at: https://www.sciencenews.org/article/california-drought-worst-least-1200-years (last accessed 9.06.2020).

Seager, R., Osborn, T. J., Kushnir, Y., Simpson, I. R., Nakamura, J. and Liu, H. (2019) Climate variability and change of Mediterraneantype climates. Journal of Climate, 32 2887–915. Doi:10.1175/JCLI-D-18-0472.1.

Secci, D., Patriche, C. V., Ursu, A. and Sfîcă, L. (2010). Spatial interpolation of mean annual precipitations in Sardinia. A comparative analysis of several methods. Geographia Technica, 9(1), 67-75.

Sellami, H., Benabdallah, S., La Jeunesse, I. and Vanclooster, M. (2016) Quantifying hydrological responses of small Mediterranean catchments under climate change projections. Science of the Total Environment, 543, 924-936. Doi. 10.1016/j.scitotenv.2015.07.006.

Sen, P.K. (1968) Estimates of the regression coefficient based on Kendall's tau, Journal of the American Statistical Association 63, 1379–1389.

Sepulcre-Canto, G., Horion, S., Singleton, A., Carrao, H. and Vogt, J. (2012). Development of a combined drought indicator to detect agricultural drought in Europe. Natural Hazards and Earth System Sciences, 12 (11), 3519–3531. Doi: 10. 5194/nhess-12-3519-2012.

Sheffield, J. and Wood, E.F. (2012) Drought: Past Problems and Future Scenarios. International Journal of Digital Earth, 5(5),1-2. Doi: 10.1080/17538947.2011.597110.

Shi, L., Chu, E., Anguelovski, I., Aylett, A., Debats, J., Goh, K., Schenk, T., Seto, K.C., Dodman, D., Roberts, D., Roberts, J.T. and VanDeveer, D. (2016) Roadmap towards justice in urban climate adaptation research. Nature Climate Change, 6(2), 131-137. Doi: 10.1038/NCLIMATE2841

Sirangelo, B., Caloiero, T., Coscarelli, R. and Ferrari, E. (2017) Stochastic analysis of long dry spells in Calabria (southern Italy). Theoretical and Applied Climatology, 127(3–4), 711–724. Doi:10.1007/s00704-015-1662-0.

Song, X., Li, L., Fu, G., Li, J., Zhang, A., Liu, W. and Zhang, K. (2014) Spatial-temporal variations of spring drought based on spring-composite index values for the Songnen Plain, Northeast China. Theoretical and Applied Climatology, 116 (3–4), 371-384. Doi: 10.1007/s00704-013-0957-2.

Spinoni, J., Barbosa, P., Bucchignani, E., Cassano, J., Cavazos, T., Christensen, J. H., Christensen, O. B., Coppola, E., Evans, J., Geyer, B., Giorgi, F., Hadjinicolaou, P., Jacob, D., Katzfey, J., Koenigk, T., Laprise, R., Lennard, C. H., Levent Kurnaz, M., Li, D., Llopart, M., McCormick, N., Naumann, G., Nikulin, G., Ozturk, T., Panitz, H.-J., Porfirio da Rocha, R., Rockel, B., Solman, S. A., Syktus, J., Tangang,

F., Teichmann, C., Vautard, R., Vogt, J. V., Winger, K., Zittis, G. and Dosio, A. (2020) Future Global Meteorological Drought Hot Spots: A Study Based on CORDEX Data. Journal of Climate, 33(9), 3635-3661. Doi: 10.1175/JCLI-D-19-0084.1.

Spinoni, J., Naumann, G., Vogt, J.V. and Barbosa, P. (2015) The biggest drought events in Europe from 1950 to 2012. Journal of Hydrology: Regional Studies, 3, 509–524. Doi: 10. 1016/j.ejrh.2015.01.001.

Stahl, K., Moore, R.D., Floyer, J.A., Asplin, M.G. and McKendry, I.G. (2006). Comparison of approaches for spatial interpolation of daily air temperature in a large region with complex topography and highly variable station density. Agricultural and forest meteorology, 139(3-4), 224-236. Doi: 10.1016/j.agrformet.2006.07.004

Stahr, A. and Langenscheidt, E. (2015) Landforms of high mountains. Springer-Verlag Berlin Heidelberg. 8, 158 ISBN 978-3-662-51478-8. Doi 10.1007/978-3-642-53715-8.

Stocker T. (2011) Introduction to climate modelling; Advances in geophysical and environmental mechanics and mathematics: Springer Verlag, Heidelberg,179 pp.

Svoboda, M. and Fuchs, B. (2016) Handbook of Drought Indicators and Indices Integrated Drought Management Programme (IDMP), Integrated Drought Management Tools and Guidelines Series 2, World Meteorological Organization and Global Water Partnership, Geneva, Switzerland, 52 pp

Tadesse, T., Wilhite, D.A., Harms, S.K., Hayes, M.J. and Goddard, S. (2004) Drought Monitoring Using Data Mining Techniques: A Case Study for Nebraska, USA. Natural Hazards, 33,137-159. Doi: 10.1023/B:NHAZ.0000035020.76733.0b.

Taylor, K.E., Stouffer, R.J. and Meehl, G.A. (2012) An overview of CMIP5 and the experiment design. Bulletin of the American Meteorological Society, 93(4), 485-498. Doi: 10.1175/BAMS-D-11-00094.1.

Terzago, S., Fratianni, S. and Cremonini, R. (2013) Winter precipitation in Western Italian Alps (1926–2010). Meteorology and Atmospheric Physics, 119(3-4), 125-136. Doi: 10.1007/s00703-012-0231-7

Teutschbein, C., and Seibert, J. (2012) Bias correction of regional climate model simulations for hydrological climate-change impact studies: Review and evaluation of different methods. Journal of hydrology, 456, 12-29. Doi: 10.1016/j.jhydrol.2012.05.052.

The Guardian South Asia floods kill 1,200 and shut 1.8 million children out of school (2017) Available online at: https://www.theguardian.com/world/2017/aug/30/mumbai-paralysed-by-floods-as-india-and-region-hit-by-worst-monsoon-rains-in-years (last accessed 13.06.2020)

Tomasino, M., Zanchettin, D. and Traverso, P. (2004) Analisi del periodo siccitoso dell'estate 2003 in riferimento alla magra eccezionale del Po misurata a Pontelagoscuro. Bollettino geofisico, XXVII (1-2).

Tomas-Burguera, M., Beguería, S. and Vicente-Serrano, S. M. (2020). Climatology and trends of reference evapotranspiration in Spain. International Journal of Climatology, 1-15. Doi: 10.1002/joc.6817

Toreti, A., Desiato, F., Fioravanti, G. and Perconti, W. (2010) Seasonal temperatures over Italy and their relationship with low-frequency atmospheric circulation patterns. Climatic Change, 99(1–2), 211–227. Doi: 10.1007/s10584-009-9640-0.

Trajkovic, S. (2005). Temperature-based approaches for estimating reference evapotranspiration. Journal of irrigation and drainage engineering, 131(4), 316-323. Doi: 10.1061/(ASCE)0733-9437(2005)131:4(316)

Travis, W.R. (2013) Design of a severe climate change early warning system, Weather and Climate Extremes. 2, 31-38. Doi: 10.1016/j.wace.2013.10.006.

Trenberth, K.E., Dai, A., van der Schrier, G., Jones, P.D., Barichivich, J., Briffa, K.R. and Sheffield, J. (2013) Global warming and changes in drought. Nature Climate Change, 4(1), 17–22. Doi: 10.1038/nclimate2067.

Trenberth, K.E., Dai, A., Rasmussen, R.M. and Parsons, D.B. (2003) The Changing Character of Precipitation. The National Center for Atmospheric Research, Boulder, Colorado. Doi: 10.1175/BAMS-84-9-1205.

Uboldi, F. and Lussana, C. (2018). Evidence of non-stationarity in a local climatology of rainfall extremes in northern Italy. International Journal of Climatology, 38(1), 506-516. Doi: 10.1002/joc.5183.

UNFCCC (2015) Adoption of the Paris Agreement. Proposal by the President. Proposal by the President. Available from: http://unfccc.int/resource/d°Cs/2015/cop21/eng/l09r01.pdf. United Nations, Geneva.

Valigi, D., Luque-Espinar, J.A., Di Matteo, L., Cambi, C., Pardo-Igúzquiza, E. and Rossi, M. (2016). Analysis of drought conditions and their effects on Lake Trasimeno (Central Italy) levels. Acque Sotterranee-Italian Journal of Groundwater, 215(2):39-47. Doi: 10.7343/as-2016-215.

Valverde, P., Serralheiro, R., de Carvalho, M., Maia, R., Oliveira, B. and Ramos, V. (2015). Climate change impacts on irrigated agriculture in the Guadiana river basin (Portugal). Agricultural Water Management, 152, 17-30. Doi: 10.1016/j.agwat.2014.12.012

van der Linden, P. and Mitchell J.F.B. (2009) ENSEMBLES: Climate Change and its Impacts: Summary of research and results from the ENSEMBLES project. Met Office Hadley Centre, FitzRoy Road, Exeter EX1 3PB, Uk, 160 pp.

Vergni, L. and Todisco, F. (2011). Spatio-temporal variability of precipitation, temperature and agricultural drought indices in Central Italy. Agricultural and Forest Meteorology, 151(3), 301-313. Doi: 10.1016/j.agrformet.2010.11.005.

Vicente-Serrano, S.M., Tomas-Burguera, M., Beguería, S., Reig, F., Latorre, B., Peña-Gallardo, M., Yolanda Luna, M., Morata, A. and González-Hidalgo, J.C. (2017) A high resolution dataset of drought indices for Spain. Data, 2(3), 22. Doi: 10.3390/data2030022.

Vicente-Serrano, S.M., Van der Schrier, G., Beguería, S., Azorin-Molina, C. and Lopez-Moreno, J.I. (2015) Contribution of precipitation and reference evapotranspiration to drought indices under different climates. Journal of Hydrology, 526, 42-54. Doi: 10.1016/j.jhydrol.2014.11.025.

Vicente-Serrano, S.M., Azorin-Molina, C., Sanchez-Lorenzo, A., Revuelto, J., Lopez-Moreno, J.I., Gonzalez-Hidalgo J.C. and Espejo, F. (2014) Reference evapotranspiration variability and trends in Spain, 1961–2011. Global and Planetary Change, 121, 26-40. Doi: 10.1016/j.gloplacha.2014.06.005.

Vicente-Serrano, S.M., Beguería, S., Lorenzo-Lacruz, J., Camarero, J.J., Lopez-Moreno, J.I., Azorin-Molina, C., Revuelto, J., Morán-Tejeda, E. and Sanchez-Lorenzo, A. (2012) Performance of drought indices for ecological, agricultural, and hydrological applications. Earth Interactions, 16(10), 1-27. Doi: 10.1175/2012EI000434.1.

Vicente-Serrano, S.M., López-Moreno, J.I., Drumond, A., Gimeno, L., Nieto, R., Morán-Tejeda, E., Lorenzo-Lacruz, J., Beguería, S. and Zabalza, J. (2011) Effects of warming processes on droughts and water resources in the NW Iberian Peninsula (1930–2006), Climate Research 48:203–212. Doi: 10.3354/cr01002.

Vicente-Serrano, S.M., Beguería, S. and López-Moreno, J.I. (2010) A multiscalar drought index sensitive to global warming: the standardized precipitation evapotranspiration index. Journal of Climate, 23(7), 1696–1718. Doi:10.1175/2009 JCLI2909.1.

Wackernagel, H. (2003) Multivariate Geostatistics: An Introduction with Applications. (3rd ed.) Heidelberg: Springer, Berlin, 388 pp.

Wallace, J.M. and Gutzler, D.S. (1981) Teleconnections in the geopotential height field during the northern hemisphere winter. Monthly Weather Review, 109(4), 784–812.

Wang, S., Huang, G.H., Lin, Q.G., Li, Z., Zhang, H. and Fan, Y.R. (2014) Comparison of interpolation methods for estimating spatial distribution of precipitation in Ontario, Canada. International Journal of Climatology, 34(14), 3745–3751. Doi: 10.1002/joc.3941.

Wang, W., Ertsen, M.W., Svoboda, M.D. and Hafeez, M. (2016) Propagation of drought: from meteorological drought to agricultural and hydrological drought. Advances in Meteorology,1-5. Doi: 10.1155/2016/6547209.

Wiesner, C.J. (1970). Climate, irrigation and agriculture. Climate, irrigation and agriculture, Angus and Robertson, Sydney,246 pp. ISBN: 020795352X.

Wilhite, D.A. and Glantz, M.H. (1985) Understanding: the Drought Phenomenon: The Role of Definitions. Water International 10(3): 111-120. Doi:10.1080/02508068508686328.

Wilhite, D.A. (2000). Drought as a Natural Hazard: Concepts and Definitions. in Drought: A Global Assessment, vol. I, edited by Donald A. Wilhite, chap. 1, pp. 3-18.

Willmott, C.J. (1982) Some comments on the evaluation of model performance. Bulletin of the American Meteorological Society, 63, 1309–1313. Doi: 10.1175/1520-0477(1982)063<1309:SCOTEO>2.0.CO;2.

Winkler K., Gessner, U. and Hochschild, V. (2017). Identifying Droughts Affecting Agriculture in Africa Based on Remote Sensing Time Series between 2000–2016: Rainfall Anomalies and Vegetation Condition in the Context of ENSO. Remote Sensing, 9, 831. Doi:10.3390/rs9080831.

World Meteorological Organization, 2018: Guide to Climatological Practices. World Meteorological Organization Rep. 100, 153pp. [Available online at https://library.wmo.int/doc_num.php?explnum_id=5541].

World Meteorological Organization (1992) International meteorological vocabulary, World Meteorological Organization Rep. 182, 802 pp [Available online at https://library.wmo.int/doc_num.php?explnum_id=4712].

Yao, Y., Liang, S., Qin, Q. and Wang, K. (2010) Monitoring drought over the conterminous United States using MODIS and NCEP Reanalysis-2 data. Journal of Applied Meteorology and Climatology, 49, 1665–1680. Doi: 10.1175/2010JAMC2328.1

Zaitchik, B.F., Macalady, A.K., Bonneau, L.R. and Smith, R.B. (2006) Europe's 2003 heat wave: a satellite view of impacts and land–atmosphere feedbacks. International Journal of Climatology: A Journal of the Royal Meteorological Society, 26(6), 743–769. Doi: 10.1002/joc.1280.

Zargar, A., Sadiq, R., Naser, B. and Khan, F.I. (2011). A review of drought indices. Environmental Reviews, 19, 333-349. Doi:10.1139/A11-013.

Zhang, Y.Q., Peña-Arancibia, J.L., McVicar, T.R., Chiew F.H.S., Vaze, J., Liu, C., Lu, X., Zheng, H., Wang, Y., Liu, Y.Y. Millares, D.G. and Pan, M. (2016) Multi decadal trends in global terrestrial evapotranspiration and its components. Scientific Reports, 6, 19124. doi:10.1038/srep19124

Zucaro, F. and Morosini, R. (2018). Sustainable land use and climate adaptation: a review of European local plans. TeMA Journal of Land Use, Mobility and Environment, 11(1), 7-26. Doi: 10.6092/1970-9870/5343.